DISSERTATION

VALIDATION OF G-PROTEIN COUPLED INWARDLY RECTIFYING POTASSIUM CHANNEL 1 (GIRK1) AS NEW PROGNOSTIC BREAST CANCER BIOMARKER

SUBMITTED BY

SARAH KAMMERER, MSC

FOR THE ACADEMIC DEGREE OF

DOCTOR OF MEDICAL SCIENCE

(DR. SCIENT. MED.)

AT THE

MEDICAL UNIVERSITY OF GRAZ

INSTITUTE OF BIOPHYSICS

UNDER THE SUPERVISION OF

PROF. DR. THOMAS BAUERNHOFER

PROF. WOLFGANG SCHREIBMAYER

DR. STEPHAN W. JAHN

PROF. DR. PETER REGITNIG

2016

Eidesstattliche Erklärung

Ich erkläre ehrenwörtlich, dass ich die vorliegende Arbeit selbstständig angefertigt und abgefasst, und jene Personen und Institutionen, die am Zustandekommen der Forschungsdaten beteiligt waren, namentlich genannt habe. Andere als die angegebenen Quellen habe ich nicht verwendet und die den benutzten Quellen wörtlich oder inhaltlich entnommenen Stellen habe ich als solche kenntlich gemacht. Die Arbeit an der Dissertation und daraus entstandener Publikationen wurde gemäß den Regeln der „Good Scientific Practice“ durchgeführt.

Graz, am 01.07.2016 *Unterschrift eh*

Declaration

I hereby declare that this thesis is my own original work and that I have fully acknowledged by name all of those individuals and organizations that have contributed to the research for this thesis. Due acknowledgement has been made in the text to all other material used. Throughout this thesis and in all related publications I followed the guidelines of “Good Scientific Practice”.

Date: 01.07.2016 *Signature*

Acknowledgements

Hereby, I would like to thank everybody who contributed in any way to the present work.

First of all, I thank Thomas Bauernhofer for being a great supervisor and mentor, for finding time slots despite his full agenda whenever necessary, for fruitful discussions, for motivating words in hard times, positive feedback in good times and all his support for and beyond this dissertation project. Thank you!

I would like to thank my co-supervisors Wolfgang Schreibmayer for providing lab space, for having always an open door, for many interesting discussions and all his feedback during my work and especially during manuscript writing; Stephan Jahn for answering all pathology-related questions, for his great input and the many ideas; and Peter Regitnig for all the preparatory work that was done before I started.

I thank my team colleagues Astrid Gorischek and Simin Rezania at the Institute of Biophysics for helping with many practical issues, for good discussions, nice chats, coffee breaks and for being friends. Thanks to Armin Sokolowski for his great work perfomed during his diploma thesis. Also, I would like to thank Klaus Groschner for his support, Alice Maier-Pilecky and Elisabeth Bischof for help and support in administrative issues and all members of the Institute of Biophysics for the good time we had.

Special thanks to Elke Winter from the Institute of Pathology. She is not only a genius in her work, but also a good friend. Thank you for instruction, advise and help, for good discussions, for chats, coffee, motivation, and the great trip to Strasbourg! From the Institute of Pathology, I would like to thank also Gerald Hoefler and Florentia Peintinger for supporting this work, the members of the “big lab” for hosting me, and Sylvia Eidenhammer and her colleagues from the immunohistochemistry lab for their help and working time.

Many thanks also to Martin Pichler from the Division of Oncology for several fruitful discussions, valuable input and great collaboration. I would like to thank “his girls” Daniela Schwarzenbacher and Verena Stiegelbauer for their collaboration and the nice coffee and lunch breaks. I thank also Amin El-Heliebi from the Institute of Cell Biology, Embryology and Histology for the many hours at the microscope and for the good collaboration not only in this project.

Thanks to all of my friends who supported me during this time and beyond. Most importantly, I am deeply grateful for all the support I got from my family, for cheering with me and suffering with me. And thanks to you, Florian, just for everything. I would not have been able to this without you.

Table of Contents

1 List of Abbreviations

a. dest.	aqua destillata
ACD	Advanced Cell Diagnostics
AGTR1	angiotensin II receptor type 1
ATCC	American Type Culture Collection
BCA	bicinchoninic acid
BP	biological process
BPE	bovine pituitary extract
BSA	bovine serum albumin
DAB	diaminobenzidine
DapB	bacterial dihydrodipicolinate reductase
DNA	deoxyribonucleic acid
CC	cellular component
CCD	charge-coupled device
ChIP	chromatin immunoprecipitation
DFS	disease free survival
DMEMhG	Dulbecco's Modified Eagle Medium high glucose
ECL	enhanced chemiluminescence
ENCODE	Encyclopedia of DNA Elements at UCSC
ER	estrogen receptor (protein)
ESR1	estrogen receptor 1 (gene)
FBS	fetal bovine serum
FCS	fetal calf serum
FDR	false discovery rate
FFPE	formalin-fixed, paraffin-embedded
GEO	Gene Expression Omnibus
GIRK1	G-protein inwardly rectifying potassium channel subtype 1 (protein)
GO	gene ontology
GPCR	G-protein coupled receptor
hEGF	human epidermal growth factor
HEK	human embryonic kidney
Her2	human epidermal growth factor receptor 2
HIER	heat induced epitope retrieval
HR	hazard ratio
HRP	horseradish peroxidase
IHC	immunohistochemistry

ISH	in situ hybridization
KCNJ3	G-protein inwardly rectifying potassium channel subtype 1 (gene)
L-Glut	L-glutamine
LN	lymph node
LSB	Laemmli sample buffer
MAS	microarray suite
MCF	Michigan Cancer Foundation
MF	molecular function
MEBM	mammary epithelial basal medium
MEM	minimum essential medium
mRNA	messenger ribonucleic acid
NE	norepinephrine
OD	optical density
OS	overall survival
Pen/Strep	penicillin and streptomycin
PBS	phosphate-buffered saline
PBST	phosphate-buffered saline containing 0.05% Tween
PIC	protease inhibitor cocktail
POLR2A	DNA-directed RNA polymerase II subunit RPB1
PR	progesterone receptor
RIPA	radio immunoprecipitation assay
RNA	ribonucleic acid
r_S	Spearman rank correlation coefficient
SDS	sodium dodecyl sulfate
SDS-PAGE	sodium dodecyl sulfate-polyacrylamide gel electrophoresis
TAM	tamoxifen
TBS	Tris-buffered saline
TCGA	The Cancer Genome Atlas
TPM	transcripts per million
UCSC	University of California Santa Cruz
WST	water soluble tetrazolium
wt	wild type
X. laevis	*Xenopus laevis*

2 List of Figures

3 List of Tables

4 Abstract

Validation of G-protein coupled inwardly rectifying potassium channel 1 (GIRK1) as new prognostic breast cancer biomarker

It has been shown in several studies that potassium channels are involved in tumor development and metastasis. Amongst them, GIRK1 has been found to correlate with lymph node metastasis in breast cancer patients and to be elevated in breast tumors when compared to normal breast tissue. The study of potential new biomarkers for distinct cancer types is crucial for the improvement of patient diagnosis, treatment and outcome.

Therefore, the aim of this project was to study GIRK1 expression levels first in the publicly available data set of The Cancer Genome Atlas (TCGA) to derive important information on expression patterns in different breast cancer subsets; second, to establish methods for the detection of GIRK1 in human formalin-fixed, paraffin-embedded (FFPE) breast cancer tissue; and third, to validate the findings of the TCGA in a well characterized cohort of FFPE breast cancer samples.

Analysis of the TCGA showed a strong correlation between GIRK1 and estrogen receptor (ER) expression levels (p<0.001). Correlation and/or association with other clinical features such as tumor size, lymph node and metastasis status, tumor grade, histology, Her2 status or age at diagnosis were not significant. GIRK1 levels were, despite the strong correlation, variable within the ER positive subgroup and survival analysis showed that ER positive patients with high GIRK1 expression had worse overall survival probabilities than the ones with low GIRK1 levels (HR=1.77 (1.04-3.02); p<0.05). A multivariate analysis showed that GIRK1 was an independent prognostic marker for ER positive breast cancer patients (HR=5.2 (1.3-21.8; p<0.05), being also independent of the PAM50 status. We then established protocols for GIRK1 immunohistochemistry and RNA *in situ* hybridization (ISH), whereby the ISH method was more robust, sensitive and specific and was therefore selected for further use on ER positive patient samples. The results of the validation set confirmed the previous findings, showing again that ER positive patients had both worse disease free (HR=3.1 (1.3-7.6) p<0.01) and overall survival (HR=2.4 (1.2-4.8); p<0.05) probabilities when GIRK1 levels in the tumor were high.

We conclude that GIRK1 might become a prognostic biomarker for ER positive breast cancer and provide a diagnostic tool for the detection of GIRK1 in FFPE tissue (RNA ISH). Further studies will elucidate the molecular mechanisms that lead to GIRK1 upregulation in breast cancer and give insights into involved signaling pathways.

5 Zusammenfassung

Validierung des G-Protein gekoppelten Kaliumkanals GIRK1 als neuen prognostischen Biomarker für Brustkrebs

Mehrere Studien zeigten, dass Kaliumkanäle an der Entstehung und Metastasierung von Tumoren beteiligt sind. Unter anderem wurde berichtet, dass die Expression von GIRK1 mit Lymphknotenmetastasen in Brustkrebspatientinnen korrelierte und dass die GIRK1 Expression in Brusttumoren höher als in normalem Brustgewebe war. Die Untersuchung von neuen potenziellen Biomarkern für verschiedene Krebsarten ist unabdingbar, um Diagnosestellung, Behandlung und Überleben von KrebspatientInnen zu verbessern.

Daher war es das Ziel der vorliegenden Arbeit, erstens die GIRK1 Expression im öffentlich zugänglichen Datenset des TCGA (The Cancer Genome Atlas) zu untersuchen, um Expressionsmuster in verschiedenen Brustkrebsformen zu identifizieren. Zweitens sollten Methoden für die Detektion von GIRK1 in humanem formalinfixierten, paraffin-eingebetteten (FFPE) Brustkrebsgewebe etabliert werden, und drittens war es Ziel, die Ergebnisse der Auswertung des TCGA in einem gut charakterisierten Set von FFPE Brustkrebsproben zu validieren.

Die Analyse des TCGA zeigte eine starke Korrelation (p<0.001) der GIRK1 Expression mit der des Östrogenrezeptors (ER). Es gab keine signifikante Korrelation und/oder Assoziation mit anderen klinischen Eigenschaften, wie z.B. Tumorgröße, Lymphknoten- oder Metastasenstatus, Tumorgrad, Histologie, Her2 Status oder Alter bei Diagnose. Trotz der starken Korrelation waren die GIRK1 Expressionswerte innerhalb der ER-positiven Patientinnen sehr variabel und Überlebensanalysen zeigten, dass ER-positive Patientinnen mit hoher GIRK1 Expression eine schlechtere Gesamtüberlebenswahrscheinlichkeit hatten als jene mit niedrigen GIRK1 Werten (HR=1.77 (1.04-3.02); p<0.05). Eine Multivariatanalyse zeigte außerdem, dass GIRK1 einen unabhängigen prognostischen Marker für ER-positive Patientinnen darstellt (HR=5.2 (1.3-21.8; p<0.05), interessanterweise auch unabhängig vom PAM50 Status. Weiters haben wir Protokolle für GIRK1 Immunhistochemie und RNA in-situ Hybridisierung (ISH) etabliert, wobei die ISH Methode robuster, sensitiver und spezifischer war und deshalb für die Analyse von ER-positive Patientinnenproben verwendet wurde. Die Ergebnisse dieses Validierungssets bestätigten die vorherigen Befunde und zeigten wiederum, dass ER-positive Patientinnen eine schlechtere krankheitsfreie Überlebenswahrscheinlichkeit (HR=3.1 (1.3-7.6) p<0.01) als auch Gesamtüberlebenswahrscheinlichkeit (HR=2.4 (1.2-4.8); p<0.05) hatten, wenn die GIRK1 Expression hoch war.

Wir schließen, dass in Zukunft GIRK1 als prognostischer Biomarker für ER-positiven Brustkrebs Verwendung finden könnte und liefern eine diagnostische Methode zum Nachweis von GIRK1 in FFPE Gewebe (RNA ISH). Zukünftige Studien werden die molekularen Mechanismen beleuchten, die zur Hochregulierung von GIRK1 in Brustkrebs führen und Einblicke in die darin involvierten Signalwege liefern.

6 Introduction

Breast cancer is the most common cancer among women worldwide and, after lung cancer, the second most common cancer type overall. It still has a high mortality rate despite dramatic improvements in diagnosis and treatment of this disease (1-4). At present, several promising multi-gene signatures which include dozens of genes are available to determine the aggressiveness of a tumor and to shed light on the heterogeneity and constitution of an individual tumor. However, single specific molecules are often more effective markers to decide on treatment options (5-7). Such markers for breast cancer include the estrogen receptor (ER), progesterone receptor (PR) and the human epidermal growth factor receptor 2 (Her2). In order to improve patient care and to select the right treatment for each individual patient, it is required to investigate the potential use of other molecules as prognostic or predictive biomarkers for breast cancer in addition to ER, PR and Her2, since patient outcomes are still unsatisfactory (8-10).

Recent publications have shown that G-protein coupled receptors (GPCR), but also tyrosine kinase and phosphatase receptors, belong to the most promising families of putative therapeutic targets and prognostic markers in cancer (3,11-13). GPCRs and their effectors are involved in in a large number of physiological functions, including hormone release, immune responses, cardiac muscle contraction, neurotransmission and blood pressure regulation, to name just a few of their functions. Their dysfunction or deregulation contributes to several human diseases including cancer (12,14-17).

In this study, we focused on G-protein coupled inward rectifier potassium channel 1 (GIRK1, encoded by the *KCNJ3* gene; synonyms: KGA, Kir3.1) and its use as prognostic marker in breast cancer. Four GIRK subunits (GIRK1-4) exist in humans and they form homo- or hetero-tetrameric ion channels within the plasma membrane (18). GIRKs are downstream effectors of many GPCRs and are involved in the regulation of the electrical transmembrane potential by influencing potassium flow through the plasma membrane. Thereby, they contribute to the regulation of cellular excitability and physiological roles include functions such as blood platelet aggregation, heartbeat, memory and learning functions, reward mechanisms, insulin secretion and lipid metabolism (18-23).

There are numerous reports in the literature about abnormal expression of ion channels in cancerous tissue (see (24) and (25) for review). It is well established that cell adhesion, proliferation, cell migration and also oncogenic potential and metastasation depend on potassium permeability and potassium channel activity (26-32). Several lines of evidence indicate that GIRKs might play a role in tumorigenesis and tumor growth: mutated GIRK4, encoded by the *KCNJ9* gene, was linked to benign adenomas of the adrenal cortex with

aldosteronism and severe hypertension as consequence (33,34). Further, up-regulation of GIRK1 mRNA and protein in pancreatic adenocarcinomas (35) and non-small cell lung cancer (36) was reported. Importantly, increased GIRK1 expression levels were shown to be correlated with breast cancer progression and patient´s prognosis: Stringer et al. (37) demonstrated that GIRK1 mRNA is highly overexpressed (up to 700 fold) in primary invasive breast cancer samples when compared to normal tissue. This upregulation correlated positively with occurrence and number of lymph node metastases. A second study by Brevet et al. (38) showed stronger immunohistochemical GIRK1 staining in breast cancer samples when compared to normal breast tissue. Studies on the MCF-7 breast cancer cell line revealed increased mRNA levels of GIRK1 as well as the expression of short GIRK1 splice variants (39). A possible functional role of GIRK1 expression in breast cancer was shown by Rezania et al. (40): stable overexpression of GIRK1 in MCF-7 cells led to increased invasiveness, motility, velocity and angiogenesis in vitro assays.

See also: "KCNJ3 is a new independent prognostic marker for estrogen receptor positive breast cancer patients" by Kammerer et al; manuscript submitted to Oncotarget.

7 Aim of the Study

Based on the findings mentioned above, it seemed worthwhile to study the use of GIRK1 as prognostic breast cancer biomarker in a clinical setting. Validation of GIRK1 expression status in larger breast cancer patient cohorts has not been performed to date. Therefore, we aimed to study GIRK1 expression levels in invasive breast cancer tissue samples and to validate it as new prognostic breast cancer biomarker. The following steps were taken to achieve this goal:

- Data analysis of the large breast cancer cohort of the TCGA:
    - comparison of GIRK1 expression levels between breast tumors and corresponding normal breast tissue
    - analysis of GIRK1 expression in clinically relevant breast cancer subsets (i.e. regarding pTNM staging, grading, age at diagnosis, histology as well as ER, PR and Her2 expression status)
    - correlation analysis and hierarchical cluster analysis to study the genes co-regulated with GIRK1
    - overall survival analysis of patients with high versus low GIRK1 expression

- Validation of the findings of the TCGA using a well characterized patient cohort:
    - analysis of GIRK1 expression in clinically relevant breast cancer subsets
    - correlation analysis to study the genes co-regulated with GIRK1
    - establishment of methods for the detection of GIRK1 on formalin-fixed, paraffin-embedded (FFPE) tissue samples
    - staining of FFPE patient samples for GIRK1
    - overall and disease free survival analysis of patients with high versus low GIRK1 expression

8 Materials and Methods

8.1 Gene expression data from The Cancer Genome Atlas (TCGA)

The gene expression levels (as RNA Seq V2 RSEM values) of GIRK1 of 950 invasive breast carcinoma samples freely available from the TCGA were downloaded from the cBioPortal for Cancer Genomics (www.cbioportal.org (41,42)) on August 4, 2013 by Armin Sokolowsky (diploma student at the Institute of Biophysics). The gene expression data were generated by using the Illumina HiSeq 2000 RNA Sequencing platform at the TCGA Genome Characterization Center of the University of North Carolina, USA (43). The corresponding clinical data of each patient were downloaded from the University of California Santa Cruz (UCSC) Cancer Genomics Browser (https://genome-cancer.ucsc.edu), also on August 4, 2013. In addition, mRNA expression levels (also as RNA Seq V2 RSEM) of 105 healthy tissue samples corresponding to 105 of the patient samples mentioned above were downloaded as individual data files from the TCGA Data Portal (https://tcga-data.nci.nih.gov). The mRNA data and the clinical data were imported into a Microsoft Excel sheet and combined to one data file containing all the relevant information. Male patients (n=9) and patients without gene expression data for GIRK1 (n=36) were excluded for further analysis (remaining n=905). Patient characteristics are summarized in Table 1. The Excel file was imported into a SigmaPlot/SigmaStat worksheet for statistical analysis and a text file was generated for the use in *R* (see “statistical analysis” section for details). *See also: “KCNJ3 is a new independent prognostic marker for estrogen receptor positive breast cancer patients” by Kammerer et al; manuscript submitted to Oncotarget.*

8.2 Cell lines and culture conditions

Lysates of cell lines were used on western blots to test five different anti-GIRK1 antibodies. Several positive and negative controls were used as described below:

a) Native or GIRK1-transfected *Xenopus (X.) laevis* oocytes
b) The HL-1 cell line, derived from mouse atrium (positive control)
c) The human embryonic kidney cell line HEK-293 (negative control)
d) The Michigan Cancer Foundation (MCF)-7 breast cancer cell line (wild type and overexpressing GIRK1 variants or vector control)

The HEK-293 and the MCF-7 cell lines were purchased from the American Type Culture Collection (ATCC®, Manassas, VA, USA), the HL-1 cell line from William C. Claycomb. Cells

Table 1: Patient characteristics of the TCGA set.

Characteristic	Number	%
Age at diagnosis (years)		
≤50	241	26.6
>50	552	61.0
NA	112	12.4
mean	58	
SD	13	
Status		
alive/lost for follow-up	726	80.2
deceased	98	10.8
NA	81	9.0
Follow-up time (months)		
mean	32	
SD	35	
Lymph node status		
negative	417	46.1
positive	450	49.7
NA	38	4.2
Metastasis status		
negative	782	86.4
positive	15	1.7
NA	108	11.9
T stage		
pT1	235	26.0
pT2	509	56.2
pT3	102	11.3
pT4	33	3.6
NA	26	2.9
Grade		
1	150	16.6
2	505	55.8
3	194	21.4
4	15	1.7
NA	41	4.5
ER status		
negative	194	21.4
positive	647	71.5
NA	64	7.1
PR status		
negative	277	30.6
positive	561	62.0
NA	67	7.4
Her2 status		
negative	635	70.2
positive	107	11.8
NA	163	18.0
PAM50 classification		
luminal A	228	25.2
luminal B	121	13.4
Her2-enriched	57	6.3
basal-like	96	10.6
normal-like	7	0.8
NA	396	43.6

NA: not available; SD: standard deviation

were cultured in corresponding culture media as recommended by ATCC® and as summarized in Table 2. Fetal calf serum (FCS) and G418 were purchased from PAA (Linz, Austria). Fetal bovine serum for HL-1 cells, penicillin/streptomycin (100 U/ml and 100 ng/ml), norepinephrine, cholera toxin, and L-glutamine were purchased from Sigma-Aldrich (St. Louis, MO, USA). The SingleQuots for MCF-10A medium were purchased from Lonza (Basel, Switzerland) and were added to the medium to a final concentration of 13 mg/ml bovine pituitary extract (BPE), 0.5 mg/ml hydrocortisone, 10 µg/ml human epidermal growth factor (hEGF) and 5 mg/ml insulin.

Stable transfections of GIRK1 variants and vector controls were performed by Astrid Gorischek and Simin Rezania (both Institute of Biophysics, Medical University of Graz) as described in Simin Rezania's thesis (planned publication date: autumn 2016). The *X. laevis* oocytes were harvested, prepared and transfected by Astrid Gorischek (Institute of Biophysics, Medical University of Graz) as described previously (39,44).

The cells were kept in a humidified atmosphere at 37 °C and 5% CO_2 The culture medium was refreshed every two to three days and cells were split at 80% confluence using 0.25% (or 0.05% for HL-1 cells) trypsin/EDTA (Sigma-Aldrich, St. Louis, MO, USA). Regular mycoplasma tests were negative. *See also: "KCNJ3 is a new independent prognostic marker for estrogen receptor positive breast cancer patients" by Kammerer et al; manuscript submitted to Oncotarget.*

Table 2: Cell culture media.

Cell line	Medium	Supplier	Additives
HEK-293	DMEMhG	Sigma-Aldrich, St. Louis, MO, USA	10% FCS, 1% Pen/Strep
HL-1	Claycomb	Sigma-Aldrich, St. Louis, MO, USA	10% FBS, 1% Pen/Strep, 0.1 mM NE, 2 mM L-glut
MCF-7^{wt}	MEM	Gibco, Vienna, Austria	10% FCS, 1% Pen/Strep
MCF-7^{T}	MEM	Gibco, Vienna, Austria	10% FCS, 1% Pen/Strep, 3 µl/ml G418
MCF-10A^{wt}	MEBM	Lonza, Basel, Switzerland	SingleQuots, 100 ng/ml cholera toxin, 1% Pen/Strep
MCF-10A^{T}	MEBM	Lonza, Basel, Switzerland	SingleQuots, 100 ng/ml cholera toxin, 1% Pen/Strep, 0.5 µl/ml G418

wt: wild type; T: transfected; DMEMhG: Dulbecco's Modified Eagle Medium high Glucose; MEM: Minimum Essential Media; MEBM: Mammary Epithelial Basal Medium; FBS: Fetal Bovine Serum; FCS: Fetal Calf Serum; Pen/Strep: Penicillin and Streptomycin; NE: Norepinephrine, L-glut: L-glutamine

8.3 Cell lysis and protein estimation

Cells were collected by centrifugation (500 rcf, 4 °C, 5 minutes), washed in ice cold PBS (phosphate-buffered saline), pelleted and stored at -20 °C until use. The cell pellets or *X. laevis* oocytes were lysed with 100 to 400 µl RIPA (radio immunoprecipitation assay) buffer (Thermo Scientific, Waltham, MA, USA; volume depending on pellet size) containing a protease inhibitor cocktail (PIC, Sigma-Aldrich, St. Louis, MO, USA), incubated for 20 minutes on ice and vortexed. The lysates were sonicated (2 cycles, 10 seconds on and 30 seconds off, amplitude 20%) on ice and centrifuged in a pre-cooled Eppendorf centrifuge (13000 rpm, 4 °C, 20 minutes) to remove the debris. The supernatant was collected, aliquoted and stored at -20 °C until use. Protein concentrations of the lysates were estimated using the BCA (bicinchoninic acid) protein assay kit (Thermo Scientific, Waltham, MA, USA) according to manufacturer's instructions. Briefly, a BSA (bovine serum albumin) standard ranging from 25 to 2000 µg/ml was prepared. Twenty-five µl of either standard solutions or samples diluted 1:10 were pipetted in triplicate in a 96-well plate and 200 µl of the BCA working solution were added to each well. The plate was shaken for 30 seconds and incubated at 37 °C for 30 minutes. The absorbance at 560 nm was measured using a plate reader. After the generation of the calibration curve and the corresponding formula, the protein concentrations of the samples could be calculated. *See also "Critical evaluation of KCNJ3 gene product detection in human breast cancer: mRNA in situ hybridization is superior to immunohistochemistry" by Kammerer et al.; accepted for publication in the Journal of Clinical Pathology.*

8.4 Western blots

Table 3 summarizes the anti-GIRK1 antibodies that were tested to determine the product with the highest specificity and also describes the dilutions which were used. In general, the cell lysates were diluted to the desired protein concentration with RIPA buffer, mixed 1:5 with 5x Laemmli sample buffer (LSB) containing 10% SDS (sodium dodecyl sulfate; from Promega, Mannheim, Germany), 300 mM Tris-HCl (pH 6.8), 25% glycerol (Sigma-Aldrich, St. Louis, MO, USA), traces of bromophenol blue (Merck, Darmstadt, Germany) and 5% β-mercaptoethanol (Sigma-Aldrich, St. Louis, MO, USA). The samples were heat-denatured at 95 °C for 5 minutes and subjected to sodium dodecyl sulfate-polyacrylamide gel electrophoresis (SDS-PAGE; 8% gels) together with a protein marker (PageRuler Prestained Protein Ladder, Thermo Scientific, Waltham, MA, USA). Gels were run at 80 V for 20 minutes (stacking gel) and then at 120 V (separation gel). After 1.5 hours electro transfer (150 mA, on ice) on a nitrocellulose membrane (GE Healthcare, Pittsburgh, PA,

USA), the membranes were stained with Ponceau S solution (Sigma-Aldrich, St. Louis, MO, USA) to check the protein transfer. Membranes were blocked with PBST (PBS with 0.05% Tween from Merck, Darmstadt, Germany) containing 5% non-fat dry milk (Bio-Rad, Hercules, CA, USA) for 1 hour at room temperature on a shaker. The membranes were washed with PBST and incubated with the primary antibody diluted in PBST containing 1% non-fat dry milk over night at 4 °C on a shaker (see Table 3 for antibody dilutions). The membranes were washed 3 times for 10 minutes with PBST before incubation with the secondary antibody (1 hour at room temperature on a shaker). As secondary antibodies sheep anti-rabbit/HRP (horseradish peroxidase), sheep anti-mouse/HRP (both kindly provided by Amir Zarnani, Teheran, Iran; both diluted 1:10000) or donkey anti-goat/HRP (Santa Cruz Biotechnology, Dallas, TX, USA; diluted 1:5000) were used in PBST containing 1% non-fat dry milk. The membranes were washed 3 times for 10 minutes with PBST, incubated for 1 minute with ECL (enhanced chemiluminescence) Select detection solution (GE Healthcare, Pittsburgh, PA, USA) and then exposed to a CCD (charge-coupled device) camera using the ChemiDoc™ MP System (Bio-Rad, Hercules, CA, USA). *See also "Critical evaluation of KCNJ3 gene product detection in human breast cancer: mRNA in situ hybridization is superior to immunohistochemistry" by Kammerer et al.; accepted for publication in the Journal of Clinical Pathology.*

Table 3: Primary anti-GIRK1 antibodies tested on Western Blots.

Product	Supplier	Source	Clonality	Dilution
C-terminal	Kurt Schmidt, Institute of Pharmaceutical Sciences, University of Graz, Austria	rabbit	polyclonal	1:1000
N-terminal	Kurt Schmidt, Institute of Pharmaceutical Sciences, University of Graz, Austria	rabbit	polyclonal	1:650
Sc-16131	Santa Cruz, Dallas, TX, USA	goat	polyclonal	1:200
APC-005	Alomone, Jerusalem, Israel	rabbit	polyclonal	1:200
ALM-031	Alomone, Jerusalem, Israel	mouse	monoclonal	1:200
Ab119246	Abcam, Cambridge, MA, USA	mouse	monoclonal	1:1000

8.5 Patient samples

Formalin-fixed, paraffin-embedded (FFPE) tissue samples of 53 primary invasive breast carcinomas were retrieved from the Biobank of the Medical University of Graz. Two male patient samples were excluded and five more samples were excluded for further analysis after pathological review by Stephan Jahn (Institute of Pathology, Medical University of

Graz) because the samples did not contain invasive tumor cells (remaining n=46). Additional 29 samples were available from the Medical University of Innsbruck. Nine of them were excluded for analysis after pathological review by Stephan Jahn (Institute of Pathology, Medical University of Graz) because they were either lacking invasive tumor cells or not containing primary tumor tissue (remaining n=20). Full clinical and pathological characterization was available for all 66 included patients and gene expression data of an Affymetrix microarray (GEO accession GSE17705; (45)) were available for 65 of 66 samples and were analyzed as described in the "statistical analysis" section. All patients underwent tamoxifen treatment for five years. The characteristics of this patient subset are summarized in Table 4. The use of the patient samples including the clinical data was approved by the ethics committee of the Medical University of Graz (number 24-081 ex 11/12). *See also: "KCNJ3 is a new independent prognostic marker for estrogen receptor positive breast cancer patients" by Kammerer et al; manuscript submitted to Oncotarget.*

8.6 Gene expression data from GEO ID GSE17705

The above mentioned patients were part of a larger set used in a previously conducted multicenter study that included the generation of microarray data of 298 out of 299 breast carcinoma samples, most of them ER positive (45). The normalized gene expression levels thereof were downloaded from the Gene Expression Omnibus (GEO, ID GSE17705). The data were generated and processed using the Affymetrix Human Genome U133A Array platform as described in (45). Briefly, tissue samples were processed by two different laboratories (MD Anderson Cancer Center, Texas, USA and Jules Bordet Institute, Brussels, Belgium; inter-laboratory reliability was assessed). Probe-level intensities were generated with Microarray Suite (MAS) version 5.0, normalized and log2 transformed. Corresponding clinical data were available from the participating study centers, namely from the Medical University of Graz, Austria; the Medical University Innsbruck, Austria; the Institut Gustave Roussy, Villejuif, France; and the Jules Bordet Institute, Brussels, Belgium. Updated patient follow up until December 2014 was only available from the two Austrian centers and detailed clinical data were not available from Brussels. The patient characteristics are summarized in Table 4. The mRNA expression data and the clinical data were imported into a Microsoft Excel sheet and combined to one data file containing all the relevant information. The Excel file was imported into a SigmaPlot/SigmaStat worksheet for statistical analysis and a text file was generated for the use in *R* (see "statistical analysis" section for details). *See also: "KCNJ3 is a new independent prognostic marker for estrogen receptor positive breast cancer patients" by Kammerer et al; manuscript submitted to Oncotarget.*

Table 4: Patient characteristics of the GEO set GSE17705

Characteristic	number (total)	% (total)	number (subset AT)	% (subset AT)
Total patient number	299	100	66	100
Age at diagnosis (years)				
≤50	16	5.4	7	10.6
>50	168	56.2	59	89.4
NA	115	38.5	0	0.0
mean±SD	63±11		64±10	
Status				
alive/lost for follow-up	114	38.1	28	42.4
deceased	70	23.4	38	57.6
NA	115	38.5	0	0.0
Follow-up time (months)				
mean±SD	142±62		157±76	
Lymph node status				
negative	176	58.8	34	51.5
positive	112	37.5	30	45.5
NA	11	3.7	2	3.0
Metastasis status				
negative	228	76.3	66	100.0
positive	71	23.7	0	0.0
T stage				
pT1	37	12.4	27	40.9
pT2	46	15.4	32	48.5
pT3	7	2.3	4	6.1
pT4	4	1.3	3	4.5
NA	205	68.6	0	0.0
Grade				
1	22	7.4	12	18.2
2	52	17.4	36	54.6
3	18	6.0	16	24.2
4	0	0.0	0	0.0
NA	207	69.2	2	3.0
ER status				
negative	13	4.3	0	0.0
positive	286	95.7	66	100.0
PR status				
negative	45	15.0	16	24.2
positive	139	46.5	30	75.8
NA	115	38.5	0	0.0
Her2 status[a]				
negative	29	9.7	0.0	0
positive	13	4.3	0.0	0
NA	257	86.0	66	100
PAM50 classification				
luminal A	68	22.7	0	0.0
luminal B	89	29.8	0	0.0
Her2-enriched	41	13.7	0	0.0
basal-like	31	10.4	0	0.0
normal-like	69	23.1	0	0.0
NA	1	0.3	66	100.0

[a]: Her2 status was not part of routine diagnosis in the early 1990s when most of the patients were first diagnosed. NA: not available; SD: standard deviation; subset AT: subset of patients of the two Austrian centers (Graz and Innsbruck) for which FFPE tissue was available for analysis.

8.7 Immunohistochemistry

Immunohistochemistry (IHC) was performed for GIRK1 and Ki-67, a proliferation marker. Three µm thick sections of FFPE tissue samples were mounted on coated glass slides (Dako, Glostrup, Denmark) by Sylvia Eidenhammer (Institute of Pathology, Medical University of Graz). For GIRK1 IHC, formalin-fixed, agarose-embedded samples of HL-1 and HEK-293 cells, produced at the Institute of Pathology (Medical University of Graz), were mounted on each slide as internal positive and negative control, respectively. Unless otherwise stated, all steps were performed at room temperature.

8.7.1 GIRK1 staining procedure

Slides were incubated at 60 °C for 1 hour or overnight, dewaxed in xylene (Merck, Darmstadt, Germany) and rehydrated in 100%, 90%, 70% and 50% ethanol (Merck, Darmstadt, Germany). Heat-induced epitope retrieval (HIER) was performed by incubating the sections in target retrieval solution pH 9.0 from Dako (Glostrup, Denmark) for 40 minutes in a microwave at 150 W/cuvette. The solution was pre-warmed for 1 min at 900 W before use. After 20 minutes in the microwave, the cuvette was refilled with a. dest. (aqua destillata) in order to compensate for evaporation. The slides were cooled for 20 minutes at room temperature, rinsed in a. dest. and incubated in wash buffer from Dako (Glostrup, Denmark) for 5 minutes to achieve pH equilibration. The tissue area was then circled using a hydrophobic barrier pen (Dako, Glostrup, Denmark) and endogenous peroxidase activity was blocked by incubation with hydrogen peroxide (H_2O_2) for 10 minutes. Slides were washed three times in Dako wash buffer, followed by antibody incubation for 1 hour (mouse monoclonal anti-GIRK1 antibody from Abcam, diluted 1:50 in antibody diluent solution from Dako, Glostrup, Denmark). Slides were washed as above and incubated with the EnVision+ dual link reagent (rabbit/mouse-HRP, from Dako, Glostrup, Denmark). After washing the slides as above, the chromogen diaminobenzidine (DAB; from Dako, Glostrup, Denmark) was allowed to react for 7 minutes while color development was observed under the microscope. The sections were rinsed in Dako wash buffer, then in warm tap water, and counterstained with Meyer's hematoxylin (from the pharmacy of the Medical University of Graz) for 20 seconds. After rinsing the slides in warm tap water for 5 minutes, the sections were dehydrated in 50%, 70%, 90% and 100% ethanol, followed by butyric acetate and cover slips were mounted with Entellan® (all from Merck, Darmstadt, Germany). The slides were scored based on signal intensity by two independent evaluators (Stephan W. Jahn and Thomas Bauernhofer). A score from 0 to 3 was possible, where 0 = negative, 1 = weak, 2 = intermediate and 3 = strong. *See also "Critical evaluation of KCNJ3 gene product*

detection in human breast cancer: mRNA in situ hybridization is superior to immunohistochemistry" by Kammerer et al.; accepted for publication in the Journal of Clinical Pathology.

8.7.2 Ki-67 staining procedure

The Ki-67 IHC was performed in the routine lab by Sylvia Eidenhammer (Institute of Pathology, Medical University of Graz) on a BenchMark automated slide staining platform (Ventana, Tucson, AZ, USA) after incubating the slides for 1 hour at 70 °C. The ready-to-use rabbit monoclonal anti-Ki-67 antibody, the iVIEW DAB detection kit, hematoxylin and bluing agent were all purchased from Ventana (Tucson, AZ, USA) and used according to the standard protocol as described below (in German as downloaded directly from the staining platform software). After finishing the automated staining procedure and rinsing the slides in tap water with dishwashing detergent, the sections were dehydrated in 50%, 70%, 90% and 100% ethanol, followed by butyric acetate, and cover slips were mounted with Entellan®. The slides were scored based on percentage of positive nuclei by two independent evaluators (Stephan W. Jahn and Thomas Bauernhofer). Thus, a score from <5% to 100% was possible.

8.7.3 Ki-67 staining protocol

Protokoll-Nr. 78: Ki-67 (04.04.2013)
Prozedur: U iVIEW DAB (v1.02.0020)
BenchMark ULTRA IHC/ISH Staining Module
LKH Unikliniken Graz, Auenbrugger Platz 25 A-8036 GRAZ

Schritt-N	Protokollschritt
1	Mixer aktivieren
2	Mixer deaktivieren
3	[Temperatur auf 72 °C als Standard einstellen]
4	Objektträger-Temperatur von [72 °C] auf Mittlere Temperaturen (Entparaffinierung) erhöhen
5	Inkubieren für 4 Minuten
6	EZPrep Vol. ausgleichen
7	Objektträger mit EZPrep spülen
8	EZPrep Vol. ausgleichen
9	Coverslip auftragen
10	Objektträger mit EZPrep spülen

11	EZPrep Vol. ausgleichen
12	Coverslip auftragen
13	Objektträger mit EZ Prep spülen
14	Deparaffinierung Vol. ausgleichen
15	Coverslip auftragen
16	Mixer aktivieren
17	Objektträger-Heizung ausschalten
18	Pausenpunkt (Landezone)
19	[Kurz- 8 Minuten Conditioning]
20	Objektträger mit EZ Prep spülen
21	Cell Conditioner Nr. 1 lang auftragen
22	Abgabe von Cell Cond. u. Coverslip lang
23	[Temperatur auf 95 °C als Standard einstellen]
24	Erwärme Objektträger auf [95 °C] und inkubiere für 8 Minuten (Cell Conditioner Nr. 1)
25	Cell Conditioner Nr. 1 auftragen
26	Cell Cond. u. Coverslip auftragen (ohne Barcode Blowoff)
27	Cell Cond. u. Coverslip auftragen (ohne Barcode Blowoff)
28	Cell Conditioner Nr. 1 auftragen
29	Cell Cond. u. Coverslip auftragen (ohne Barcode Blowoff)
30	Objektträger-Heizung ausschalten
31	Inkubieren für 8 Minuten
32	Spülen mit Reaktionspuffer
33	Feineinstellung des Reaktionspuffervolumens
34	Coverslip auftragen
35	Spülen mit Reaktionspuffer
36	Feineinstellung des Reaktionspuffervolumens
37	Coverslip auftragen
38	Pausenpunkt (Landezone)
39	Aufwärmen der Objektträger auf 36 Grad C
40	Spülen mit Reaktionspuffer
41	Feineinstellung des Reaktionspuffervolumens
42	1 Tropfen I-VIEW INHIBITOR auftragen. Coverslip auftragen, und für 4 Minuten inkubieren (ein Tropfen entspricht einer Reagenzienabgabe)
43	Spülen mit Reaktionspuffer
44	Feineinstellung des Reaktionspuffervolumens
45	Coverslip auftragen

46	Aufheizen des Objektträgers bis 36 Grad C, und für 4 Minuten inkubieren
47	Spülen mit Reaktionspuffer
48	Feineinstellung des Reaktionspuffervolumens
49	1 Tropfen von [Ki-67 (30-9)] (Antikörper) auftragen, LCS auftragen u. für [0 Stunden 32 Min] inkubieren
50	Spülen mit Reaktionspuffer
51	Feineinstellung des Reaktionspuffervolumens
52	Coverslip auftragen
53	Aufwärmen der Objektträger auf 36 Grad C
54	Spülen mit Reaktionspuffer
55	Feineinstellung des Reaktionspuffervolumens
56	1 Tropfen I-VIEW BIOTIN Ig auftragen, Coverslip auftragen, und für 8 Minuten inkubieren
57	Spülen mit Reaktionspuffer
58	Feineinstellung des Reaktionspuffervolumens
59	1 Tropfen I-VIEW SA-HRP auftragen, Coverslip auftragen, und für 8 Minuten inkubieren
60	Spülen mit Reaktionspuffer
61	Feineinstellung des Reaktionspuffervolumens
62	Coverslip auftragen
63	Spülen mit Reaktionspuffer
64	Feineinstellung des Reaktionspuffervolumens
65	1 Tropfen I-VIEW DAB und einen Tropfen I-VIEW H2O2 auftragen, LCS auftragen und für 8 Minuten inkubieren
66	Spülen mit Reaktionspuffer
67	Feineinstellung des Reaktionspuffervolumens
68	1 Tropfen I-VIEW COPPER auftragen, Coverslip auftragen, und für 4 Minuten inkubieren
69	Spülen mit Reaktionspuffer
70	Feineinstellung des Reaktionspuffervolumens
71	1 Tropfen [HEMATOXYLIN] (Gegenfärbung) auftragen, LCS auftragen u. für [4 Minuten] inkubieren
72	Spülen mit Reaktionspuffer
73	Feineinstellung des Reaktionspuffervolumens
74	Coverslip auftragen
75	Spülen mit Reaktionspuffer
76	Feineinstellung des Reaktionspuffervolumens

77	1 Tropfen von [BLUING AGENT] (Nach-Gegenfärbung) auftragen, LCS auftragen u. für [4 Minuten] inkubieren
78	Spülen mit Reaktionspuffer
79	Coverslip auftragen
80	Objektträger-Heizung ausschalten
81	Spülen mit Reaktionspuffer

8.8 RNA in-situ hybridization

Of each sample, three 4 µm thick sections of FFPE tissue were mounted on Superfrost Plus coated slides from Thermo Scientific (Waltham, MA, USA). In order to avoid RNA contamination, the microtome was carefully cleaned with RNase Away (Thermo Scientific, Waltham, MA, USA) before and after each new sample. For the same reason, needles were used instead of brushes to handle the sections. Fatty tissue and regions not containing invasive tumor cells were carefully removed from the slide using a scalpel. The slides were processed according to manufacturer's instructions for the RNAscope® 2.0 High Definition - BROWN kit (from ACD, Hayward, CA, USA; see section below for the detailed protocol and Figure 1 for an overview). Briefly, the slides were incubated at 60 °C for 1 hour and then pretreated as described. Three sections of each sample were used and stained with the following probes:

a) Negative control: DapB (bacterial dihydrodipicolinate reductase)
b) Positive control: POLR2A (DNA-directed RNA polymerase II subunit RPB1)
c) GIRK1: probe designed by ACD in order to detect GIRK1a and GIRK1d variants

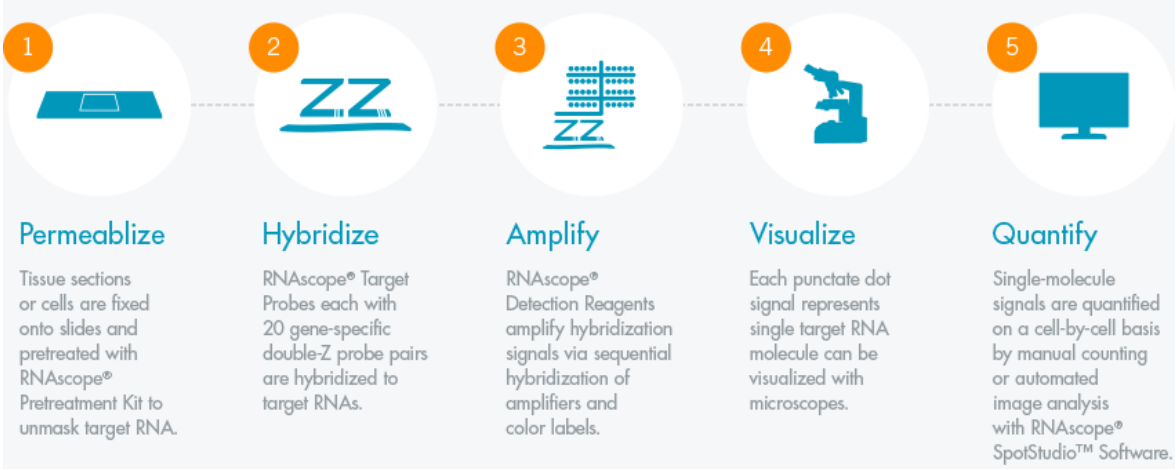

Figure 1: RNAscope in situ hybridization workflow.

Downloaded from http://www.acdbio.com/.

Probes were incubated for 2 hours at 40 °C and then, a total of six amplification steps, followed by the signal detection with DAB were performed as described. Slides were counterstained with 50% hematoxylin and dehydrated, and cover slips were mounted. All incubation steps requiring 40 °C were performed using the HybEZ oven with the humidity control tray from ACD (Hayward, CA, USA).

8.8.1 RNA-ISH protocol

The following “Quick Guide for FFPE Tissues” (Catalogue Number 320498) for the RNAscope® 2.0 HD Detection Kit (BROWN) was downloaded from http://www.acdbio.com/.

Introduction

This quick guide is intended for advanced users who are familiar with the procedures in the Sample Preparation Pre-treatment Guide for Formalin-Fixed Paraffin-Embedded (FFPE), see Catalogue No. 320511 and RNAscope® 2.0 HD Detection Kit (BROWN) User Manual Part 2 (Catalogue No. 320497). Refer to the user manual for safety guidelines. For every chemical, read the Material Safety Data Sheet (MSDS) and follow handling instructions. Wear appropriate protective eyewear, clothing, and gloves. For the latest services and support information, go to: www.acdbio.com/support.

Part 1: Prepare and Pre-treat Samples

PREPARE FFPE SECTIONS:

1. Immediately place dissected tissue sample in fresh 10% NBF for 16–32 HRS at ROOM TEMPERATURE (RT).
2. Dehydrate, embed in paraffin, and cut sample into 5 +/- 1 µm sections. Mount sections on Superfrost® Plus slides.

OPTIONAL STOPPING POINT (1). Use sectioned tissue within 3 months. Store sections with desiccants at RT.

PREPARE SLIDES:

Bake Slides:

1. Bake slides in a dry oven for 1 HR at 60°C.

OPTIONAL STOPPING POINT (2). Use sectioned tissue within 1 week. Store sections with desiccants at RT.

Deparaffinise FFPE Sections:

2. In a fume hood:
    - Fill two Tissue-Tek® Clearing Agent dishes with ~200 mL fresh xylene.
    - Fill two Tissue-Tek® Staining dishes with ~200 mL fresh 100% EtOH.
3. Place slides in a Tissue-Tek® Slide Rack in xylene 2 x 5 MIN.
4. Incubate slides in 100% EtOH 2 x 1 MIN.
5. Remove slides from rack. Air dry slides for 5 MIN at RT.

OPTIONAL STOPPING POINT (3). Air dry overnight at RT (must use within 24 hrs) or proceed directly to the next step.

PRETREAT SAMPLES:

Prepare Oven and Reagents (30 MIN at 40°C):

1. Set HybEZ™ oven to 40°C and warm HybEZ™ Humidity Control Tray containing wet Humidifying Paper for 30 MIN before use. Keep tray warm during assay.
2. Prepare 700 mL fresh 1X Pre-treat 2 in a beaker. Cover with foil, bring to a mild boil, and maintain. Do not boil more than 30 MIN before use.

Apply Pre-treat 1 (10 MIN at RT):

1. Add ~5–8 drops of Pre-treat 1 to each section for 10 MIN at RT.
2. Place slides into a Tissue-Tek® Slide Rack submerged in distilled water.
3. Wash slides in the distilled water by moving the rack up and down 3–5 times and repeat with fresh distilled water.

Apply Pre-treat 2:

1. With a pair of forceps very slowly submerge the slide rack into boiling 1X Pre-treat 2 solution. Refer to Appendix A of the Part 1, Sample Preparation and Pre-treatment

Guide (Cat. No. 320511) for FFPE Tissue for specific pre-treatment time, depending on your tissue type.

2. Immediately transfer hot slide rack to a Staining Dish containing distilled water.
3. Wash slides in the distilled water by moving the rack up and down 3–5 times and repeat with fresh distilled water.
4. Wash slides in fresh 100% EtOH by moving the rack up and down 3–5 times, and air dry.

Create Barrier:

1. Draw 2–4 times around tissue using the Immedge™ hydrophobic barrier pen. Dry completely ~2 MIN or OVERNIGHT at RT.

Apply Pre-treat 3:

1. Remove excess liquid from slides, place in the HybEZ™ Slide Rack, and add ~5 Drops of Pre-treat 3 to each section.
2. Place the HybEZ™ Slide Rack in the prewarmed HybEZ™ Humidity Control Tray. Seal tray and insert back into the HybEZ™ Oven. Incubate at 40°C for 30 MIN.

Note: If needed, prepare RNAscope® 2.0 assay materials during this step.

3. Wash slides in the distilled water by moving the rack up and down 3–5 times and repeat with fresh distilled water.

Part 2: RNAscope® 2.0 Assay

PREPARE THE MATERIALS:

1. Prepare 3 L of 1X WASH BUFFER by adding 2.94 L distilled water and 1 bottle (60 mL) of 50X Wash Buffer to a large carboy. Mix well.
2. Prepare 50% HEMATOXYLIN and 0.02% AMMONIA WATER.
3. Prepare dehydrating reagents: 200 mL XYLENE in a Clearing Agent Dish, 2 x 200 mL 100% ETOH and 200 mL 70% ETOH in Staining Dishes.
4. Equilibrate reagents and equipment:
    - Place AMP 1–6 at RT.
    - Warm probes for 10 MIN at 40°C and cool to RT.

RUN THE ASSAY:

Hybridize Probe (2 HRS at 40°C):

1. Remove excess liquid from slides, place in the HybEZ™ Slide Rack, and add ~4 drops probe to each section.
2. Insert sealed tray containing HybEZ™ Slide Rack back into the HybEZ™ Oven for 2 HRS at 40°C. Remove slide rack.
3. Wash slides in 1X Wash Buffer for 2 MIN at RT. Repeat with fresh 1X Wash Buffer.

Hybridize Amp 1 (30 MIN at 40°C):

1. Remove excess liquid from slides, place in the HybEZ™ Slide Rack, and add ~4 drops AMP 1 to each section.
2. Insert sealed tray containing HybEZ™ Slide Rack into the HybEZ™ Oven for 30 MIN at 40°C. Remove slide rack.
3. Wash slides in 1X Wash Buffer for 2 MIN at RT. Repeat with fresh 1X Wash Buffer.

Hybridize Amp 2 (15 MIN at 40°C):

1. Remove excess liquid from slides, place in the HybEZ™ Slide Rack, and add ~4 drops AMP 2 to each section.
2. Insert sealed tray containing HybEZ™ Slide Rack into the HybEZ™ Oven for 15 MIN at 40°C. Remove slide rack.
3. Wash slides in 1X Wash Buffer for 2 MIN at RT. Repeat with fresh buffer.

Hybridize Amp 3 (30 MIN at 40°C):

1. Remove excess liquid from slides, place in the HybEZ™ Slide Rack, and add ~4 drops AMP 3 to each section.
2. Insert sealed tray containing HybEZ™ Slide Rack into the HybEZ™ Oven for 30 MIN at 40°C. Remove slide rack.
3. Wash slides in 1X Wash Buffer for 2 MIN at RT. Repeat with fresh buffer.

Hybridize Amp 4 (15 MIN at 40°C):

1. Remove excess liquid from slides, place in the HybEZ™ Slide Rack, and add ~4 drops AMP 4 to each section.
2. Insert sealed tray containing HybEZ™ Slide Rack into the HybEZ™ Oven for 15 MIN at 40°C. Remove slide rack, but do not place tray back into the oven.
3. Wash slides in 1X Wash Buffer for 2 MIN at RT. Repeat with fresh buffer.

Hybridize Amp 5 (30 MIN at RT):

1. Remove excess liquid from slides, place in the HybEZ™ Slide Rack, and add ~4 drops AMP 5 to each section.
2. Incubate sealed tray containing HybEZ™ Slide Rack for 30 MIN at RT.
3. Wash slides in 1X Wash Buffer for 2 MIN at RT. Repeat with fresh buffer.

Hybridize Amp 6 (15 MIN at RT):

1. Remove excess liquid from slides, place in the HybEZ™ Slide Rack, and add ~4 drops AMP 6 to each section.
2. Incubate sealed tray containing HybEZ™ Slide Rack for 15 MIN at RT.
3. Wash slides in 1X Wash Buffer for 2 MIN at RT. Repeat with fresh buffer.

Detect the Signal (10 MIN at RT):

1. Mix equal volumes of BROWN-A and BROWN-B.
2. Remove excess liquid from slides, place in the HybEZ™ Slide Rack, and pipette ~120 µL of DAB onto each tissue section.
3. Incubate sealed tray containing HybEZ™ Slide Rack for 10 MIN at RT.
4. Remove DAB from slides and wash 3–5 times in distilled water.

Counterstain the Slides (2 MIN at RT):

1. Place slides in 50% Hematoxylin I for 2 MIN at RT. Wash 3–5 times in distilled water and repeat with fresh distilled water.
2. Wash slides 10 SEC in 0.02% ammonia water, and then wash 3–5 times in distilled water.

Mount the Slides:

1. Incubate slides in 70% EtOH for 2 MIN with occasional agitation.
2. Incubate slides in 100% EtOH for 2 MIN with occasional agitation. Repeat with fresh EtOH.
3. Incubate slides in xylene for 5 MIN with occasional agitation.
4. Add 1–2 drops of cytoseal and place coverslip over section and air dry.

EVALUATE THE RESULTS

Examine tissue sections under a standard bright field microscope at 20–40X magnification.

8.8.2 RNA ISH evaluation

Ten z-stacks of a representative region of each slide were photographed at 40x magnification by Amin El-Heliebi (Institute of Cell Biology, Histology and Embryology, Medical University of Graz) using a Zeiss Observer.Z1 inverted microscope (Zeiss, Jena, Germany). Multiple single adjacent images (3 x 3 tiles) were acquired and aligned using the MosaiX module of the AxioVision software (Zeiss, Jena Germany). Each assembled image covered an estimated area of 0.62 x 0.45 mm. Files were converted to the TIF file format

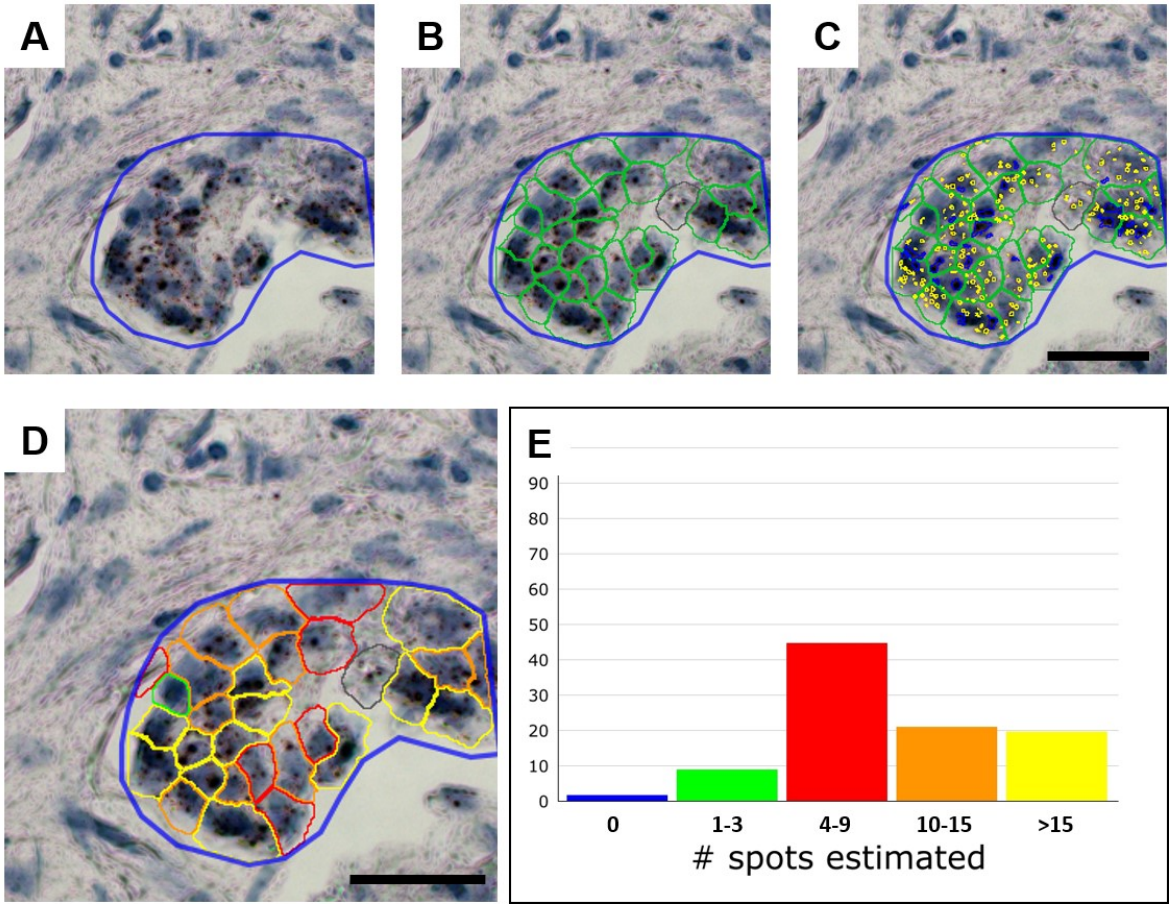

Figure 2: Detail of digital image analysis of RNA in situ hybridization.

Single steps during image analysis include **A.** definition of the area of interest (blue), **B.** detection of single cells (green) and **C.** detection of single spots (yellow) and clusters (blue). **D.** Graphical visualization of results. Colours correspond to the bars in E, grey cells were excluded for analysis by manual quality control. **E.** Bar graph of final results.

The average number of spots estimated for this sample was 10.11. Scale bar: 25 µm in all images.

Figure taken from: "Critical evaluation of KCNJ3 gene product detection in human breast cancer: mRNA in situ hybridization is superior to immunohistochemistry" by Kammerer et al.; accepted for publication in the Journal of Clinical Pathology.

and image sequences were imported into ImageJ, a freely available image processing and analysis software (http://imagej.nih.gov/ij/). Image sequences were stacked using the minimal intensity projection type and then used for analysis and determination of average numbers of spots per cell with the SpotStudio software from ACD (Hayward, CA, USA). An example on how image analysis was performed is given in Figure 2. Samples were excluded from final scoring if the negative control was positive (on average more than 0.5 spots/cell) or the positive control was negative (on average less than 2.5 spots/cell). *See also "Critical evaluation of KCNJ3 gene product detection in human breast cancer: mRNA in situ hybridization is superior to immunohistochemistry" by Kammerer et al.; accepted for publication in the Journal of Clinical Pathology.*

8.9 Statistical analyses

Statistical analyses were performed using the SigmaPlot/SigmaStat v12.5 software (Systat Software Inc., San Jose, CA, USA) and *R* (www.r-project.org). The Shapiro-Wilk test showed that the populations were not normally distributed. The Mann-Whitney rank sum test and the Kruskal-Wallis one-way analysis of variance on ranks test were used to test differences in gene expression levels between two or more groups, respectively. The Kruskal Wallis test was followed by all pairwise multiple comparison procedures (Dunn's Method). The Wilcoxon signed rank test was used for paired samples. Spearman rank correlation, association and Cox proportional hazard analysis were performed in *R*, while SigmaPlot/SigmaStat was used for the generation of scatter plots. Genesis 1.7.6 (by Alexander Sturm and Rene Snajder, Institute for Genomics and Bioinformatics, Graz University of Technology) was used for mean centring of data, calculation of Euclidean distance and hierarchical cluster analysis. The online tool DAVID (http://david.abcc.ncifcrf.gov/) was used for functional annotations of genes to gene ontology (GO) terms and pathways. For overall and disease free survival analysis including the calculation of the corresponding long rank *p*-values and the hazard ratios, an *R* code with an auto-cut-off option adapted from Györffy et al. (46) was used. All results were considered as statistically significant when $p<0.05$. All *R* codes used are provided in the following sections. *See also "Critical evaluation of KCNJ3 gene product detection in human breast cancer: mRNA in situ hybridization is superior to immunohistochemistry" by Kammerer et al.; accepted for publication in the Journal of Clinical Pathology; and "KCNJ3 is a new independent prognostic marker for estrogen receptor positive breast cancer patients" by Kammerer et al; manuscript submitted to Oncotarget.*

8.10 *R* codes

This section includes the *R* codes used for different statistical and bioinformatical analysis. Unless otherwise stated, the codes were generated in collaboration with Hubert Hackl (Division of Bioinformatics, Innsbruck Medical University). Comments after the hashtags serve for additional information and explanation and are not functional parts of the code.

8.10.1 Correlation analysis

```
set.seed(123)

GENLIST<-c("gene1", "gene2")        # define genes of interest here

unlink("correlation.txt")
EXPR<-read.table("file_name.txt", header=TRUE, sep="\t", dec = ".",
check.names=FALSE)            # define table name
rowl<-length(EXPR[2,])
M1<-as.matrix(EXPR[,2:rowl])
M<-log2(M1+1)                       # log2 transformation of expression
values
G<-as.vector(EXPR$row_title)        # enter the title of the row
                                    # containing the gene names here

G1<-c()
G2<-c()
COR1<-c()
P1<-c()
COR2<-c()
P2<-c()
COR3<-c()
P3<-c()
Z<-c()
pvalue<-c()
ZP<-c()
VP<-c()
pvalueP<-c()
i<-1
GEN1<-c("gene1")                    # re-enter the name of gene1 here
IND1<-which(G==GEN1)
X<-M1[IND1,]
CUTOFF<-c(1.5)                      # enter the desired cut-off for the
                                    # bootstrap and permutation functions
GL_IND<-which(X<CUTOFF)
LGL<-length(GL_IND)
GH_IND<-which(X=CUTOFF)
LGH<-length(GH_IND)
co1<-c()

      for (GEN2 in G) {
            IND2<-which(G==GEN2)[1]
            Y<-M1[IND2,]
            MX<-mean(Y[GL_IND])
            Yvec<-c()

            # bootstrap function starts here
            for (j in 1:1000) {
```

```
            co<-sample(GH_IND,LGL, replace=TRUE)
            GH_B<-Y[co]
            Yvec[j]<-MX-mean(GH_B)
      }
      ME<-mean(Yvec)
      SD<-sd(Yvec)
      if (SD<0.0000000000001) {
            Z[i]=NA
            pvalue[i]=NA
      } else {
            Z[i]<-(-ME/SD)
            pvalue[i]<-2*pnorm(-abs(Z[i]))
      }
      YPvec<-c()
      GLPV<-mean(Y[GL_IND])
      GHPV<-mean(Y[GH_IND])
      VP[i]<-GHPV-GLPV

      # permutation function starts here
      for (j in 1:1000) {
            co1<-sample(1:length(X), replace=FALSE)
            YP<-Y[co1]
            GLP<-mean(YP[GL_IND])
            GHP<-mean(YP[GH_IND])
            YPvec[j]<-GHP-GLP
      }
      MEP<-mean(YPvec)
      SDP<-sd(YPvec)
      if (SDP<0.0000000000001) {
            ZP[i]=NA
            pvalueP[i]=NA
      } else {
            ZP[i]<-((VP[i]-MEP)/SDP)
            pvalueP[i]<-2*pnorm(-abs(ZP[i]))
      }



      res1<-cor.test(X,Y,method = "pearson")
      res2<-cor.test(X,Y,method = "spearman")
      res3<-cor.test(X,Y,method = "kendall")
      G1[i]<-GEN1
      G2[i]<-GEN2
      COR1[i]<-res1$estimate
      P1[i]<-res1$p.value
      COR2[i]<-res2$estimate
      P2[i]<-res2$p.value
      COR3[i]<-res3$estimate
      P3[i]<-res3$p.value
      i<-i+1
}

DF<-data.frame(G1,G2,COR1,P1, COR2,P2,COR3,P3,Z,pvalue,VP, ZP,pvalueP)
write.table(DF, file="new_file_name.txt", sep="\t", quote=FALSE,
row.names=FALSE)                    # define the desired file name here
```

8.10.2 Association analysis

```
library(ltm)

S<-read.table("file_name.txt", header=TRUE, sep="\t", dec = ".",
check.names=FALSE)                    # read table with clinical
                                      # information, all information must
                                      # be numerical

AGE<-as.vector(S$AGE)                 # all titles in this section must
S1<-as.vector(S$SAMPLE)               # correspond to the row titles of
MET<-as.vector(S$M)                   # the table
LN<-as.vector(S$N)
T<-as.vector(S$T)
ST<-as.vector(S$Stage)
ER<-as.vector(S$ER)
PR<-as.vector(S$PR)
HER2<-as.vector(S$HER2)
PAM50<-as.factor(S$PAM50)

CL<-read.table("file_name.txt", header=TRUE, sep="\t", dec = ".",
check.names=FALSE)                    # read normalized gene expression
                                      # from table

TCG<-as.vector(CL[,1])
index<-which(TCG=="gene_name")        # enter gene of interest here
GI<-CL[index,2:length(CL[1,])]
GIR<-as.numeric(CL[index,2:length(CL[1,])])
GIR1<-log2(GIR+1)
GIN<-names(GI)
id<-new.env(hash=TRUE)
for (i in 1:length(GIN)) {
      id[[GIN[i]]] <- GIR1[i]
}
GIE<-c()
for (i in 1:length(S1)) {
      GIE[i]<-id[[S1[i]]]
}
ag<-cor.test(GIE, AGE, use ="complete.obs",method="pearson")
agepval<-as.numeric(ag$p.value)
agecor<-as.numeric(ag$estimate)

metcor<-biserial.cor(GIE, MET, use ="complete.obs", level = 2)
lymphcor<-biserial.cor(GIE, LN, use ="complete.obs", level = 2)
t<-cor.test(GIE, T, use ="complete.obs",method="spearman")
tpval<-as.numeric(t$p.value)
tcor<-as.numeric(t$estimate)
st<-cor.test(GIE, ST, use ="complete.obs",method="spearman")
stpval<-as.numeric(st$p.value)
stcor<-as.numeric(st$estimate)
ercor<-biserial.cor(GIE, ER, use ="complete.obs", level = 2)
prcor<-biserial.cor(GIE, PR, use ="complete.obs", level = 2)
her2cor<-biserial.cor(GIE, HER2, use ="complete.obs", level = 2)
y<-anova(lm(GIE ~ PAM50))
pam50_eta<-sqrt(y[2][1,1]/(y[2][2,1]+y[2][1,1]))
pam50_pval<-y[1,5]
DF<-data.frame(AGE_COR=agecor, AGE_PVAL=agepval, M=metcor, N=lymphcor,
T_COR=tcor, T_PVAL=tpval, STAGE_COR=stcor, STAGE_PVAL=stpval,
ER=ercor,PR=prcor, HER2=her2cor, PAM50_ETA=pam50_eta,
PAM50_PVAL=pam50_pval)
```

```
write.table(DF, file="new_file_name.txt", sep="\t", quote=FALSE,
row.names=FALSE)                    # enter desired file name here
```

8.10.3 Combination of genes with corresponding expression values

```
S<-read.table("file_name.txt", header=FALSE, sep="\t", dec = ".",
check.names=FALSE)                  # read table with selected genes

id<-new.env(hash=TRUE)
SV<-as.vector(S[,1])

for (i in 1:length(SV)) {
      id[[SV[i]]] <- SV[i]
}

EX<-read.table("file_name.txt", header=TRUE, sep="\t", dec = ".",
check.names=FALSE)                  # read table with normalized gene
                                    # expression values

ID<-as.vector(EX$row_title)         # row title of gene IDs
V<-c()
index<-1
for (i in 1:length(EX[,1])) {
      if (exists(as.vector(EX[i,1]), envir = id, inherits=FALSE)) {
            V[index]<-i
            index<-index+1
            ID[i]<-id[[as.vector(EX[i,1])]]
      }
}
EX1<-EX[V,2:length(EX[2,])]
D<-data.frame(ID=ID[V],EX1)
write.table(D, file="new_file_name.txt", sep="\t", quote=FALSE,
row.names=FALSE)                    # enter desired file name here
```

8.10.4 Clinical data for the cluster analysis

```
S<-read.table("file_name.txt", header=TRUE, sep="\t", dec = ".",
check.names=FALSE)                  # read table with clinical
                                    # information in numerical form

SV<-as.vector(S$SAMPLE)             # enter correct column title
M<-as.matrix(S[,5:7])
id1<-new.env(hash=TRUE)
id2<-new.env(hash=TRUE)
id3<-new.env(hash=TRUE)
for (i in 1:length(S$SAMPLE)) {     # enter correct column title
  id1[[SV[i]]] <- as.vector(M[i,1])
  id2[[SV[i]]] <- as.vector(M[i,2])
  id3[[SV[i]]] <- as.vector(M[i,3])
}

CL<-read.table("file_name.txt", header=TRUE, sep="\t", dec = ".",
check.names=FALSE)                  # enter name of table downloaded from
                                    # Genesis
CL_NAMES<-names(CL)
MN<-matrix(rep("0",2718),ncol=906)
for (i in 2:(length(CL_NAMES))) {
  MN[1,i]<-id1[[CL_NAMES[i]]]
  MN[2,i]<-id2[[CL_NAMES[i]]]
```

```
  MN[3,i]<-id3[[CL_NAMES[i]]]
}
MN[1,1]<-"ER"                          # enter correct column title
MN[2,1]<-"PR"                          # enter correct column title
MN[3,1]<-"HER2"                        # enter correct column title
colnames(MN)<-CL_NAMES
DF<-as.data.frame(MN)
write.table(DF, file="new_file_name.txt", sep="\t",
quote=FALSE,row.names=FALSE)           # enter desired file name here
```

8.10.5 PAM50 data for the cluster analysis

```
S<-read.table("FS_PAM50_num.txt", header=TRUE, sep="\t", dec = ".",
check.names=FALSE)                     # read table with PAM50 information
                                       # in numeric form
SV<-as.vector(S$Sample)                # enter correct column title
M<-as.matrix(S[,2])
id1<-new.env(hash=TRUE)
for (i in 1:length(S$Sample)) {        # enter correct column title
  id1[[SV[i]]] <- as.vector(M[i,1])
}

CL<-read.table("file_name.txt", header=TRUE, sep="\t", dec = ".",
check.names=FALSE)                     # enter name of table downloaded from
                                       # Genesis
CL_NAMES<-names(CL)
MN<-matrix(rep("0",299),ncol=299)
for (i in 2:(length(CL_NAMES))) {
  MN[1,i]<-id1[[CL_NAMES[i]]]
}
MN[1,1]<-"PAM50"
colnames(MN)<-CL_NAMES
DF<-as.data.frame(MN)
write.table(DF, file="new_file_name.txt", sep="\t", quote=FALSE,
row.names=FALSE)                       # enter desired file name here
```

8.10.6 Replacement of gene IDs with gene names for PAM50 classification

```
S<-read.table("file_name.txt", header=TRUE, sep="\t", dec = ".",
check.names=FALSE)                     # read table with gene IDs and
                                       # corresponding gene names
id<-new.env(hash=TRUE)
SV<-as.vector(S$ID)                    # enter correct column title
SW<-as.vector(S$GENE)                  # enter correct column title
for (i in 1:length(SV)) {

      if (!is.na(SW[i])) {
            id[[SV[i]]] <- SW[i]
      }
}

EX<-read.table("file_name.txt", header=TRUE, sep="\t", dec = ".",
check.names=FALSE)                     # read gene expression table
ID<-as.vector(EX$ID_REF)               # enter correct column title
V<-c()
index<-1
for (i in 1:length(EX[,1])) {
      if (exists(as.vector(EX[i,1]), envir = id, inherits=FALSE)) {
            V[index]<-i
```

```
            index<-index+1
            ID[i]<-id[[as.vector(EX[i,1])]]
      }
}
EX1<-EX[V,2:length(EX[2,])]
D<-data.frame(ID=ID[V],EX1)
# write file with normalized gene expression (TCGA) with available (AS)
clinical information
write.table(D, file="new_file_name.txt", sep="\t", quote=FALSE,
row.names=FALSE)                    # enter new file name here
```

8.10.7 Combination of PAM50 genes with corresponding expression values

```
S<-read.table("PAM50_gene_list.txt", header=FALSE, sep="\t", dec = ".",
check.names=FALSE)                  # read list of the PAM50 genes
id<-new.env(hash=TRUE)
SW<-as.vector(S[,1])
for (i in 1:length(SW)) {
      id[[SW[i]]] <- SW[i]
}

EX<-read.table("file_name.txt", header=TRUE, sep="\t", dec = ".",
check.names=FALSE)                  # read gene expression table
ID<-as.vector(EX$ID)                # enter correct column title
V<-c()
index<-1
for (i in 1:length(ID)) {
      if (exists(as.vector(ID[i]), envir = id, inherits=FALSE)) {
            V[index]<-i
            index<-index+1
      }
}
EX1<-EX[V,]
write.table(EX1, file="new_file_name.txt", sep="\t", quote=FALSE,
row.names=FALSE)                    # enter new file name here
```

8.10.8 PAM50 classification

This code is freely available on https://genome.unc.edu/pubsup/breastGEO/ and was generated by Parker et al. (47) in their original work on breast cancer intrinsic subtype prediction. No changes were made to the original code.

```
###
# input variables for the subtype prediction script
###
library(ctc)
library(heatmap.plus)

paramDir<- "C:/Users/Sarah Kammerer/Desktop/bioclassifier_R"
                                    # the location of unchanging files
                                    # such as the function library and
                                    # main program
inputDir<- "C:/Users/Sarah Kammerer/Desktop/PAM50/"
                                    # the location of the data matrix,
                                    # and where output will be located

inputFile<- "file_name.txt"         # the input data matrix as a tab
```

```
                                    # delimited text file as generated in
                                    # section 11.1.7
short<-"new_file_name"              # short name that will be used for
                                    # output files

calibrationParameters<- NA          # the column of the
                                    # "mediansPerDataset.txt" file to use
                                    # for calibration;

                                    # NA will force centring within the
                                    # test set & -1 will not do any

                                    # adjustment (when adjustment
                                    # performed by used)

hasClinical<-FALSE                  # may include tumor size as second
                                    # row, with 'T' as the gene name, and
                                    # encoded as binary (0 for size <=
                                    # 2cm or 1 for size > 2cm)
                                    #set this variable to FALSE if tumor
                                    # size is not available

collapseMethod<-"mean"              # can be mean or iqr (probe with max
                                    # iqr is selected)
                                    # typically, mean is preferred for
                                    # long oligo and iqr is preferred for
                                    # short oligo platforms


####
# run the assignment algorithm, output files will be generated
####

source(paste(paramDir,"subtypePrediction_functions.R",sep="/"))
source(paste(paramDir,"subtypePrediction_distributed.R",sep="/"))
```

8.10.9 Survival analysis

This code is freely available on http://kmplot.com/analysis/studies/Supplemental%20R%20script%201.R and was generated by Mihaly et al. (48). Minor modifications and additions were made to the original code in collaboration with Dieter Platzer (Institute of Biophysics, Medical University of Graz) in order to change the output information and the graphics output.

```
#----------------------------------------
#          Kaplan-Meier plot script
#----------------------------------------
#
# Supplemental R script for following study:
# Zsuzsanna Mihály, Máté Kormos, András Lánczky, Magdolna Dank, Jan
# Budczies, A. Marcell Szász, Balázs Győrffy
# A meta-analysis of gene expression based biomarkers predicting outcome
# after tamoxifen treatment in breast cancer
# Breast Cancer Res Treat. 2013 Jul;140(2):219-32.
# doi: 10.1007/s10549-013-2622-y.
#
#
```

```
# Input:
# - gene expression data:
#           +----------------------------------------
#           | AffyId | Gene Expr 1 | Gene Expr 2 ...
#           +----------------------------------------
# - clinical data
#           +----------------------------------------
#           | AffyId | Survival time | Survival event
#           +----------------------------------------
# Note: If there are other columns in the clinical table, you can specify
# which column has to be used for the survival data.
# Note: The ordering of the tables has to be same.
#
# Running the script:
#     expr: expression data
#     clin: clinical data
#     event_index: column containing the survival event,
#     time_index:  column containing the survival time,
#     affyid: if you are interested in one Affymetrix probe ID,
#     auto_cutoff: if this parameter is set to "true", the script finds
#                  the best cut-off value
#     quartile: if the auto_cutoff is not set, you can use the quartile
#                  option. This parameter runs from 1 to 100 as a
#                  percentile, where the data has to be split into the two
#                  groups. 50 means the median, 25 the lower, 75 the upper
#                  quartile.
#
# Example 1:
# d = loadData(expr="@supplemental table 1_GEO expression data
# sorted.txt", clin="@supplemental table 2_GEO clinical data
# sorted.txt");
#     kmplot(d$expr, d$clin, event_index=3, time_index=4,
#     auto_cutoff="true")
#
# Example 2:
# d = loadData(expr="@supplemental table 1_GEO expression data
# sorted.txt", clin="@supplemental table 2_GEO clinical data
# sorted.txt");
#     kmplot(d$expr, d$clin, event_index=3, time_index=4,
#     affyid="213324_at", auto_cutoff="true")
#
# Example 3:
# d = loadData(expr="expression_table.txt", clin="clinical_table.txt");
#     kmplot(d$expr, d$clin, event_index=2, time_index=3,
#     auto_cutoff="false", quartile=50);
#

library(survival)
library(survplot)


checkData = function(expr, clin){

      affyid_expr = as.character(expr[[1]]);
      affyid_clin = as.character(clin[[1]]);

      # check number of entries
      if(length(affyid_expr) != length(affyid_clin)){
            stop("The dimensions of data is not equal.");
      }
```

```
	for(i in 1:length(affyid_expr)){
	if(affyid_expr[[i]] != affyid_clin[[i]]){
		stop(paste("STOP: The ", i, "the ID of data is different.",
		sep="") )
		}
	}

}


auto_cutoff = function(row, gene_db, time_index, event_index, expr){

	ordered_row = order(row);
	q1 = round(length(ordered_row)*0.25);
	q3 = round(length(ordered_row)*0.75);

	# m = sortedrow[round(i)];
	surv = Surv(gene_db[,time_index], gene_db[,event_index]);

	p_values = vector(mode="numeric", length = q3-q1+1)
	min_i = 0
	min_pvalue=1

	for(i in q1:q3){

		gene_expr = vector(mode="numeric", length=length(row))
		gene_expr[ordered_row[i:length(ordered_row)]] = 1

		cox = summary(coxph(surv ~ gene_expr, ties="breslow"))

		pvalue = cox$sctest['pvalue']

		p_values[i-q1+1] = pvalue

		if(pvalue < min_pvalue){
			min_pvalue = pvalue
			min_i = i
		}

	}
	print(c('min_pvalue', min_pvalue), quote = FALSE)
	print(c('min_i', min_i), quote = FALSE)
	print(c('cutoff',expr[min_i,2]), quote = FALSE)


	gene_expr = vector(mode="numeric", length=length(row))
	gene_expr[ordered_row[min_i:length(ordered_row)]] = 1


	m = row[ordered_row[min_i]]
}


loadData = function(exprFile="@supplemental table 1_GEO expression
data_sorted.txt", clinFile="@supplemental table 2_GEO clinical
data_sorted.txt"){

	if(file.exists(exprFile)){
		expr = read.table(exprFile, header=TRUE, sep="\t");
	}else{
		stop("The gene expression table is not exists!");
```

```
	}

	if(file.exists(clinFile)){
		clin = read.table(clinFile, header=TRUE, sep="\t");
	}else{
		stop("The gene expression table is not exists!");
	}

	list("expr"=expr, "clin"=clin);
}

mySurvplot = function(surv, gene_expr, xlab="Time (months)", ylab="OS
probability", snames = c('low', 'high'), stitle = "Expression",
hr.pos=NA){
	survplot(surv ~ gene_expr, xlab=xlab, ylab=ylab, snames = snames,
stitle = stitle, hr.pos=hr.pos);

	cox = summary(coxph(surv ~ gene_expr, ties="breslow"))
	print('-----------------')
	print('with subgroups')
	print(cox)

	pvalue=cox$sctest['pvalue']
	hr = round(cox$conf.int[1],2)
	hr_left = round(cox$conf.int[3],2)
	hr_right = round(cox$conf.int[4],2)

	conf_int =  paste(" (", hr_left, " - ", hr_right, ")", sep="");

	txt = paste("HR = ", hr, conf_int, "\nlogrank P = ", signif(pvalue,
	2), sep="")
	text(grconvertX(0.98, "npc"), grconvertY(.97, "npc"),
		labels=txt,
		adj=c(1, 1))

	list(pvalue, hr, hr_left, hr_right)
}

createDirectory = function(base){
	i="";
	while(file.exists(paste(base, i, sep=""))){
		if(i==""){
			i=1;
		}else{
			i=i+1;
		}
	}
	toDir = paste(base, i, sep="")
	dir.create(toDir)

	toDir
}


getCutoff = function(quartile, median_row, manual_cutoff="false",
verbose=FALSE){

	sortedrow=order(median_row);
	minValue = median_row[sortedrow[1]]
	maxValue = median_row[sortedrow[length(sortedrow)]]
```

```
	# if manual_cutoff is true, then the user can specify a discrete
	# Cut-off value

	if(manual_cutoff=="true"){
		m = as.numeric(quartile);
		indices = which(median_row>m)
	}else{
		quartile = as.numeric(quartile);

		if(is.na(quartile) || !is.numeric(quartile)){
			stop("The quartile parameter isn't numeric.")
		}else if(quartile<5){
			quartile = 5
		} else if(quartile > 95){
			quartile = 95
		}

		i=length(sortedrow)*quartile/100;
		m=median_row[sortedrow[round(i)]];

		indices = which(m<median_row)
		#sortedrow[round(i):length(sortedrow)]
	}

	if(verbose){
		print(m)
		print(minValue)
		print(maxValue)
	}

	list(m, minValue, maxValue, indices)
}

getParameter = function(c_args, id){
	res = ""
	for(i in 1:length(c_args)){

		tmp = strsplit(c_args[i], "=")
		filter_id = tmp[[1]][1]
		value = tmp[[1]][2]

		if(filter_id == paste("-", id, sep="")){
			res = value
			break
		}

	}

	res

}

kmplot = function(expr, clin, event_index=3, time_index=4, affyid="",
auto_cutoff="true", quartile=50){

	# checks the input: if the expression data and clinical data don't
	# match, the script will fail.

	checkData(expr, clin);
```

```
      survival_data = cbind(as.numeric(clin[[time_index]]),
as.numeric(clin[[event_index]]));

      resTable=rbind();

      index_arr = 2:dim(expr)[2];
      if(affyid != ""){
            index = which(colnames(expr) == paste(affyid, sep=""));
            if(length(index) > 0){
                  index_arr = c(index);
            }
      }
      for(j in 1:length(index_arr)){
            i=index_arr[j]
            print(paste("Processing...", colnames(expr)[i]));

            row = as.numeric(expr[[i]]);

    # ---------------------- CUTOFF ----------------------
            if(auto_cutoff == "true"){
                  m = auto_cutoff(row, survival_data, 1, 2, expr)
            }else{
                  # calculates lower quartile, median, or upper quartile
                  tmp = getCutoff(quartile, row)

                  m = tmp[[1]]
                  minValue = tmp[[2]]
                  maxValue = tmp[[3]]
                  indices = tmp[[4]]

            }

      # gene_expr consists 1 if m smaller than the gene expression value,
      # 0 if m bigger then the gene expression value
            gene_expr=vector(mode="numeric", length=length(row))
            gene_expr[which(m < row)] = 1

    # ---------------------- KMplot ----------------------
            tryCatch({
                  surv<-Surv(survival_data[,1], survival_data[,2]);

                  res = mySurvplot(surv, gene_expr)
                  pvalue = res[[1]]
                  hr = res[[2]]
                  hr_left = res[[3]]

                  hr_right = res[[4]]

                  resTable = rbind(resTable, c(pvalue, hr, hr_left,
                  hr_right));

                  cox_simple = summary(coxph(surv ~ expr[,2],
                  ties="breslow"))
                  print('--------------')
                  print('no subgroups')
                  print(cox_simple)

            }, interrupt = function(ex){
                  cat("Interrupt during the KM draw");
                  print(ex);
                  dim(gene_expr);
```

```
            }, error = function(ex){
                  cat("Error during the KM draw");
                  print(ex);
                  dim(gene_expr);
            }
            );


      }

}

EXPR<-read.table("file_name.txt", header=TRUE, sep="\t", dec = ".",
check.names=FALSE)                  # read table with gene expression and
                                    # clinical information

names(EXPR)                         # show column titles with numbering

gexpr<-EXPR[,c(x,y)]                # make gene expression table for a
                                    # certain gene, whereas x=column
                                    # number of patient ID and y=column
                                    # number of gene of interest

kmplot(gexpr, EXPR, event_index=a, time_index=b,  affyid="c",
auto_cutoff="true")                 # draw KM plot with gene expression
                                    # table and full table, whereas
                                    # a=column number of event status,
                                    # b=column number of event time and
                                    # c=gene ID or name

# to select subgroups of the full table; enter column title and selection
criterion as below and repeat procedure above with the new subgroup table

ER<-subset(EXPR,EXPR$ER_Status=="Positive")
ISH<-subset(EXPR, ISH_result==0 | ISH_result==4)
```

8.10.10 Cox proportional hazard model

```
library(survival)

########################
### OS TCGA ER+ MULTIVARIATE COX MODEL
########################

b<-read.table("TCGA_ER.txt",  header=TRUE,  sep="\t",  dec  =  ".",
check.names=FALSE )                 # read table with survival times
                                    # and clinical information

SURV<-b$OS_months                   # enter row name with survival
                                    # times
EVENT<-b$Event                      # enter row name with event status

#pT
T<-as.vector(b$pathologic_T)     #enter row name with pT status
ind0<-which(T=="T1")
ind1<-which(T=="T2" | T=="T3"| T=="T4")
T[ind0]<-0
T[ind1]<-1
```

```
#pN
N<-as.vector(b$pathologic_N)     # enter row name with LN status
ind0<-which(N=="N0")
ind1<-which(N=="N1" | N=="N2" | N=="N3" | N=="N4")
N[ind0]<-0
N[ind1]<-1

#pM
M<-as.vector(b$pathologic_M)     # enter row name with pM status
ind0<-which(M=="M0")
ind1<-which(M=="M1")
M[ind0]<-0
M[ind1]<-1

#Age
AGE<-as.vector(b$Age)            # enter row name with age at
                                 # diagnosis
ind0<-which(AGE<=50)
ind1<-which(AGE>50)
AGE[ind0]<-0
AGE[ind1]<-1

#Her2
HER2<-as.vector(b$Her2)          # enter row name with Her2 status
ind0<-which(HER2=="Negative")
ind1<-which(HER2=="Positive")
HER2[ind0]<-0
HER2[ind1]<-1

#Menopause
MENO<-as.vector(b$Menopause)     # enter row name with menopausal
                                 # status
ind0<-which(MENO=="Pre")
ind1<-which(MENO=="Post" | MENO=="Peri")
MENO[ind0]<-0
MENO[ind1]<-1

#Histology
HISTO<-as.vector(b$Histology)    # enter row name with histological
                                 # subtype
ind0<-which(HISTO=="Ductal")
ind1<-which(HISTO=="Lobular")
HISTO[ind0]<-0
HISTO[ind1]<-1

#PAM50
PAM50<-as.vector(b$PAM50)        # enter row name with PAM50 status
ind0<-which(PAM50=="Luminal A")
ind1<-which(PAM50=="Luminal B")
PAM50[ind0]<-0
PAM50[ind1]<-1

# dichozomize samples based onquantile expr
hiloquant<-function(x,pr) {
  qu<-as.vector(quantile(x,pr))
```

```
  a<-which(x>qu)
  b<-which(x<=qu)
  x[a]<-1
  x[b]<-0
  return(x)
}
KCNJ3<-hiloquant(b$KCNJ3,0.72)   # define gene of interest and
                                 # cutoff percentile



sink(file = "er_coxmodels_univariate_os.txt")
vp<-NULL
vp[1]<-0.0


d1<-which(!is.na(T))
v1<-coxph(Surv(as.numeric(SURV[d1]),as.numeric(EVENT[d1]))        ~
as.factor(T[d1]))
vp[2]<-summary(v1)[[9]][3]
print (summary(v1)[[7]])
print (summary(v1)[[8]])

d2<-which(!is.na(N))
v2<-coxph(Surv(as.numeric(SURV[d2]),as.numeric(EVENT[d2]))        ~
as.factor(N[d2]))
vp[3]<-summary(v2)[[9]][3]
print (summary(v2)[[7]])
print (summary(v2)[[8]])

d3<-which(!is.na(M))
v3<-coxph(Surv(as.numeric(SURV[d3]),as.numeric(EVENT[d3]))        ~
as.factor(M[d3]))
vp[4]<-summary(v3)[[9]][3]
print (summary(v3)[[7]])
print (summary(v3)[[8]])

d4<-which(!is.na(HISTO))
v4<-coxph(Surv(as.numeric(SURV[d4]),as.numeric(EVENT[d4]))        ~
as.factor(HISTO[d4]))
vp[5]<-summary(v4)[[9]][3]
print (summary(v4)[[7]])
print (summary(v4)[[8]])

d7<-which(!is.na(HER2))
v7<-coxph(Surv(as.numeric(SURV[d7]),as.numeric(EVENT[d7]))        ~
as.factor(HER2[d7]))
vp[8]<-summary(v7)[[9]][3]
print (summary(v7)[[7]])
print (summary(v7)[[8]])

d8<-which(!is.na(MENO))
v8<-coxph(Surv(as.numeric(SURV[d8]),as.numeric(EVENT[d8]))        ~
as.factor(MENO[d8]))
vp[9]<-summary(v8)[[9]][3]
```

```
print (summary(v8)[[7]])
print (summary(v8)[[8]])

d9<-which(!is.na(AGE))
v9<-coxph(Surv(as.numeric(SURV[d9]),as.numeric(EVENT[d9]))        ~
as.factor(AGE[d9]))
vp[10]<-summary(v9)[[9]][3]
print (summary(v9)[[7]])
print (summary(v9)[[8]])


d10<-which(!is.na(PAM50))
v10<-coxph(Surv(as.numeric(SURV[d10]),as.numeric(EVENT[d10]))     ~
as.factor(PAM50[d10]))
vp[11]<-summary(v10)[[9]][3]
print (summary(v10)[[7]])
print (summary(v10)[[8]])

d11<-which(!is.na(KCNJ3))
v11<-coxph(Surv(as.numeric(SURV[d11]),as.numeric(EVENT[d11]))     ~
KCNJ3[d11])
vp[12]<-summary(v11)[[9]][3]
print (summary(v11)[[7]])
print (summary(v11)[[8]])


sink()

pw<-
paste("covariate",vp[1],vp[2],vp[3],vp[4],vp[5],vp[8],vp[9],vp[10]
,vp[11],vp[12], sep="\t")
dfw<-data.frame(P=pw)
write.table(dfw, file = "er_pvalues_covariates_os.txt", append =
FALSE, quote = FALSE, sep = "\t", eol = "\n", na = "NA", dec = ".",
row.names = FALSE, col.names = FALSE)


sink(file = "er_coxmodels_os.txt")
print (summary(v1))
print (summary(v2))
print (summary(v3))
print (summary(v4))
print (summary(v7))
print (summary(v8))
print (summary(v9))
print (summary(v10))
print (summary(v11))
sink()

sink(file = "er_mv_coxmodel_os.txt")
indALL<-which(!is.na(T) & !is.na(N) & !is.na(M) & !is.na(HISTO) &
!is.na(HER2) & !is.na(MENO) & !is.na(PAM50) & !is.na(AGE))
ma<-coxph(Surv(as.numeric(SURV[indALL]),as.numeric(EVENT[indALL]))
~
as.factor(T[indALL])+as.factor(N[indALL])+as.factor(M[indALL])+as.
```

```
factor(HISTO[indALL])+as.factor(HER2[indALL])+as.factor(MENO[indAL
L])+as.factor(PAM50[indALL])+as.factor(AGE[indALL]))
print (summary(ma))
mb<-coxph(Surv(as.numeric(SURV[indALL]),as.numeric(EVENT[indALL]))
~
as.factor(T[indALL])+as.factor(N[indALL])+as.factor(M[indALL])+as.
factor(HISTO[indALL])+as.factor(HER2[indALL])+as.factor(MENO[indAL
L])+as.factor(AGE[indALL])+as.factor(PAM50[indALL])+as.factor(KCNJ
3[indALL]))
print (summary(mb))
sink()
```

9 Results

9.1 Analysis of the TCGA data set

First, in order to screen for GIRK1 (*KCNJ3* gene) mRNA expression patterns in breast cancer and especially in distinctive breast cancer subtypes, we performed a detailed statistical analysis of the gene expression data available from the TCGA on invasive breast cancer samples. Some of the following analyses and figures were produced in collaboration with Armin Sokolowski (diploma student at the Institute of Biophysics, Medical University of Graz) and are also part of his diploma thesis.

9.1.1 GIRK1 mRNA expression in normal and cancerous breast tissue

Of 105 patients, data were available for both the tumor tissue and surrounding normal tissue; thus, we were able to compare the GIRK1 mRNA expression in normal and cancerous tissue of the same patient. Figure 3 shows that GIRK1 mRNA expression is significantly higher in tumor than in surrounding normal tissue (Wilcoxon signed rank test, $p<0.005$). The median was 6.8 and 14.6 in normal and tumor tissue, respectively, while the 75% percentile was 19.6 and 326.4, respectively.

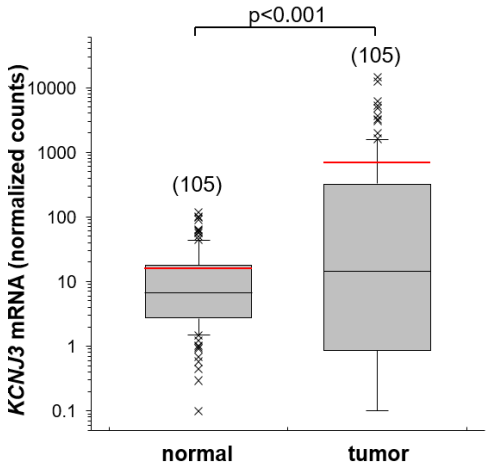

Figure 3: GIRK1 mRNA expression in normal and in corresponding tumor tissue.
TCGA, n=105, $p<0.001$. Median: 6.8 vs. 14.6; 75th percentile: 19.6 vs. 326.4.
Whiskers represent the 10th and the 90th percentile, crosses represent outliers. Black line marks the median, red line the mean value. A Wilcoxon signed rank test was used for analysis.
Figure taken from: "KCNJ3 is a new independent prognostic marker for estrogen receptor positive breast cancer patients" by Kammerer et al; manuscript submitted to Oncotarget.

This indicates that GIRK1 mRNA is overexpressed in primary breast tumors. *See also: "KCNJ3 is a new independent prognostic marker for estrogen receptor positive breast cancer patients" by Kammerer et al; manuscript submitted to Oncotarget.*

9.1.2 GIRK1 mRNA expression in different breast cancer subtypes

Next, we examined whether the GIRK1 mRNA expression is higher in certain subgroups of breast cancer patients. First, we built four categories taking into account the hormone receptors (ER and PR) and the Her2 status. We found significantly higher GIRK1 mRNA expression in hormone receptor positive patients which seemed to be independent of the patient's Her2 status (see Figure 4A). Thus, we grouped the patients regarding their ER and PR status irrespective of their Her2 status. As shown in Figure 4B, the GIRK1 mRNA

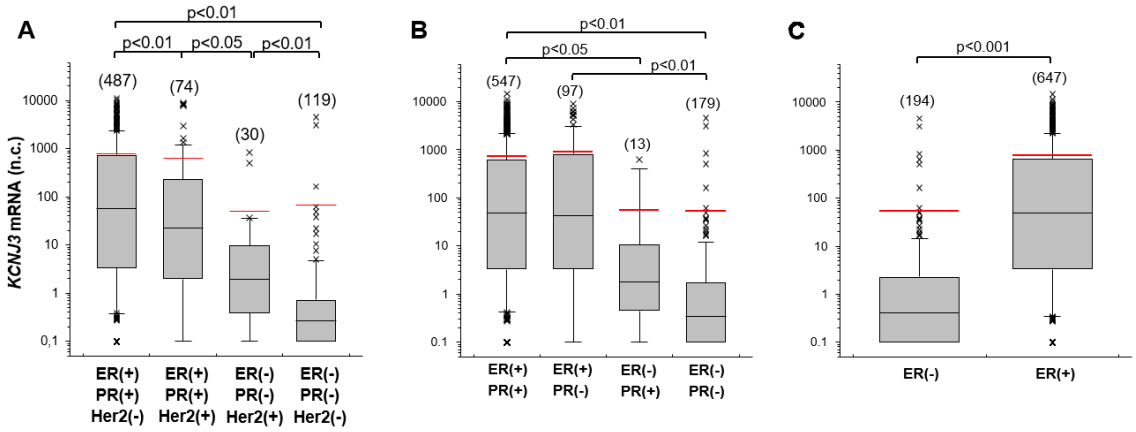

Figure 4: GIRK1 mRNA expression in different breast cancer subtypes.

A. Breast cancer subtypes regarding estrogen receptor (ER), progesterone receptor (PR) and Her2 expression status (n=710, $p<0.01$). **B.** Breast cancer subtypes regarding ER and PR expression status (n=836, $p<0.001$). **C.** ER negative and ER positive patients (n=841, p<0.001).

Whiskers represent the 10th and the 90th percentile, crosses represent outliers, the red line marks the mean value. Number of samples analyzed is given in brackets above each box. A Kruskal Wallis test with Dunn's post-hoc tests for pairwise comparison was used for analysis in (A) and (B) and a Wilcoxon rank sum test in (C); *p*-values are given on top of each plot. n.c.: normalized counts.

Figure panels B and C taken from: "KCNJ3 is a new independent prognostic marker for estrogen receptor positive breast cancer patients" by Kammerer et al; manuscript submitted to Oncotarget.

expression was significantly higher in ER positive than in ER negative patients (p<0.001). Finally, we grouped the patients regarding their ER status only, and we could show that ER positive patients have indeed statistically higher GIRK1 mRNA levels irrespective of PR or Her2 status (p<0.001, median 0.4 vs. 49.0, see Figure 4C). *See also: "KCNJ3 is a new independent prognostic marker for estrogen receptor positive breast cancer patients" by Kammerer et al; manuscript submitted to Oncotarget.* To display the expression values for single patients, and to show the differences in GIRK1 expression between ER negative and positive patients, a bar graph was generated (Figure 5).

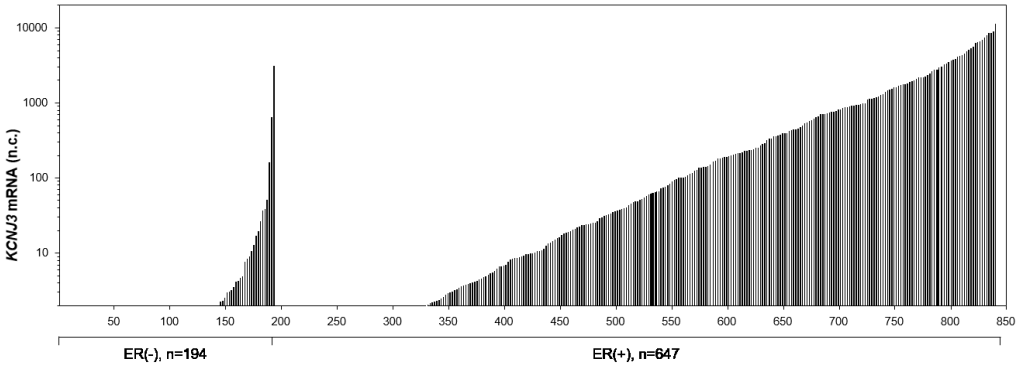

Figure 5: GIRK1 mRNA expression in ER negative and positive patients.
n.c.: normalized counts.

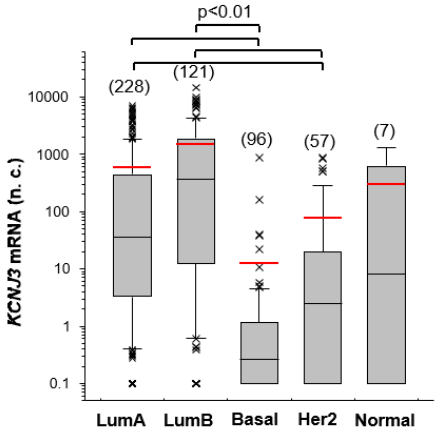

Figure 6: GIRK1 mRNA expression in different PAM50 subgroups.
Whiskers represent the 10th and the 90th percentile, crosses represent outliers, the red line marks the mean value. Number of samples analyzed is given in brackets above each box. A Kruskal Wallis test with Dunn's post-hoc tests for pairwise comparison was used
LumA: luminal A, LumB: luminal B, Basal: basal-like, Her2: Her2-enriched, Normal: normal-like, n.c.: normalized counts.
Figure taken from: "KCNJ3 is a new independent prognostic marker for estrogen receptor positive breast cancer patients" by Kammerer et al; manuscript submitted to Oncotarget.

Since the TCGA data also included the PAM50 information for most of the patients, we grouped the patients into the five PAM50 classification subtypes and analyzed the differences in GIRK1 mRNA expression. Figure 6 shows that the luminal A and luminal B subtypes had the highest GIRK1 expression values, which fits well to the above mentioned results since the luminal A and B subtype comprise the hormone receptor positive patients. *See also: "KCNJ3 is a new independent prognostic marker for estrogen receptor positive breast cancer patients" by Kammerer et al; manuscript submitted to Oncotarget.*

Next, we analyzed possible differences in GIRK1 mRNA expression levels regarding distinct clinical features. We found statistically significant higher GIRK1 mRNA levels in patients who had positive lymph nodes (LN) at first diagnosis than in LN negative patients (see Figure 7A). In addition, GIRK1 mRNA expression was analyzed in patients who presented with or without metastasis at first diagnosis. We did not find a statistically significant difference between these two groups, probably due to the low patient number with metastasis (n=15). However, a trend towards higher GIRK1 mRNA levels in patients with metastasis could be observed (Figure 7B).

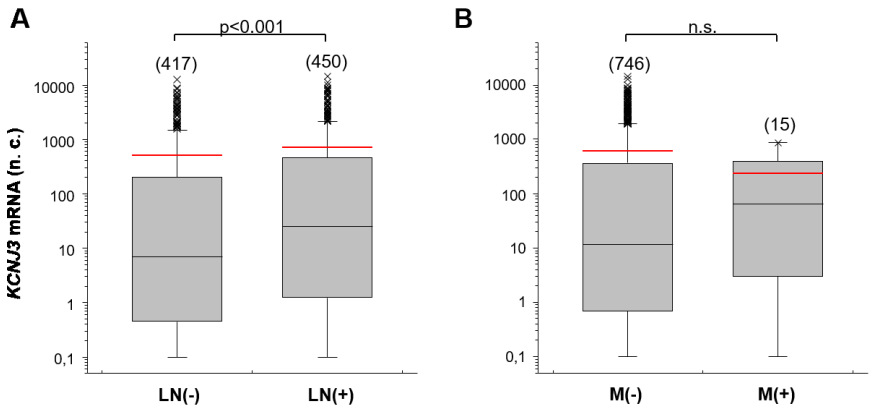

Figure 7: GIRK1 mRNA expression at different clinical stages.

A. LN negative and positive patients (n=867, *p*<0.001). **B.** Metastasis (M) negative and positive patients (n=760, n.s.).

Whiskers represent the 10th and the 90th percentile, crosses represent outliers, the red line marks the mean value. Number of samples analyzed is given in brackets above each box. Mann-Whitney rank sum tests were used for analysis.

Figure panel A taken from: "KCNJ3 is a new independent prognostic marker for estrogen receptor positive breast cancer patients" by Kammerer et al; manuscript submitted to Oncotarget.

GIRK1 expression levels were not significantly altered regarding the age at diagnosis, menopausal status (both in Figure 8A), tumor size (Figure 8B), tumor stage (Figure 8C) and histology (Figure 8D). *See also: "KCNJ3 is a new independent prognostic marker for estrogen receptor positive breast cancer patients" by Kammerer et al; manuscript submitted to Oncotarget.*

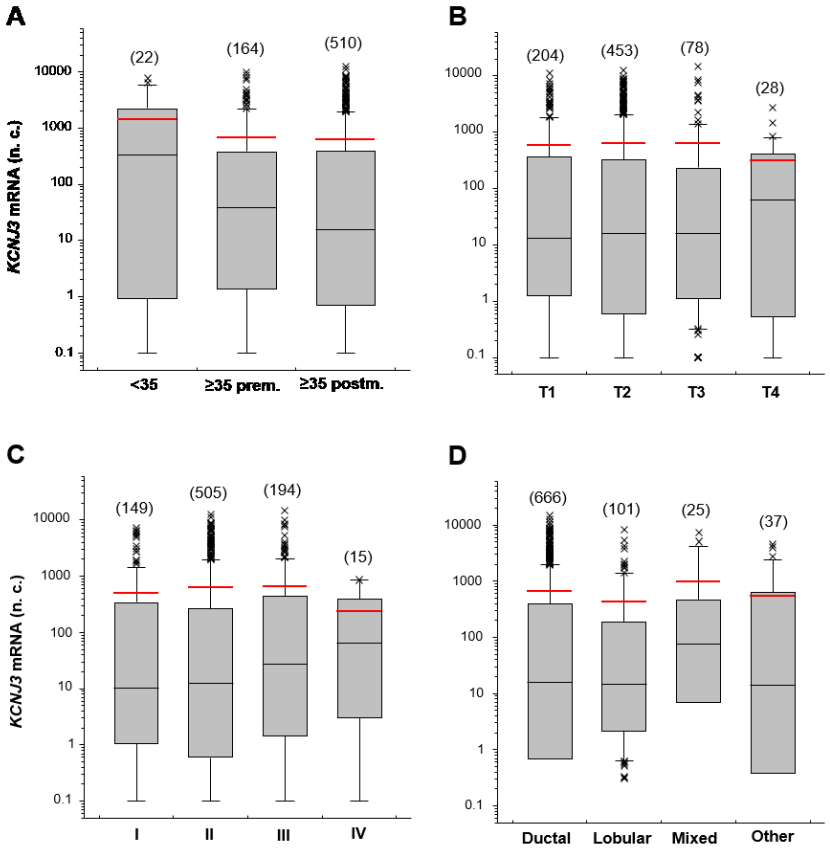

Figure 8: GIRK1 mRNA expression in different clinical subgroups.

A. Patients younger than 35 years old, older than 35 and pre-menopausal (prem.) and older than 35 and post-menopausal (postm.). **B.** Patients with tumors of size T1 (<2 cm), T2 (2-5 cm), T3 (>5 cm) and T4 (any size, but growing into chest wall or skin). **C.** Patients with tumors of stage I, stage II, stage III and stage IV. **D.** Patients with ductal, lobular, mixed and other tumor histology.

Whiskers represent the 10th and the 90th percentile, crosses represent outliers, the red line marks the mean value. Number of samples analyzed is given in brackets above each box. Kruskal Wallis tests with Dunn's post-hoc tests for pairwise comparison were used for analysis. Results were not statistically significant.

Figure panels taken from: "KCNJ3 is a new independent prognostic marker for estrogen receptor positive breast cancer patients" by Kammerer et al; manuscript submitted to Oncotarget.

9.1.3 Association analysis

Association analysis was performed in addition to the analysis above to detect positive or negative associations of GIRK1 mRNA expression levels with any clinical features. Corresponding *p*-values were calculated where possible, i.e. where the clinical feature comprised more than two groups. GIRK1 mRNA was highly associated with the ER status and the PAM50 classification. Table 5 summarizes the results.

Table 5: Association analysis of GIRK1 mRNA and clinical features.

Clinical feature	association coefficient	*p*-value
Age at diagnosis	-0.0062	0.860887
ER status	0.4593	---
PR status	0.3243	---
Her2 status	-0.0651	---
PAM50 classification	0.5048	2.16E-51
Tumor size (T)	-0.0080	0.813675
Lymph nodes (N)	0.1177	---
Metastasis (M)	0.0233	---
Tumor stage	0.0544	0.109871

9.1.4 Correlation analysis

In order to investigate which genes are positively or negatively correlating with GIRK1, we performed Spearman rank correlation analysis of GIRK1 with all other genes. The analysis was performed in *R*. Table 6 shows the 25 genes with the highest and lowest Spearman rank correlation coefficients. Next, we performed functional annotations of genes positively and negatively correlating with GIRK1 to gene ontology (GO) terms and pathways using the DAVID tool. The cut-off values were set at $r_S \geq 0.4$ and $r_S \leq (-0.4)$. Results were considered as relevant when the false discovery rate (FDR) was below 10 and the *p*-value was smaller than 0.05. Twenty-four GO terms could be identified for the genes positively correlating with GIRK1, while only three GO terms (Table 7) could be identified for the negative correlations. Several genes positively correlating with GIRK1 are involved in membrane and secretion functions (Table 7). Regarding the pathway analysis, only one pathway could be identified for both positively and negatively correlating genes using the above mentioned criteria. For positively correlating genes, we identified the pathway hsa04144: Endocytosis (9 counts, 4.3% of genes, $p<0.001$, FDR=0.074%) and for negatively correlating genes the pathway hsa00601: Glycosphingolipid biosynthesis (4 counts, 2.5% of genes, $p<0.01$, FDR=2.08%).

Table 6: Genes positively and negatively correlating with GIRK1

Gene 1	Genes$^{(pos)}$	$r_S^{(pos)}$	*p*-value$^{(pos)}$	Genes$^{(neg)}$	$r_S^{(neg)}$	*p*-value$^{(neg)}$
KCNJ3	KCNJ3	1	0	PADI2	-0.4759995	2.32E-52
KCNJ3	SLC39A6	0.6268108	5.90E-100	PRKX	-0.4768779	1.42E-52
KCNJ3	DNAJC12	0.61701742	4.71E-96	CDCA7	-0.4769103	1.39E-52
KCNJ3	TBC1D9	0.59814375	6.56E-89	TRPV6	-0.477555	9.72E-53
KCNJ3	DACH1	0.58869445	1.65E-85	TTLL4	-0.4784517	5.87E-53
KCNJ3	AFF3	0.58547113	2.25E-84	PTK7	-0.4866702	5.42E-55
KCNJ3	FSIP1	0.56134045	2.87E-76	TES	-0.4871972	4.00E-55
KCNJ3	FAM134B	0.55848895	2.36E-75	GPR156	-0.491044	4.25E-56
KCNJ3	CACNA2D2	0.5553	2.43E-74	RBM38	-0.4911667	3.96E-56
KCNJ3	CDK17	0.55270108	1.59E-73	TMEM123	-0.4922149	2.14E-56
KCNJ3	ARSG	0.55219048	2.30E-73	GSDMC	-0.4936209	9.32E-57
KCNJ3	APBB2	0.5459033	2.01E-71	PSAT1	-0.4938317	8.23E-57
KCNJ3	AGTR1	0.54069761	7.62E-70	ENO1	-0.4939727	7.57E-57
KCNJ3	CLSTN2	0.53657072	1.30E-68	ACE2	-0.4948096	4.61E-57
KCNJ3	MAST4	0.53240426	2.18E-67	PROM1	-0.495256	3.53E-57
KCNJ3	SLC19A2	0.52704212	7.80E-66	BTG3	-0.4994001	2.96E-58
KCNJ3	LMX1B	0.52660581	1.04E-65	NCK2	-0.5020067	6.10E-59
KCNJ3	LONRF2	0.52619546	1.36E-65	CD82	-0.5033247	2.73E-59
KCNJ3	ELP2	0.52322939	9.53E-65	LMO4	-0.5078893	1.65E-60
KCNJ3	SLC22A5	0.52086707	4.43E-64	MSL3	-0.5104217	3.41E-61
KCNJ3	ESR1	0.52070989	4.90E-64	C11orf75	-0.5125588	8.91E-62
KCNJ3	MKL2	0.51755597	3.73E-63	MID1	-0.5141244	3.32E-62
KCNJ3	THSD4	0.51523634	1.64E-62	NFIL3	-0.5178436	3.10E-63
KCNJ3	IGF1R	0.51444564	2.71E-62	UBE2E3	-0.5263286	1.25E-65
KCNJ3	RGS22	0.51300162	6.74E-62	MPZL2	-0.5346529	4.78E-68

$^{(pos)}$: positive correlation, $^{(neg)}$: negative correlation, r_S: Spearman rank correlation coefficient

Table 7: Functional annotation analysis of genes positively correlating with GIRK1

Cat.	Term	#	%	*p*-value	FDR [%]
Positive correlation:					
BP	GO:0032940~ secretion by cell	12	5.797	1.14E-05	0.019
BP	GO:0046903~ secretion	14	6.763	1.63E-05	0.027
BP	GO:0006887~ exocytosis	9	4.348	2.77E-05	0.046
CC	GO:0044425~ membrane part	93	44.93	2.20E-04	0.286
MF	GO:0017137~ Rab GTPase binding	5	2.415	2.66E-04	0.372
BP	GO:0051179~ localization	51	24.64	2.51E-04	0.412
BP	GO:0048858~ cell projection morphogenesis	11	5.314	2.59E-04	0.426
BP	GO:0006810~ transport	46	22.22	3.44E-04	0.566
BP	GO:0032990~ cell part morphogenesis	11	5.314	3.67E-04	0.604
BP	GO:0051234~ establishment of localization	46	22.22	4.34E-04	0.713
BP	GO:0051649~ establishment of localization in cell	21	10.14	5.81E-04	0.954
CC	GO:0016020~ membrane	98	47.34	8.10E-04	1.047

Cat.	Term	#	%	*p*-value	FDR [%]
Positive correlation:					
BP	GO:0051641~ cellular localization	22	10.63	6.77E-04	1.111
BP	GO:0030182~ neuron differentiation	14	6.763	7.06E-04	1.159
BP	GO:0048666~ neuron development	12	5.797	8.91E-04	1.460
BP	GO:0007409~ axonogenesis	9	4.348	9.75E-04	1.596
BP	GO:0031175~ neuron projection development	10	4.831	0.00151	2.468
BP	GO:0048667~ cell morphogenesis involved in neuron differentiation	9	4.348	0.00162	2.641
BP	GO:0048812~ neuron projection morphogenesis	9	4.348	0.00183	2.970
BP	GO:0008104~ protein localization	20	9.662	0.00218	3.538
BP	GO:0048699~ generation of neurons	15	7.246	0.00224	3.624
BP	GO:0045184~ establishment of protein localization	18	8.696	0.00288	4.641
BP	GO:0016192~ vesicle-mediated transport	15	7.246	0.00293	4.732
CC	GO:0016021~ integral to membrane	73	35.27	0.00494	6.227
Negative correlation:					
MF	GO:0003700~transcription factor activity	19	11.95	0.00327	4.433
BP	GO:0021915~neural tube development	5	3.145	0.00462	7.255
BP	GO:0042127~regulation of cell proliferation	17	10.69	0.00495	7.748

Cat.: Category, #: number of genes involved in GO, %: percentage of genes involved in GO, FDR: false discovery rate, BP: biological process, CC: cellular component, MF: molecular function.

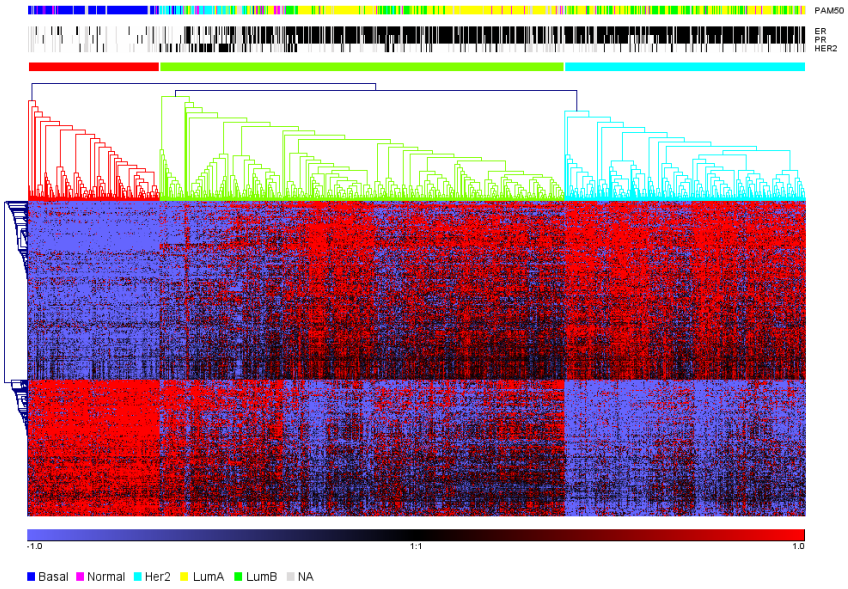

Figure 9: Hierarchical cluster analysis of genes correlating with GIRK1 expression. Clinical information is included on top. Gene expression data were log2 transformed and mean centered. The Euclidean distance was calculated for genes and patients (n=905). Basal: basal-like, Normal: normal-like, Her2: Her2-enriched, LumA: luminal A, LumB: luminal B, NA: information not available.

9.1.5 Hierarchical cluster analysis

Using the Spearman rank correlation analysis, we selected the genes positively and negatively correlating with GIRK1 ($r_S \geq 0.4$ and $r_S \leq (-0.4)$, respectively) and performed hierarchical cluster analysis using the Genesis software. The PAM50, ER, PR and Her2 information were included for each patient sample. The genes cluster in three main groups according to the PAM50 and ER/PR classification (**Fehler! Verweisquelle konnte nicht g efunden werden.**), showing again that GIRK1 upregulation correlates with ER positive breast cancer subtypes (luminal A and B), while GIRK1 expression is low in basal like/triple negative breast cancers. In order to get a clearer view on how GIRK1 gene expression clusters with the gene expression of the three known estrogen receptor status, we performed cluster analysis using only GIRK1, estrogen receptor alpha (ESR1), beta (ESR2) and the G-protein coupled estrogen receptor (GPER or GPR30). Figure 10 shows clearly that three groups can be formed based on GIRK1 and estrogen receptor expression levels.

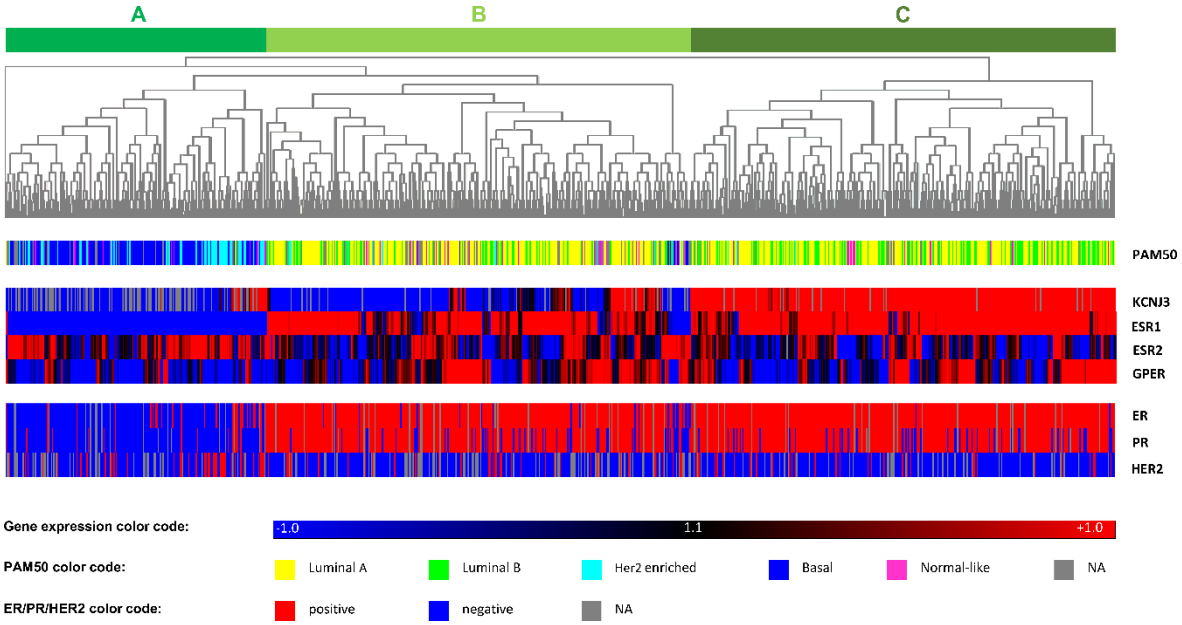

Figure 10: Heatmap of hierarchical cluster analysis.

Hierarchical cluster analysis of mRNA levels of GIRK1 and the estrogen receptors α (ESR1), β (ESR2), and GPR30 (GPER). The gene expression relative to the median expression value across all samples (n=905) is shown (blue: values below median; red: values above median. PAM50 classification (multicolor panel) and pathological ER, PR and Her2 expression status (blue: negative; red: positive) are given for each patient sample. The dendrogram on top shows that patients were divided into three main branches (A, B and C) based on the expression levels of the four genes analyzed.

Figure taken from: "KCNJ3 is a new independent prognostic marker for estrogen receptor positive breast cancer patients" by Kammerer et al; manuscript submitted to Oncotarget.

Group A consists of patients with low GIRK1 and ESR1 expression levels, being negative for ER and PR status and belonging to the basal like or Her2-enriched PAM50 subclasses. Groups B and C are mostly ER and PR positive and also have positive ESR1 gene expression. The difference is only in GIRK1 expression, which is negative in group B, but positive in group C. ESR2 and GPER did not correlate with GIRK1 expression. *See also: "KCNJ3 is a new independent prognostic marker for estrogen receptor positive breast cancer patients" by Kammerer et al; manuscript submitted to Oncotarget.*

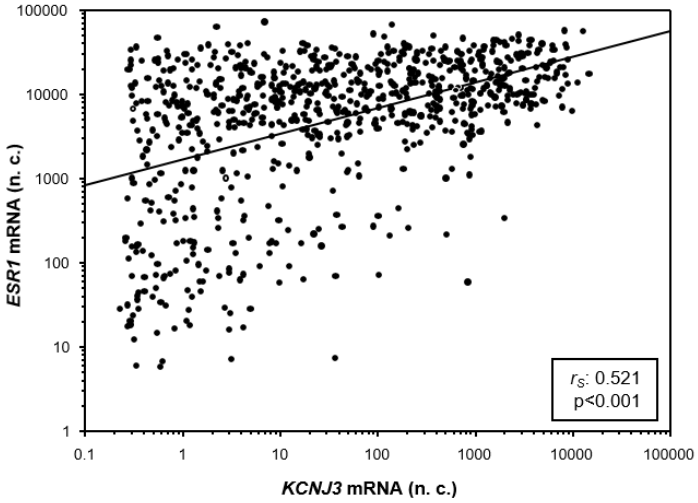

Figure 11: Scatter plot of GIRK1 and ESR1 mRNA expression levels.
905 breast cancer patient samples were analysed. Spearman rank correlation analysis revealed a statistical significant correlation between the expression of the two genes (r_S=0.521). n.c.: normalized counts.
Figure taken from: "KCNJ3 is a new independent prognostic marker for estrogen receptor positive breast cancer patients" by Kammerer et al; manuscript submitted to Oncotarget.

In line of these results it was of interest to study the correlation of GIRK1 and ESR1 mRNA expression. As shown in Figure 11 and by Spearman rank correlation analysis, the expression of the two genes correlated significantly with a correlation coefficient of 0.521 (p<0.001). *See also: "KCNJ3 is a new independent prognostic marker for estrogen receptor positive breast cancer patients" by Kammerer et al; manuscript submitted to Oncotarget.*

9.1.6 Survival analysis

Based on the results described above we further focused on the ER positive patient samples and wanted to study whether there was a difference between group B and C, i.e. between ER positive patients with high and ER positive patients with low GIRK1 expression levels. Overall survival was performed for ER positive patients using an auto-cutoff function for GIRK1 expression levels in *R*. The Kaplan Meier plot in Figure 12 shows that patients with high GIRK1 levels have a worse overall survival probability than patients with low GIRK1 levels in the tumor (p<0.05; HR=1.77). Disease free survival analysis could not be performed, since the data were not available from the TCGA. In addition to the Kaplan-Meier analysis shown above, also a uni- and multivariate Cox proportional hazard model was calculated to test whether GIRK1 is an independent prognostic biomarker for breast cancer. As shown in Table 8, the lymph node status, the metastasis status, the age at diagnosis, the PAM50 status and the GIRK1 expression had a significant influence on survival of the patients when the univariate model was used. In the multivariate analysis, only GIRK1 expression has a significant prognostic value for estrogen receptor positive breast cancer patients, meaning that it represents an independent prognostic biomarker for this disease. *See also: "KCNJ3 is a new independent prognostic marker for estrogen receptor positive breast cancer patients" by Kammerer et al; manuscript submitted to Oncotarget.*

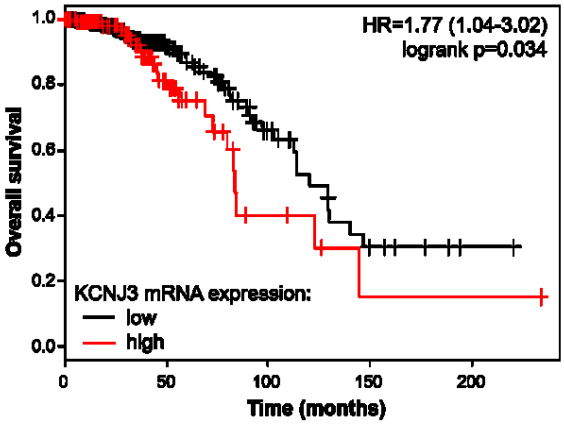

Figure 12: Overall survival of ER positive patients.

Kaplan-Meier plot of ER positive patient samples (n=647) with low and high GIRK1 expression levels as determined by RNAseq. Hazard ratio (HR) and logrank *p*-value is given.

Figure taken from: "KCNJ3 is a new independent prognostic marker for estrogen receptor positive breast cancer patients" by Kammerer et al; manuscript submitted to Oncotarget.

Table 8: Cox-proportional hazard models for ER positive breast cancer patients.

		univariate Cox model[a]		multivariate Cox model[b]	
		HR (95%-CI)	***p*-value**	**HR (95%-CI)**	***p*-value**
Size (T)	T1 vs. T2|T3|T4	1.0 (0.6-1.8)	0.985	5.9 (0.7-53.9)	0.113
LN status	neg. vs. pos.	1.8 (1.0-3.2)	0.042	0.7 (0.2-2.2)	0.513
M status	neg. vs. pos.	3.5 (1.5-8.3)	0.004	4.3 (0.8-23.2)	0.092
Histology	ductal vs. lobular	0.6 (0.1-2.4)	0.454	0.5 (0.1-3.3)	0.539
Her2 status	neg. vs. pos.	1.1 (0.4-2.8)	0.845	2.2 (0.2-22.5)	0.517
Menopause status	prem. vs. postm.	2.5 (0.9-7.0)	0.092	0.6 (0.02-20.9)	0.753
Age at diagnosis	≤50 vs. >50 years	1.9 (1.0-3.4)	0.038	2.7 (0.1-116.0)	0.589
PAM50 status	Lum A vs. Lum B	2.6 (1.3-5.3)	0.006	1.5 (0.4-5.9)	0.589
GIRK1 expression	low vs. high	1.8 (1.0-3.0)	0.036	5.2 (1.3-21.8)	0.021

[a]n=646; [b]n=228; LN: lymph node; M: metastasis; neg.: negative; pos.: positive; prem.: premenopausal; postm.: postmenopausal; Lum A: luminal A; Lum B: luminal B; low: (≤72th %ile); high: (>72th %ile); HR: hazard ratio; CI: confidence interval.

Table taken from: "KCNJ3 is a new independent prognostic marker for estrogen receptor positive breast cancer patients" by Kammerer et al; manuscript submitted to Oncotarget.

9.1.7 Genetic alterations and mutations of GIRK1

Using the information available from the TCGA, we aimed to test whether GIRK1 mRNA upregulation is a result of changes on DNA level, i.e. whether gene amplification causes the observed increased mRNA copy number. As shown in Figure 13, only two patients display

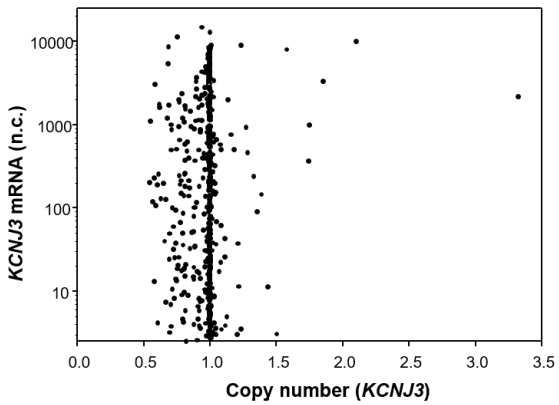

Figure 13: GIRK1 gene copy numbers versus mRNA expression.

890 breast cancer patient samples were analysed. A copy number of 1.0 indicates that no gene amplification or deletion on DNA level has happened. Spearman rank correlation analysis revealed no statistical significant increase or decrease in KCNJ3 gene copy number (r_S= -0.0207; not significant).

Figure taken from: "KCNJ3 is a new independent prognostic marker for estrogen receptor positive breast cancer patients" by Kammerer et al; manuscript submitted to Oncotarget.

GIRK1 gene amplification. The majority of patients have a normal GIRK1 copy number, while some patients display small deletions. *See also: "KCNJ3 is a new independent prognostic marker for estrogen receptor positive breast cancer patients" by Kammerer et al; manuscript submitted to Oncotarget.* Furthermore, we screened the TCGA data for genetic alterations and mutations using the cBioPortal (41,42). As shown in Figure 14A, only a negligible number (0.4%) display genetic alterations: one having a genetic amplification, one a genetic deletion and one a truncating mutation (Figure 14B).

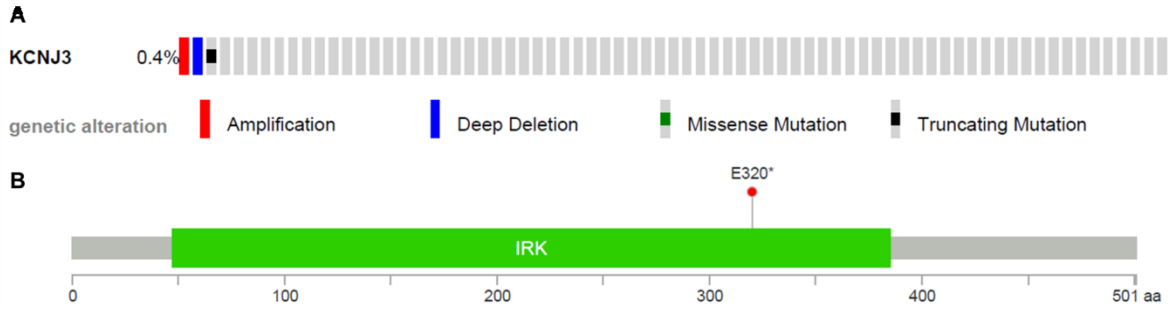

Figure 14: Genetic alterations of the GIRK1 gene in breast cancer patients.
A. Genetic alterations of single breast cancer patients of the TCGA. Each bar represents one patient. Not all patients without genetic alterations are shown for more clarity. **B.** Detailed view of the position of the truncating mutation. IRK: inwardly rectifying potassium channel. Both A and B were generated using the cBioPortal (41,42).

9.1.8 Promoter analysis

Since we were able to rule out genetic amplifications as cause for GIRK1 mRNA upregulation, and since we found a strong correlation between GIRK1 expression and ER positive breast cancer subtypes, we analyzed putative transcription binding sites within and upstream of the GIRK1 gene using the UCSC Genome Browser in order to test whether GIRK1 is a direct target of the transcriptional activity of ER. As shown in Figure 15, there are several putative transcription factor binding sites within the selected genetic region. However, there is only one putative binding site for ER in the second intron of the GIRK1 gene (highlighted by the red arrow). Details on the experimental procedures regarding the transcription factor of interest were available from ENCODE (Encyclopedia of DNA Elements at UCSC). The results for ER were generated using a ChIP (chromatin immunoprecipitation) method on an endometrial adenocarcinoma cell line. Five more ChIP assays in the same lab (two of them on the same cell line, three of them on a breast cancer

cell line) did not find ER hits within the same genetic region (49-51). Therefore, it remains elusive which factors are required for the transcription of the GIRK1 gene.

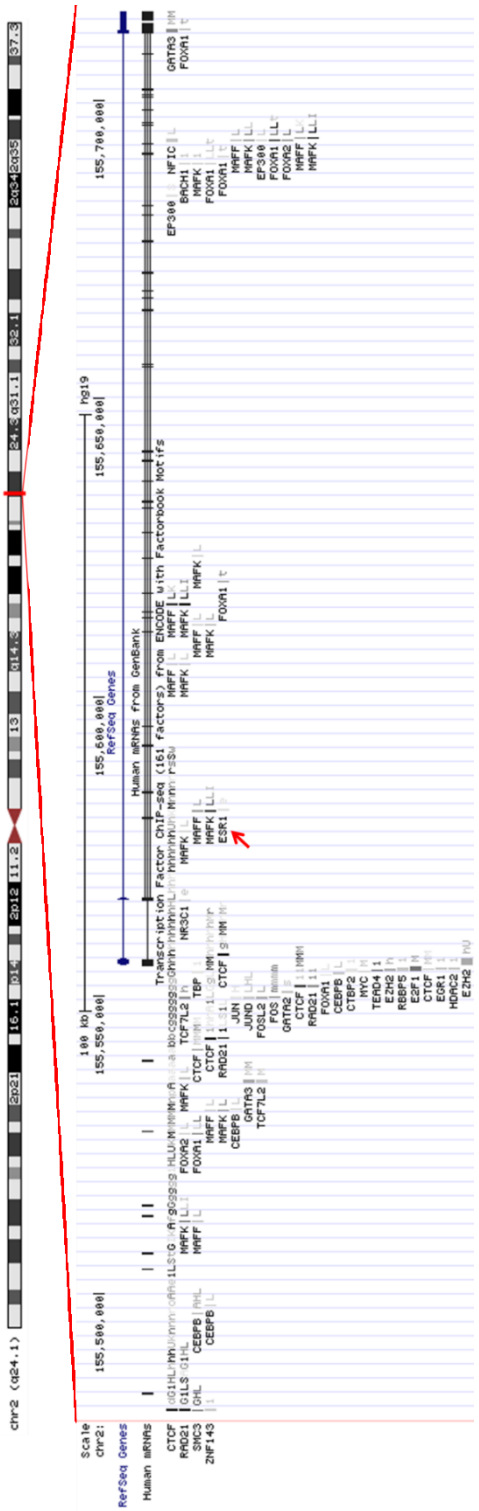

Figure 15: Putative transcription factor binding sites for the GIRK1 gene.

The section of chromosome 2 encoding for GIRK1 and an upstream part are shown as detail. Bars mark the putative binding sites and are labelled with the putative transcription factor. *The arrow highlights the putative binding site of ESR1.*

9.2 Establishment of methods for the detection of GIRK1 in FFPE tissue

The screening of the TCGA data set for expression patterns of GIRK1 mRNA in different breast cancer subtypes showed a link between GIRK1 upregulation and ER positive breast cancer. Thus, our next aim was to detect and validate GIRK1 mRNA and/or protein in a set of ER positive breast cancer patients.

9.2.1 Specificity and sensitivity of anti-GIRK1 antibodies in western blots

First, it was necessary to identify an anti-GIRK1 antibody with high sensitivity and specificity that could further be used in IHC. After carefully studying the literature and data sheets of antibody selling companies, we decided to test four commercially available antibodies (two polyclonal ones from Santa Cruz and Alomone and two monoclonal ones from Abcam and Alomone). In addition, two custom made polyclonal antibodies were generated by Kurt Schmidt (Institute of Pharmacological Sciences, University of Graz), one directed against the N- and one against the C-terminus of the GIRK1 protein. Before testing the antibodies in IHC, we did western blot analysis to see whether the antibodies produce specific bands. Out of the six anti-GIRK1 antibodies tested (see Table 3 and Figure 16), the two custom-made rabbit polyclonal antibodies and the Abcam and Alomone mouse monoclonal antibody revealed specific bands at 56 kD and 72 kD (representing the native and glycosylated form of GIRK1, respectively) on western blots using GIRK1 transfected *X. laevis* oocytes or cell lines as controls (Figure 16B-D and G). The rabbit polyclonal antibody directed against the N-terminus of GIRK1 antibody had to be excluded for further analysis due to low sensitivity in positive controls together with strong unspecific bands at 120 kD in negative controls (Figure 16D). Also the Alomone monoclonal antibody was excluded due to low sensitivity (Figure 16G) It was not possible to produce clear specific signals with the remaining two antibodies (Figure 16E-F). During the test phase, antibody dilutions ranging from 1:100 to 1:1500 were used to determine the optimal concentration for each antibody.

Based on these results, the Abcam monoclonal antibody was selected for further testing in IHC. *See also "Critical evaluation of KCNJ3 gene product detection in human breast cancer: mRNA in situ hybridization is superior to immunohistochemistry" by Kammerer et al.; accepted for publication in the Journal of Clinical Pathology.*

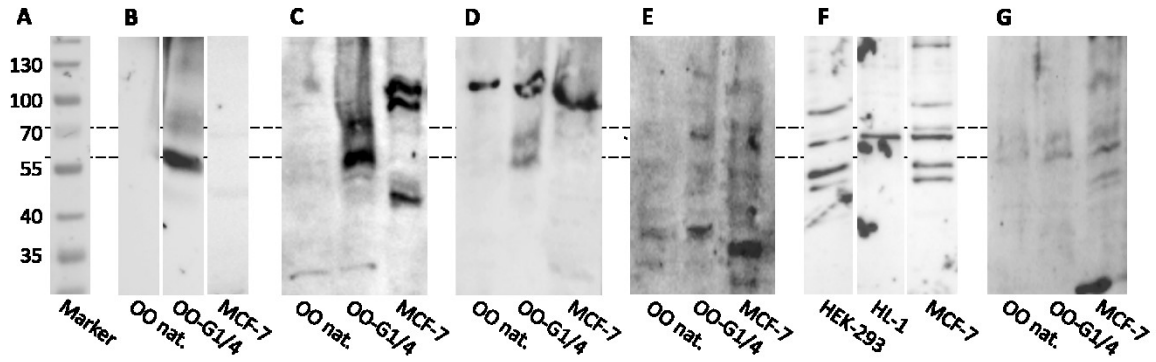

Figure 16: Testing of anti-GIRK1 antibodies on western blots.

A. Protein marker (molecular weight in kiloDalton is given to the left of each band). **B.** Abcam monoclonal antibody, diluted 1:1000, produced specific bands at 56 kD and 72 kD in the positive control (OO-G1/4: *Xenopus laevis* oocytes overexpressing human GIRK1/GIRK4 heterotetrameric channels). The negative control (native *X. laevis* oocytes) and MCF-7 breast cancer cells were negative. **C.** Custom-made polyclonal antibody (C-terminal), diluted 1:1000, produced specific bands at reasonable intensity in the positive control (OO-G1/4). The negative control (OO nat.) and MCF-7 cells resulted in additional bands that did not represent the expected band sizes for GIRK1. **D.** Custom-made polyclonal antibody (N-terminal), diluted 1:650, produced specific signals but at low intensity in the positive control (OO-G1/4), deemed unsuitable for sensitive GIRK1 protein detection in immunohistochemistry (IHC). In addition, strong bands at approx. 120 kD were present with equal intensity in all three lanes. **E.** Santa Cruz polyclonal antibody, diluted 1:200, did not display any bands that could be unequivocally attributed to GIRK1 protein expression and produced high background. **F.** Alomone polyclonal antibody, diluted 1:200, might display a positive signal in the positive control (HL-1 cells), but resulted in additional bands in both the negative control (HEK-293) and in MCF-7 cells that could not be clearly attributed to GIRK1. HEK-293 and HL-1 cells served as alternative negative and positive controls since they were used as controls also in IHC and *X. laevis* oocytes were not available. **G.** Alomone monoclonal antibody, diluted 1:200, produced specific bands but at low intensity in the positive control (OO-G1/4). MCF-7 cells resulted in additional bands that did not represent the expected band sizes for GIRK1.

30 µg total protein were loaded for oocytes, 75 µg protein for cell lines. The dashed line represents the expected locations of specific bands for GIRK1 in its native and glycosylated form at 56 and 72 kD.

Figure taken from: "Critical evaluation of KCNJ3 gene product detection in human breast cancer: mRNA in situ hybridization is superior to immunohistochemistry" by Kammerer et al.; accepted for publication in the Journal of Clinical Pathology.

9.2.2 Specificity and sensitivity of the selected anti-GIRK1 antibody in IHC

We tested the Abcam monoclonal antibody in IHC on formalin-fixed, agarose-embedded HL-1, HEK-293, MCF-7 wild type and MCF-7 GIRK1 overexpressing cells. The staining was negative in HEK-293 (negative control, Figure 17A) and MCF-7 cells (Figure 17C) and positive in HL-1 and MCF-7 GIRK1 overexpressing cells (positive controls, Figure 17B and D). Membrane staining could be observed in HL-1 cells, while the staining was predominantly located in the cytoplasm of GIRK1 overexpressing MCF-7 cells. In order to test the anti-GIRK1 antibody also on mammalian tissue sections, we used a mouse heart, where the atrium served as positive control and the ventricle as negative control. As expected and depicted in Figure 17E-F, the staining of the mouse atrium is strong, specific and localized both in the cytoplasm and on the membrane, while the ventricle remained negative. *See also: "Critical evaluation of KCNJ3 gene product detection in human breast cancer: mRNA in situ hybridization is superior to immunohistochemistry" by Kammerer et al.; accepted for publication in the Journal of Clinical Pathology.*

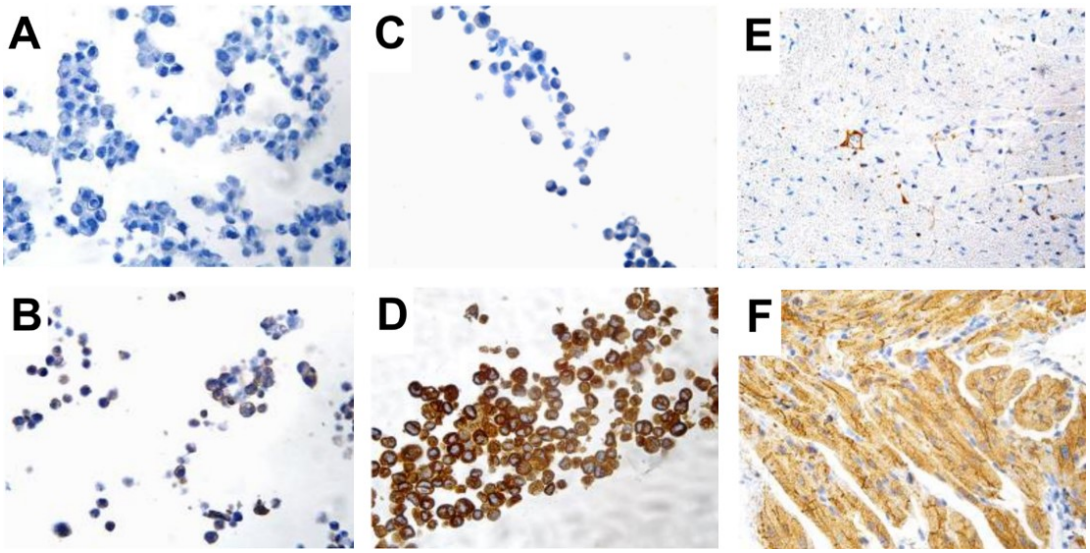

Figure 17: GIRK1 IHC on cell lines and mouse heart.

Formalin-fixed, agarose-embedded **A.** HEK-293 cells (negative control); **B.** HL-1 cells (positive control); **C.** MCF-7 cells; and **D.** MCF-7 cells overexpressing GIRK1. FFPE mouse **E.** ventricle; and **F.** atrium.

The mouse monoclonal anti-GIRK-1 antibody from Abcam was used in 1:50 dilution. Pictures were taken at 40x magnification.

Figure panels taken from: "Critical evaluation of KCNJ3 gene product detection in human breast cancer: mRNA in situ hybridization is superior to immunohistochemistry" by Kammerer et al.; accepted for publication in the Journal of Clinical Pathology

9.2.3 Specificity and sensitivity of RNA *in situ* hybridization

In addition, we also established a RNA *in situ* hybridization (ISH) protocol for the detection of GIRK1 mRNA in human FFPE tissue. The method was directly established on FFPE patient samples without previous testing on cell lines and mouse tissue, since the protocol is different in some crucial points depending on the material used. Thus, we selected patient samples from our cohort with high, intermediate and low GIRK1 expression as determined by microarray analysis previously. As quality control, sections were stained in addition to the GIRK1 staining with a negative (DapB) and a positive control probe (POLR2A). Figure 18 shows representative images of these stainings for GIRK1 and the corresponding controls. GIRK1 RNA signals were present as expected (shown in the top pictures of Figure 18). The lower left images display the corresponding negative controls which were negative in all instances. Corresponding positive controls (lower right images) were positive with at least 2.5 spots per cell as determined using the image analysis software (see Figure 2). As additional control, and to test whether the ISH method was stable between different runs, we stained the same sample several times using the positive control probe. Figure 19 shows that the method was highly stable and reproducible between runs. *See also: "Critical evaluation of KCNJ3 gene product detection in human breast cancer: mRNA in situ hybridization is superior to immunohistochemistry" by Kammerer et al.; accepted for publication in the Journal of Clinical Pathology.*

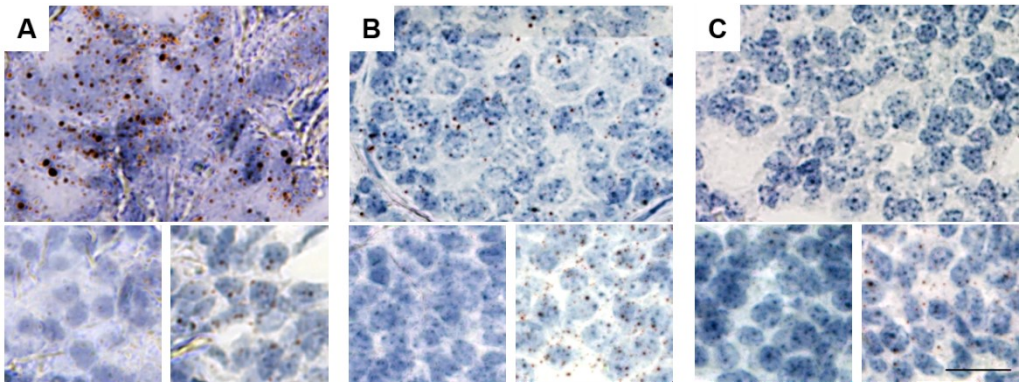

Figure 18: RNA ISH of GIRK1 and controls on FFPE breast cancer samples.

Generic micrographs for patients with **A.** high, **B.** intermediate, and **C.** low GIRK1 expression according to corresponding microarray data are shown.

Micrograph on top of each panel: GIRK1 probe; lower left micrographs: DapB probe (negative control); lower right micrographs: POLR2A probe (positive control). Scale bar: 20 µm; all images shown at identical magnification.

Figure panels taken from: "Critical evaluation of KCNJ3 gene product detection in human breast cancer: mRNA in situ hybridization is superior to immunohistochemistry" by Kammerer et al.; accepted for publication in the Journal of Clinical Pathology.

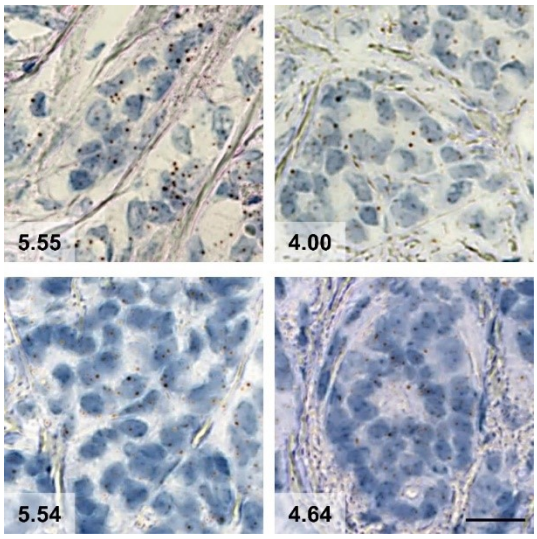

Figure 19: Reproducibility of RNA *in situ* hybridization.

Consecutive sections of the same patient sample were hybridized in different runs using the *POLR2A* probe (positive control). Numbers in boxes indicate the average number of spots per cell as determined with the SpotStudio software, and indicate that results were comparable between runs.

Scale bar: 20 µm; all images shown at identical magnifications.

Figure taken from: "Critical evaluation of KCNJ3 gene product detection in human breast cancer: mRNA in situ hybridization is superior to immunohistochemistry" by Kammerer et al.; accepted for publication in the Journal of Clinical Pathology.

9.3 Analysis of the validation set

Since the TCGA data clearly demonstrated that GIRK1 expression plays a role not in all, but in ER positive breast cancer patients only, we used a ER positive patient cohort as validation set. The patient characteristics are given in "Material and Methods". The microarray data set consisted of 298 patients, while tissue blocks were available from 66 patients. After having established two protocols for the detection of GIRK1 in human tissue, we performed immunohistochemical staining of GIRK1 and Ki-67 on the 46 patient samples available from the Medical University of Graz. In addition, RNA *in situ* hybridization was performed on all tissue samples of the validation set. Results were used to perform survival analysis. Since also microarray data were available from this cohort, we first analyzed the gene expression as we did with the TCGA data. Details are described in the following sections.

9.3.1 Association analysis

Despite clinical data were not fully available, we performed association analysis with the existing data to detect positive or negative associations of GIRK1 mRNA expression levels with any clinical features. Corresponding *p*-values were calculated where possible, i.e. where the clinical feature comprised more than two groups. GIRK1 mRNA was highly associated with the PAM50 classification. Borderline significance with low association coefficients could be observed for the age of diagnosis and the tumor size. Table 9 summarizes the results.

Table 9: Association analysis of GIRK1 mRNA and clinical features.

Clinical feature	association coefficient	*p*-value
Age at diagnosis	0.209	0.038327
PR status	0.021	---
Her2 status	-0.138	---
PAM50 classification	0.321	1.89E-06
Tumor size (T)	0.193	0.055917
Lymph nodes (N)	-0.063	---
Tumor stage	0.008	0.940282

9.3.2 Correlation analysis

Again, we performed Spearman rank correlation analysis of GIRK1 with all other genes to get insights into which genes are co-expressed or -repressed with GIRK1. Table 10 shows the 25 genes with the highest and lowest Spearman rank correlation coefficients. Functional annotations of genes positively and negatively correlating with GIRK1 to gene ontology (GO) terms and pathways was performed using the DAVID tool. The cut-off values were set at $r_S \geq 0.4$ and $r_S \leq (-0.4)$. Results were considered as relevant when the false discovery rate (FDR) was below 10 and the *p*-value was smaller than 0.05. Eight GO terms could be identified for the genes positively correlating with GIRK1, and 41 GO terms could be identified for the negative correlations (Table 11). Several genes positively correlating with GIRK1 are involved in membrane or ion functions, while some genes negatively correlating with GIRK1 rather have nucleotide binding functions (Table 11).

Table 10: Genes positively and negatively correlating with GIRK1

Gene 1	Genes$^{(pos)}$	$r_S^{(pos)}$	*p*-value$^{(pos)}$	Genes$^{(neg)}$	$r_S^{(neg)}$	*p*-value$^{(neg)}$
KCNJ3	KCNJ3	1	0	HIVEP2	-0.3435883	1.42E-09
KCNJ3	KCNJ3	0.60388015	0	NQO1	-0.3442871	1.31E-09
KCNJ3	DNAJC12	0.38976531	4.16E-12	AMMECR1	-0.3443592	1.30E-09
KCNJ3	CCBL1	0.38025765	1.53E-11	TAB2	-0.3467149	9.91E-10
KCNJ3	SPR	0.35280529	4.83E-10	LMO4	-0.346957	9.63E-10
KCNJ3	NTNG1	0.35258128	4.96E-10	ADD3	-0.3479039	8.62E-10
KCNJ3	ORAI3	0.35131568	5.77E-10	DDX19A	-0.3484439	8.09E-10
KCNJ3	ESR1	0.35123677	5.82E-10	CEP170	-0.3492851	7.33E-10
KCNJ3	BMPR1B	0.35096833	6.01E-10	HIVEP1	-0.3510731	5.94E-10
KCNJ3	GLRB	0.35023508	6.56E-10	PTGIS	-0.3517995	5.45E-10
KCNJ3	EML2	0.34975396	6.94E-10	MTMR2	-0.3544096	3.99E-10
KCNJ3	MAGEC2	0.34375154	1.40E-09	SLC10A3	-0.3551356	3.66E-10
KCNJ3	AGTR1	0.343026	1.52E-09	FOXN3	-0.3564057	3.14E-10
KCNJ3	SLC7A4	0.34073377	1.97E-09	GALNT3	-0.3600425	2.02E-10
KCNJ3	RPL23A	0.34043676	2.04E-09	ACTR3	-0.3603336	1.95E-10
KCNJ3	RPL23A	0.33937113	2.31E-09	RECK	-0.362536	1.48E-10
KCNJ3	GGA2	0.3383445	2.59E-09	RSU1	-0.3641082	1.22E-10
KCNJ3	TCTN1	0.33755548	2.83E-09	IDH2	-0.3650877	1.08E-10
KCNJ3	RPL23A	0.33748248	2.85E-09	ACTR3	-0.3667976	8.73E-11
KCNJ3	RAB17	0.33676783	3.09E-09	OPN3	-0.3682301	7.29E-11
KCNJ3	BTF3	0.3356886	3.49E-09	UBE2E3	-0.3727987	4.07E-11
KCNJ3	STRADA	0.33531177	3.64E-09	MINA	-0.3766903	2.45E-11
KCNJ3	P4HTM	0.3350592	3.75E-09	HIVEP2	-0.3828079	1.09E-11
KCNJ3	PHF7	0.33344897	4.48E-09	MGA	-0.388711	4.83E-12
KCNJ3	MLPH	0.3332041	4.61E-09	MINA	-0.3982046	1.22E-12

$^{(pos)}$: positive correlation, $^{(neg)}$: negative correlation, r_S: Spearman rank correlation coefficient

Table 11: Functional annotation analysis of genes positively correlating with GIRK1

Cat.	Term	#	%	*p*-value	FDR [%]
Positive correlation:					
CC	GO:0019898~extrinsic to membrane	10	9.434	0.00238	2.874
MF	GO:0043167~ion binding	37	34.906	0.00308	4.100
CC	GO:0031226~intrinsic to plasma membrane	16	15.094	0.00443	5.287
MF	GO:0046914~transition metal ion binding	27	25.472	0.00438	5.778
BP	GO:0048666~neuron development	8	7.547	0.00403	6.217
CC	GO:0044459~plasma membrane part	23	21.698	0.00737	8.641
MF	GO:0016705~oxidoreductase activity, acting on paired donors, with incorporation or reduction of molecular oxygen	5	4.717	0.00701	9.091
MF	GO:0046872~metal ion binding	35	33.019	0.00757	9.791

Cat.	Term	#	%	*p*-value	FDR [%]
Negative correlation:					
MF	GO:0000166~nucleotide binding	32	2.691	3.77E-05	0.051
MF	GO:0046983~protein dimerization activity	13	1.093	2.57E-04	0.345
MF	GO:0032555~purine ribonucleotide binding	26	2.187	3.37E-04	0.453
MF	GO:0032553~ribonucleotide binding	26	2.187	3.37E-04	0.453
BP	GO:0030183~B cell differentiation	5	0.421	3.63E-04	0.588
MF	GO:0005524~ATP binding	22	1.850	6.41E-04	0.858
MF	GO:0017076~purine nucleotide binding	26	2.187	6.53E-04	0.874
MF	GO:0032559~adenyl ribonucleotide binding	22	1.850	7.64E-04	1.022
BP	GO:0048518~positive regulation of biological process	28	2.355	7.09E-04	1.144
CC	GO:0005737~cytoplasm	65	5.467	0.00101	1.271
CC	GO:0043231~intracellular membrane-bounded organelle	69	5.803	0.00120	1.519
CC	GO:0043227~membrane-bounded organelle	69	5.803	0.00124	1.564
MF	GO:0030554~adenyl nucleotide binding	22	1.850	0.00148	1.979
MF	GO:0001883~purine nucleoside binding	22	1.850	0.00179	2.384
MF	GO:0001882~nucleoside binding	22	1.850	0.00195	2.592
CC	GO:0016323~basolateral plasma membrane	7	0.589	0.00216	2.707
CC	GO:0044424~intracellular part	84	7.065	0.00237	2.971
MF	GO:0004672~protein kinase activity	12	1.009	0.00234	3.102
BP	GO:0048522~positive regulation of cellular process	25	2.103	0.00205	3.278
BP	GO:0042113~B cell activation	5	0.421	0.00206	3.290
CC	GO:0043229~intracellular organelle	74	6.224	0.00268	3.354
CC	GO:0043226~organelle	74	6.224	0.00281	3.513
MF	GO:0016773~phosphotransferase activity, alcohol group as acceptor	13	1.093	0.00303	4.004
MF	GO:0042802~identical protein binding	12	1.009	0.00356	4.678
BP	GO:0046777~protein amino acid autophosphorylation	5	0.421	0.00310	4.907
BP	GO:0030335~positive regulation of cell migration	5	0.421	0.00365	5.767
CC	GO:0009898~internal side of plasma membrane	8	0.673	0.00469	5.800
CC	GO:0005622~intracellular	85	7.149	0.00519	6.394
MF	GO:0004713~protein tyrosine kinase activity	6	0.505	0.00507	6.605
BP	GO:0001775~cell activation	8	0.673	0.00427	6.714
BP	GO:0042981~regulation of apoptosis	14	1.177	0.00435	6.824
BP	GO:0043067~regulation of programmed cell death	14	1.177	0.00472	7.393
BP	GO:0010941~regulation of cell death	14	1.177	0.00487	7.615
CC	GO:0030055~cell-substrate junction	5	0.421	0.00624	7.644
BP	GO:0051272~positive regulation of cell motion	5	0.421	0.00515	8.039
BP	GO:0040017~positive regulation of locomotion	5	0.421	0.00515	8.039
CC	GO:0044428~nuclear part	22	1.850	0.00666	8.141
BP	GO:0006403~RNA localization	5	0.421	0.00553	8.609
MF	GO:0042803~protein homodimerization activity	8	0.673	0.00699	9.006
MF	GO:0005515~protein binding	68	5.719	0.00716	9.213
BP	GO:0030098~lymphocyte differentiation	5	0.421	0.00614	9.508

Table 11: Cat.: Category, #: number of genes involved in GO, %: percentage of genes involved in GO, FDR: false discovery rate, BP: biological process, CC: cellular component, MF: molecular function.

We also performed pathway analysis as for the TCGA, but no pathway fulfilled the above mentioned criteria neither for the positively nor the negatively correlating genes. Hierarchical cluster analysis was not performed for the validation set since all samples were ER positive and therefore, no additional insights were expected. Spearman rank correlation analysis was performed to study the correlation between GIRK1 and ESR1 mRNA expression (Figure 20). The expression of the two genes correlated significantly with a correlation coefficient of 0.351 (p<0.001). *See also: "KCNJ3 is a new independent prognostic marker for estrogen receptor positive breast cancer patients" by Kammerer et al; manuscript submitted to Oncotarget.*

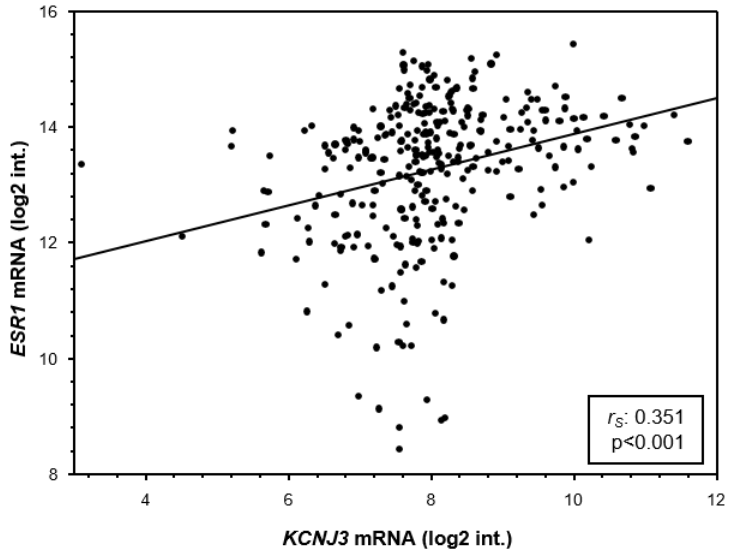

Figure 20: Scatter plot of GIRK1 and ESR1 mRNA expression levels.
298 breast cancer patient samples were analysed. Spearman rank correlation analysis revealed a statistical significant correlation between the expression of the two genes (r_S=0.351). log2 int.: log2 intensities.
Figure taken from: "KCNJ3 is a new independent prognostic marker for estrogen receptor positive breast cancer patients" by Kammerer et al; manuscript submitted to Oncotarget.

9.3.3 Ki-67 IHC on patient samples

We next moved on to stain the available tissue as follows. Ki-67 staining was first performed on the patient samples available from the Medical University of Graz only. The staining was successful in 44 patients. As the scoring was performed based on percentage of positive nuclei, we grouped the scores in low (up to 15% positive nuclei), intermediate (16-29% positive nuclei) and high (more than 30% positive nuclei) Ki-67 expression. Most patients (n=31) had a low Ki-67 score, while 7 patients had an intermediate and 6 patients a high score. Figure 21 shows representative images of low (A), intermediate (B) and high (C) Ki-67 expression.

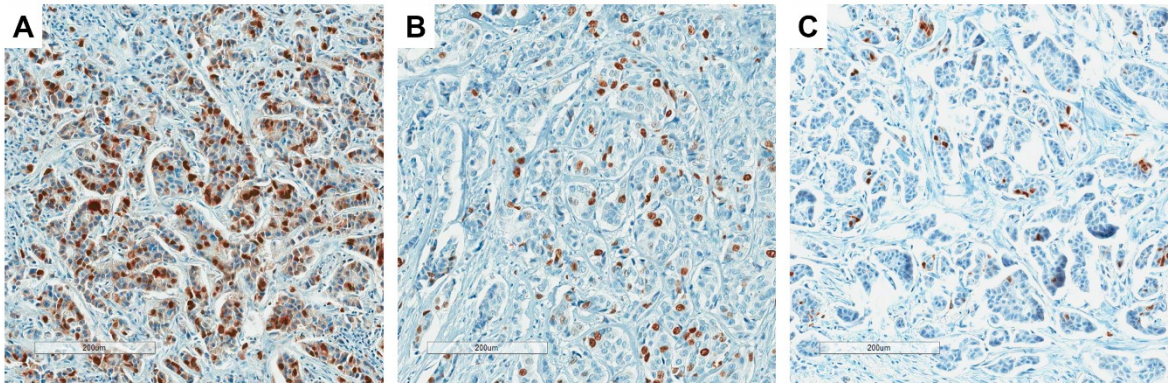

Figure 21: Ki-67 IHC on patient samples.

A. Representative image of a patient sample with low (5%) Ki-67 expression. **B.** Representative image of a patient sample with intermediate (20%) Ki-67 expression. **C.** Representative image of a patient sample with high (75%) Ki-67 expression.
Pictures were taken at 10x magnification.

We next wanted to know whether the Ki67 staining had an influence on survival times of our patients, since it represents an important marker in breast cancer. Figure 22 shows that there was no statistical significant difference in disease free or overall survival times when patients with low and high Ki67 expression were compared. Therefore, we did not stain the remaining samples for Ki67 and proceeded with analysis of GIRK1 expression levels.

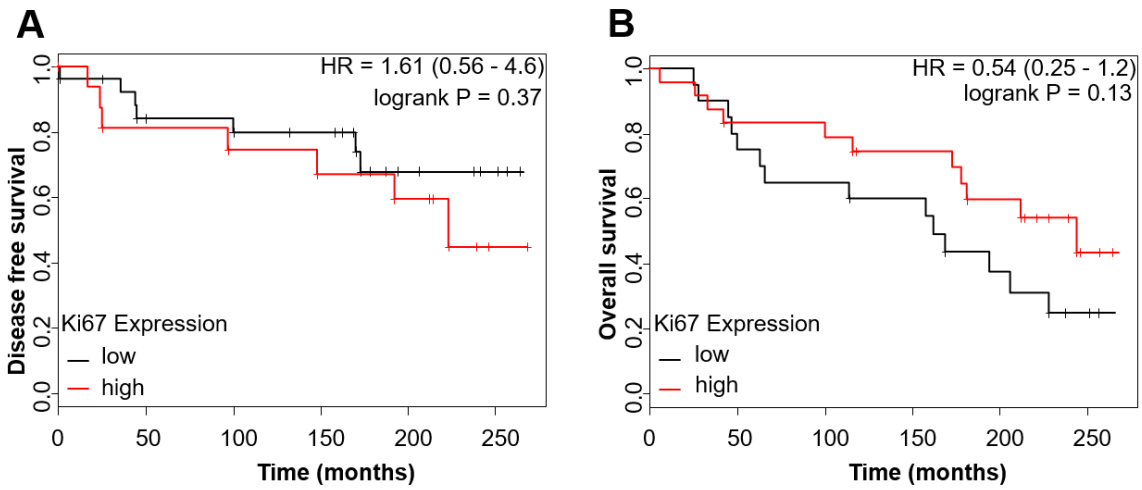

Figure 22: Survival analysis based on Ki67 IHC scoring.

A. Kaplan-Meier plot showing disease free survival probabilities for patients with low (≤15% positive nuclei) or high Ki67 expression (>15% positive nuclei). **B.** Same as A., but showing overall survival probabilities.

Hazard ratios (HR) and logrank *p*-values are given; n=44.

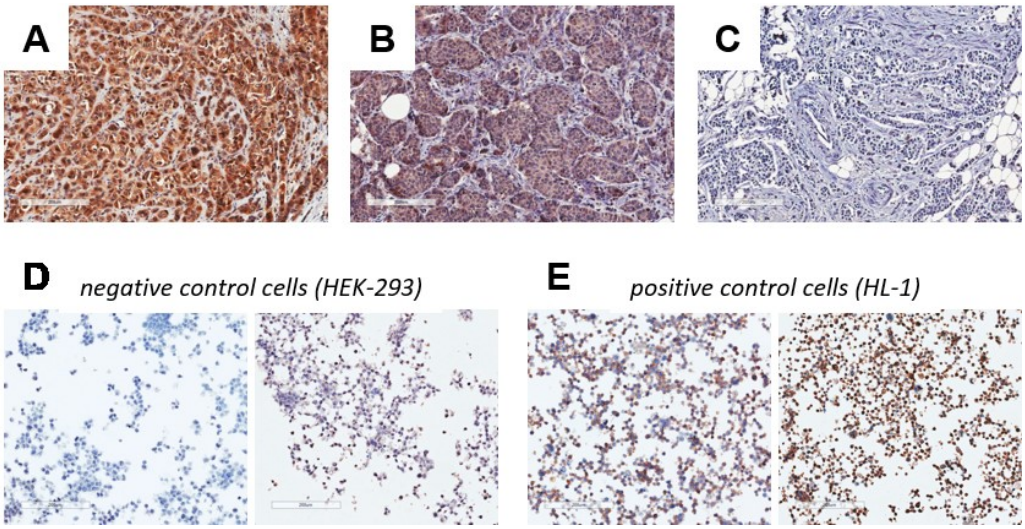

Figure 23: GIRK1 IHC on patient samples and controls.

Generic micrographs of patients with **A.** high, **B.** intermediate, and **C.** low GIRK1 protein expression. **D.** Two examples of on slide negative control cells (HEK-293), and **E.** positive control cells (HL-1).

Figure panels taken from: "Critical evaluation of KCNJ3 gene product detection in human breast cancer: mRNA in situ hybridization is superior to immunohistochemistry" by Kammerer et al.; accepted for publication in the Journal of Clinical Pathology.

9.3.4 GIRK1 IHC on patient samples

Out of 46 patients, GIRK1 IHC could be performed on 45 samples. The remaining sample had to be excluded, because the corresponding tissue block had only little material remaining which did not contain any tumor cells. Most patients (n=17) had a staining score 1, or score 0 (12 patients). Six patients had an IHC score of 2 and 10 patients a score of 3. Figure 23 shows representative pictures of high (A), intermediate (B), and negative (C) GIRK1 staining. Figure 23D-E shows representative pictures of negative (HEK-293) and positive on-slide controls (HL-1). These images show that the staining of the on-slide controls was not very stable and reproducible, even within same runs. Negative controls displayed slight positivity in several instances and positive controls were not always as strong as expected. *See also: "Critical evaluation of KCNJ3 gene product detection in human breast cancer: mRNA in situ hybridization is superior to immunohistochemistry" by Kammerer et al.; accepted for publication in the Journal of Clinical Pathology.* Therefore, before continuing with the IHC staining of the remaining patient samples, we performed interim survival analysis. Figure 24 shows that there was no significant difference between disease free or overall survival probabilities when patients with low or high GIRK1 protein expression were compared.

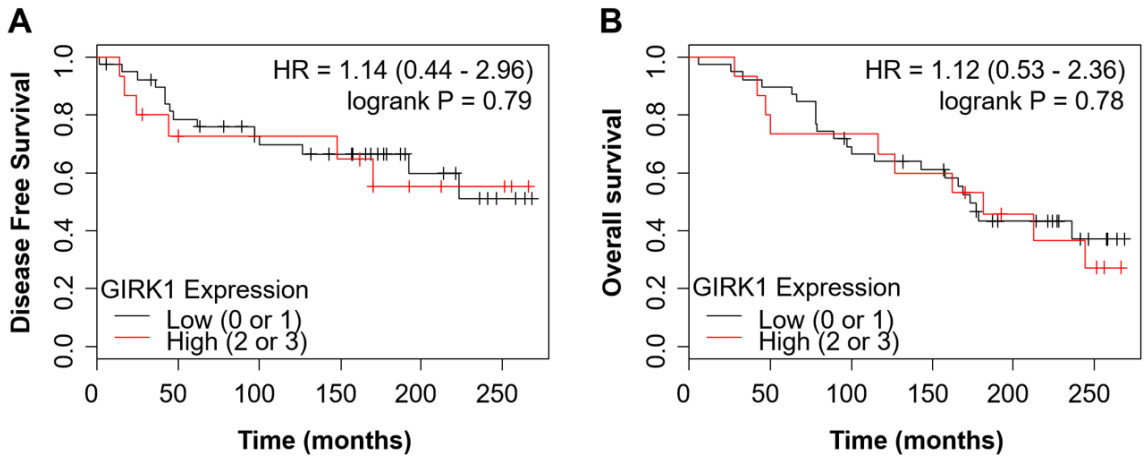

Figure 24: Survival analysis based on GIRK1 IHC scoring.

A. Kaplan-Meier plot showing disease free survival probabilities for patients with low (IHC score 0 or 1) or high GIRK1 protein expression (IHC score 2 or 3). **B.** Same as A., but showing overall survival probabilities.

Hazard ratios (HR) and logrank *p*-values are given; n=45.

9.3.5 Correlation of different GIRK1 expression results

In order to test whether the survival data above are true findings or rather due to methodological issues, we decided to compare the findings of the IHC with ISH. To do so, we selected 15 patient samples with known GIRK1 mRNA expression as determined by microarray analysis – each five of them with high, intermediate and low GIRK1 expression levels. IHC was already performed previously and we stained the samples using the ISH method described. Table 12 summarizes the patient characteristics of the selected patient samples and the results of GIRK1 expression as determined by microarray analysis, IHC and RNA ISH. As already seen from Table 12, microarray and RNA ISH data seem to fit well, while IHC data do not look highly convincing. We performed Spearman rank correlation analysis to study to what extend the results generated by the different methods would

Table 12: Patient characteristics and GIRK1 expression levels.

	Clinicopathological patient characteristics							Results of GIRK1 expression		
#	**AAD**	**Grade**	**pT**	**LN**	**pM**	**ER**	**PR**	**Microarray**	**IHC**	**RNA ISH**
8905	78	2	2	3/20	-	+	+	11.407	3	33.33
1057	60	2	2	5/20	-	+	+	9.417	3	10.11
313	56	2	2	3/23	-	+	+	9.393	3	9.01
1299	71	2	2	0/29	-	+	+	9.109	2	2.69
1098	68	3	2	0/18	-	+	-	8.917	1	0.33
527	68	2	1	11/18	-	+	+	8.239	3	1.28
1113	43	2	3	2/8	-	+	-	8.207	1	2.10
961	50	1	4	0/11	-	+	-	8.061	3	0.28
765	70	3	2	0/17	+	+	+	8.042	2	1.53
684	63	2	2	0/14	-	+	-	7.919	0	0.16
856	62	3	2	9/27	+	+	+	7.205	1	0.07
652	50	1	1	3/16	-	+	+	7.174	1	0.28
854	63	2	1	0/0	+	+	+	6.918	1	1.26
1129	53	2	4	16/19	-	+	+	6.740	2	0.07
1280	70	2	2	3/14	-	+	-	5.656	0	0.07

#: patient sample number; AAD: age at diagnosis; pT: tumor size staging; LN: lymph nodes (positive/total examined); pM: distant metastasis status; ER: estrogen receptor; PR: progesterone receptor; Microarray: log2-intensities of GIRK1 expression; IHC: immunohistochemical score of GIRK1 protein expression; RNA ISH: GIRK1 RNA in situ hybridization results as spots/cell; -: negative; +: positive.

Table taken from: "Critical evaluation of KCNJ3 gene product detection in human breast cancer: mRNA in situ hybridization is superior to immunohistochemistry" by Kammerer et al.; accepted for publication in the Journal of Clinical Pathology.

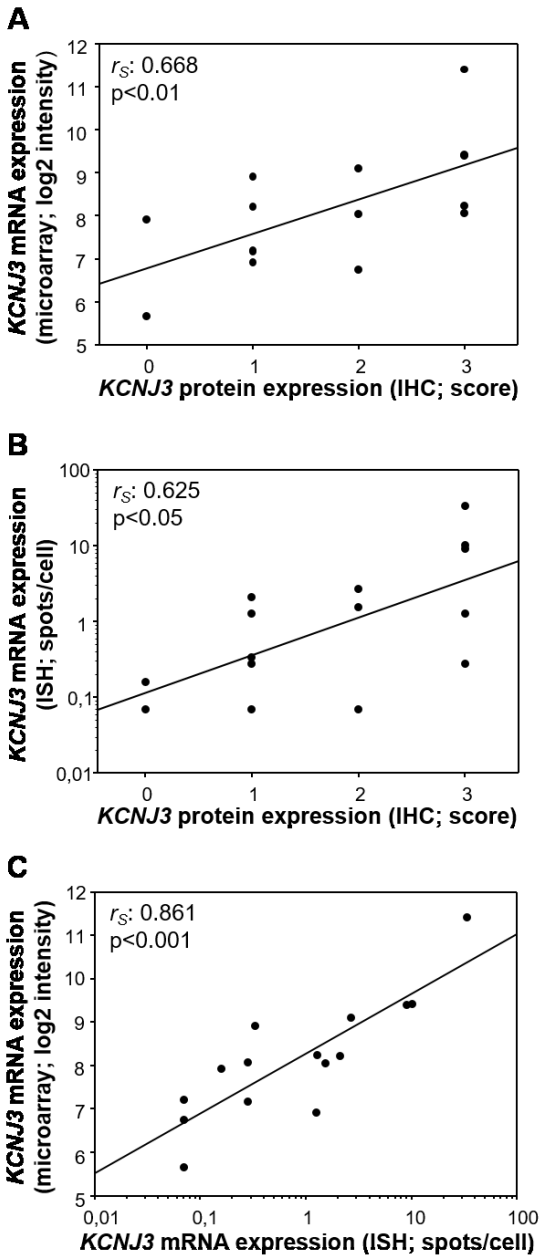

Figure 25: Correlation of GIRK1 expression as assessed by different methods.

A. Scatter plot of GIRK1 expression levels in 15 breast cancer patients as assessed by microarray (log2 intensity) and immunohistochemistry (IHC) score. **B.** RNA *in situ* hybridization (ISH; spots/cell) vs. IHC (score) are plotted. **C.** Log2 intensity of microarray vs. RNA ISH (spots/cell) are plotted.

Spearman rank correlation coefficients (r_S) and *p*-values are given for each plot; n=15.

Figure taken from: "Critical evaluation of KCNJ3 gene product detection in human breast cancer: mRNA in situ hybridization is superior to immunohistochemistry" by Kammerer et al.; accepted for publication in the Journal of Clinical Pathology.

correlate. It became evident that IHC results correlated moderately with microarray (r_S: 0.668; Figure 25A) and RNA ISH data (r_S: 0.625; Figure 25B), but microarray and RNA ISH data correlated very well (r_S: 0.861; Figure 25C). Based on these results and the fact that the selected anti-GIRK1 antibody did not display stable staining results on on-slide controls, we decided to use RNA ISH as primary detection method for GIRK1 in our patient samples. *See also: "Critical evaluation of KCNJ3 gene product detection in human breast cancer: mRNA in situ hybridization is superior to immunohistochemistry" by Kammerer et al.; accepted for publication in the Journal of Clinical Pathology.*

9.3.6 RNA-ISH on patient samples

Out of the 66 patient samples available from the Medical Universities of Graz and Innsbruck, 64 could be stained successfully. The two other samples could not be evaluated due to detachment of the tissue from the glass slide during the treatment. Further, ten samples were excluded for subsequent analysis because the positive control stainings did not fulfill the cut-off criterion of having ≥2.5 spots/cells which indicates poor RNA quality. The staining was repeated for these 12 samples, but led to the same results. Table 13 summarizes the results of GIRK1 expression as determined by microarray analysis and RNA ISH as well as corresponding RNA ISH controls. The mean value for negative controls was 0.14±0.13

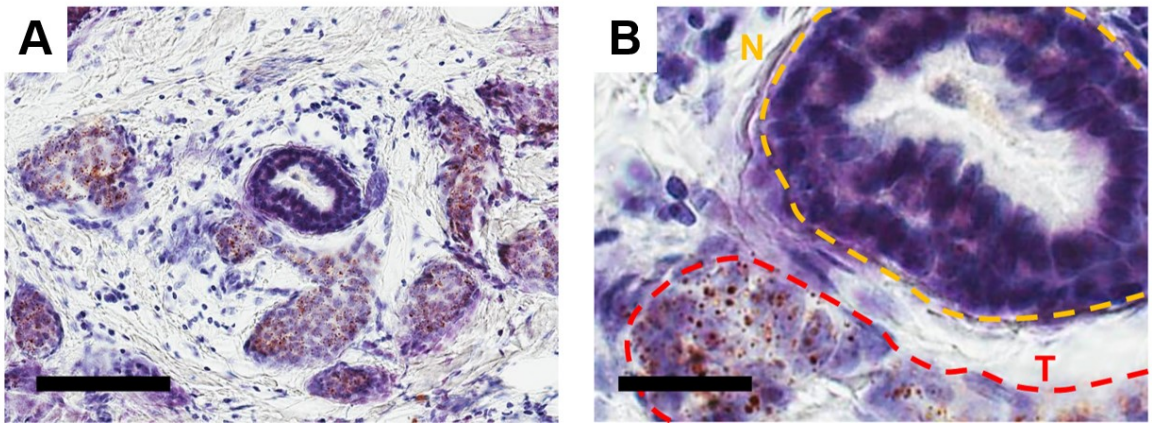

Figure 26: Example of GIRK1 RNA ISH.

A. GIRK1 RNA in situ hybridization of a patient sample with high GIRK1 expression. Positive signals (brown spots) are present in tumor cells only. Scale bar: 100 µm. **B.** Detail of A. N (yellow): normal duct; T (red): tumor area. Scale bar: 25 µm.

Figure panels taken from: "KCNJ3 is a new independent prognostic marker for estrogen receptor positive breast cancer patients" by Kammerer et al; manuscript submitted to Oncotarget.

Table 13: Summary of GIRK1 expression results and controls in patient samples.

#	GIRK1 microarray (log2 int.)	RNA ISH neg. ctrl. (s/c)	RNA ISH pos. ctrl. (s/c)	RNA ISH GIRK1 (s/c)
11	n.a.	n.a.	2.55	5.97
88	8.50	0.13	3.55	2.32
313	9.39	n.a.	8.42	9.01
318	8.32	0.04	4.39	2.56
323	*8.51*	*n.a.*	*n.a.*	*n.a.*
325	8.27	0.21	3.98	0.79
409	9.08	n.a.	n.a.	7.89
453	8.84	0.1	3.52	6.69
474	8.79	n.a.	2.80	0.13
484	8.30	n.a.	2.52	1.89
487	7.71	0.04	3.25	0.61
503	8.55	0.26	5.19	1.60
525	*8.56*	*n.a.*	*1.08*	*n.a.*
527	8.24	0.38	5.55	1.28
528	7.66	n.a.	3.55	0.74
652	7.17	0.04	4.30	0.28
684	7.92	0.13	5.01	0.16
714	8.91	0.2	13.6	7.94
732	7.22	n.a.	2.97	1.88
733	8.52	n.a.	3.67	0.22
756	7.87	0.15	6.68	0.18
765	8.04	0.02	4.96	1.53
779	*7.98*	*n.a.*	*n.a.*	*n.a.*
784	7.79	0.04	9.22	0.15
785	8.29	0.19	13.5	5.23
854	6.92	0.02	2.57	1.26
856	7.20	0.07	5.00	0.07
961	8.06	0.02	2.82	0.28
1015	6.99	n.a.	3.24	0.15
1053	7.55	n.a.	2.57	0.58
1057	9.42	0.06	3.07	10.1
1098	8.92	n.a.	3.29	0.33
1113	8.21	0.43	4.91	2.10
1129	6.74	0.05	3.56	0.07
1147	7.87	0.19	3.09	0.44
1197	7.71	0.13	5.07	0.30
1241	7.79	n.a.	2.96	1.97
1262	8.36	0.49	3.69	1.25
1280	5.66	0.04	2.51	0.07
1288	7.78	0.06	3.89	0.01
1299	9.11	n.a.	4.40	2.69
1350	*7.12*	*n.a.*	*n.a.*	*n.a.*

#	GIRK1 microarray (log2 int.)	RNA ISH neg. ctrl. (s/c)	RNA ISH pos. ctrl. (s/c)	RNA ISH GIRK1 (s/c)
1359	*7.21*	*n.a.*	*2.15*	*n.a.*
1471	9.55	n.a.	2.63	0.67
1521	7.84	n.a.	3.21	0.11
1526	7.63	n.a.	4.33	0.17
1733	7.74	n.a.	2.92	0.94
1942	7.92	n.a.	3.48	0.75
2087	8.14	n.a.	2.57	0.12
2298	8.61	n.a.	5.89	0.23
2448	8.19	n.a.	4.21	0.08
2506	8.14	n.a.	6.90	0.48
2560	*8.38*	*n.a.*	*n.a.*	*n.a.*
2633	*8.47*	*n.a.*	*n.a.*	*n.a.*
2640	*8.44*	*n.a.*	*n.a.*	*n.a.*
2783	*7.89*	*n.a.*	*n.a.*	*n.a.*
3613	7.57	n.a.	2.57	0.34
3650	9.00	n.a.	2.76	4.48
3815	*7.89*	*0.06*	*2.12*	*0.11*
3839	9.48	n.a.	5.65	0.12
3881	7.64	n.a.	3.60	0.24
3974	7.82	n.a.	2.76	0.2
4142	*6.97*	*n.a.*	*n.a.*	*n.a.*
8905	11.41	0.34	9.45	33.3
8957	*7.67*	*n.a.*	*1.61*	*n.a.*
8958	7.87	0.08	5.61	0.32

#: patient sample number; microarray: log2-intensities of GIRK1 expression; RNA ISH: RNA in situ hybridization; s/c: spots/cell; n.a.: not available. Samples excluded for further analysis are written in grey italics.

spots/cell for 27 negative controls evaluated with the SpotStudio software. Negative controls were also performed for the remaining samples, but slides were assessed under the microscope instead of using the image analysis software due to economic reasons. For one sample, it was not possible to perform negative and positive controls, since there was not enough tissue left on the block. Positive controls were all evaluated using the SpotStudio software. The mean for positive controls of the 54 included samples was 4.50±2.42 spots/cell, which indicates good RNA quality of the samples. The results for GIRK1 staining ranged from 0.01 to 33.3 spots/cell with a mean of 2.28±4.93 spots/cell. Figure 26 gives an example of GIRK1 staining in a patient sample with high GIRK1 expression levels. Importantly, positive signals can be found in tumor cells only, but not in surrounding normal

cells such as normal ducts or stromal cells (Figure 26B). *See also: "KCNJ3 is a new independent prognostic marker for estrogen receptor positive breast cancer patients" by Kammerer et al; manuscript submitted to Oncotarget.*

9.3.7 Survival analysis

We now used the results of the GIRK1 mRNA expression for survival analysis. Since this patient cohort had a complete clinical characterization and good follow-up documentation, we were able to perform both disease free and overall survival analysis. First, we used the results of the pre-existing microarray data in order to get insight into the possible prognostic role of GIRK1 mRNA expression in breast cancer. Figure 27 shows that there was no statistical significant difference in disease free survival when patients with low and high GIRK1 expression were compared. However, the difference was borderline significant when overall survival was calculated (p=0.052). A clear trend towards worse overall survival probabilities was observed for patients with high GIRK1 expression levels in their tumor. Then, we repeated this analysis, but used the RNA ISH results instead of the microarray data. Figure 28 shows impressively that patients with high GIRK1 expression levels have a worse disease free and overall survival probability. For disease free survival, the hazard ratio was 3.1 (1.26-7.63) with p<0.01 and for overall survival 2.39 (1.19-4.82) with p<0.05.

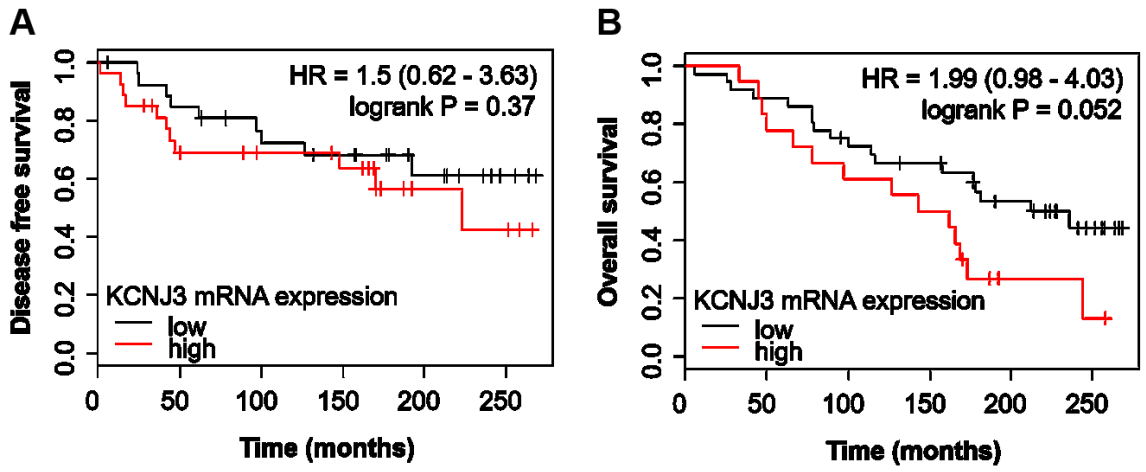

Figure 27: Survival analysis based on GIRK1 microarray data.

A. Kaplan-Meier plot showing disease free survival probabilities for patients with low or high GIRK1 expression as determined by microarray analysis (log2 intensity) **B.** Same as A., but showing overall survival probabilities.

Hazard ratios (HR) and logrank p-values are given; n=54.

Despite both the microarray and the RNA ISH method measure mRNA expression levels, the results of survival analysis are different: significant for RNA ISH, but not the microarray. This might be explained by methodological differences: While a bulk mass of cells is used for microarrays, the ISH method allows to exclude all non-tumor cells from analysis which makes the result more accurate in terms of being specific for tumor cells. *See also: "KCNJ3 is a new independent prognostic marker for estrogen receptor positive breast cancer patients" by Kammerer et al; manuscript submitted to Oncotarget.*

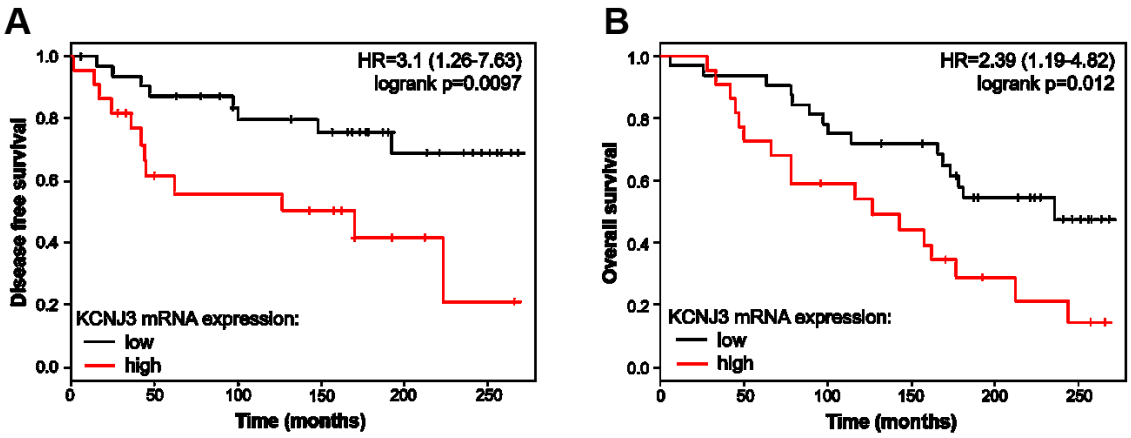

Figure 28: Survival analysis based on GIRK1 ISH data.

A. Kaplan-Meier plot showing disease free survival probabilities for patients with low or high GIRK1 expression as determined by RNA ISH analysis (spots/cell) **B.** Same as A., but showing overall survival probabilities.

Hazard ratios (HR) and logrank *p*-values are given; n=54.

Figure taken from: "KCNJ3 is a new independent prognostic marker for estrogen receptor positive breast cancer patients" by Kammerer et al; manuscript submitted to Oncotarget.

9.4 Integrative summary of both data sets

We could show in both data sets and by two different methods (RNA sequencing and RNA *in situ* hybridization) that GIRK1 expression is higher in tumor tissue than in corresponding normal tissue (see Figure 3 and Figure 26). Despite significant higher GIRK1 levels in LN positive patients in the TCGA data set (Figure 7A), the association coefficient was low in this data set (0.118; Table 5) as well as in the validation set (-0.063; Table 9). Age at diagnosis and tumor size had a borderline significant association coefficient in our validation

set (Table 9), but not in the TCGA data set (Table 5). In both data sets, a strong association of GIRK1 expression with the PAM50 status of the patient could be observed (Figure 6, Table 5, Table 9). This result was expected after having found a strong correlation of GIRK1 with ER positive breast cancer samples (Figure 4, Figure 10, Figure 11, Table 5, Table 6) and two groups of the PAM50 classification (luminal A and luminal B type) represent ER positive subsets. Positive correlation of gene expression between GIRK1 and ESR1 could also be found in the validation set (Figure 20).

We now used the correlation analysis of both data sets and searched for overlaps, i.e. for genes that had a high or low correlation coefficient in both data sets studied. Figure 29 shows Venn diagrams for positively and negatively correlating genes of both data sets. Six genes were in common when the genes positively correlating with GIRK1 were analyzed, and three when we looked at the genes negatively correlating with GIRK1. Table 14 gives an overview of the functions of these genes. The estrogen receptor gene was present again

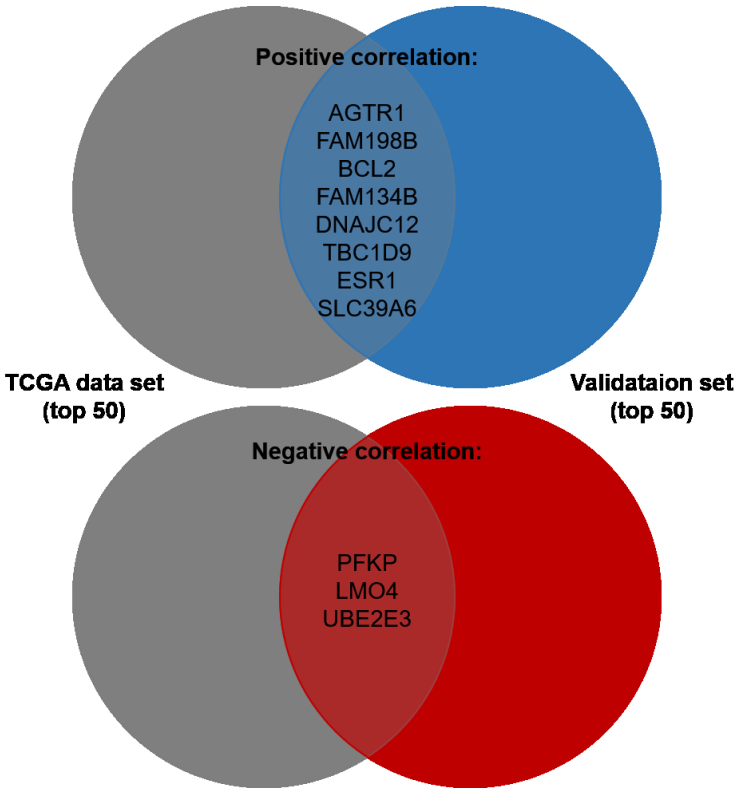

Figure 29: Venn diagram of genes correlating with GIRK1 in both data sets.
Grey circles represent the top 50 genes positively (top) and negatively (bottom) correlating with GIRK1. The blue circle (positive correlation with GIRK1 and) and the red circle (negative correlation with GIRK1) represent the top 50 of the validation set. Genes present in both lists are named in the overlapping region.

in this list, underlining its importance when studying GIRK1 in breast cancer. Of special interest are also DNAJC12 and AGTR1. It was shown that the transcription of DNAJC12 is directly activated by ESR1 due to estrogen response elements in its promotor region which explains its co-expression with ESR1 (52). It is also known that AGTR1 is expressed in ER positive breast cancer subtypes and that there is an association between AGTR1 expression and resistance to tamoxifen treatment. However, the molecular mechanisms behind these findings remain unclear (53-56). A potential hypothesis is that AGTR1 might activate GIRK1 via the phospholipase C pathway. Further studies are needed to elucidate whether there are functional mechanisms between GIRK1 and its co-expressed and/or -repressed genes. When we looked at the GOterm analysis of both data sets, we could only find one GOterm that was common to both: GO:0048666~neuron development. In addition, several GOterms in both data sets deal with secretion and membrane localization. None of the GOterms linked to genes negatively correlating with GIRK1 and no pathway yielded overlapping results.

Table 14: Description of genes correlating with GIRK1 in both data sets.

Gene	Description	Summary
AGTR1	Angiotensin II Receptor, Type 1	Receptor for angiotensin II. Mediates its action by association with G proteins that activate a phosphatidylinositol-calcium second messenger system.
FAM189B	Family With Sequence Similarity 189, Member B	Potential binding partner of a WW domain-containing protein which is involved in apoptosis and tumor suppression.
BCL2	B-Cell CLL/Lymphoma 2	Suppresses apoptosis in a variety of cell systems including factor-dependent lymphohematopoietic and neural cells. Regulates cell death by controlling the mitochondrial membrane permeability. Appears to function in a feedback loop system with caspases. Inhibits caspase activity either by preventing the release of cytochrome c from the mitochondria and/or by binding to the apoptosis-activating factor (APAF-1).
FAM134B	Family With Sequence Similarity 134, Member B	Endoplasmic reticulum-anchored autophagy receptor that mediates ER delivery into lysosomes through sequestration into autophagosomes. Promotes membrane remodeling and ER scission via its membrane bending capacity and targets the fragments into autophagosomes via interaction with ATG8 family proteins. Required for long-term survival of nociceptive and autonomic ganglion. neurons.
DNAJC12	DnaJ (Hsp40) Homolog, Subfamily C, Member 12	This gene encodes a member of a subclass of the HSP40/DnaJ protein family. Members of this family of proteins are associated with complex assembly, protein folding, and export.
TBC1D9	TBC1 Domain Family, Member 9 (With GRAM Domain)	May act as a GTPase-activating protein for Rab family protein(s).

Gene	Description	Summary
ESR1	Estrogen Receptor 1	Estrogen controls many cellular processes including growth, differentiation and function of the reproductive system. Estrogen is also responsible for the growth and maintenance of the skeleton and the normal function of the cardiovascular and nervous systems.
SLC39A6	Solute Carrier Family 39 (Zinc Transporter), Member 6	May act as a zinc-influx transporter.
PFKP	Phosphofructo-1-Kinase Isozyme C	Catalyzes the phosphorylation of D-fructose 6-phosphate to fructose 1,6-bisphosphate by ATP, the first committing step of glycolysis.
LMO4	LIM Domain Only 4	Probable transcriptional factor.
UBE2E3	Ubiquitin-Conjugating Enzyme E2E 3	Accepts ubiquitin from the E1 complex and catalyzes its covalent attachment to other proteins. In vitro catalyzes Lys-11- and Lys-48-, as well as Lys-63-linked polyubiquitination. Participates in the regulation of transepithelial sodium transport in renal cells. May be involved in cell growth arrest.

Gene description and summaries are taken from the Human Gene Database (genecards.org).

Regarding the survival analysis, we could show in both data sets that ER positive patients with high GIRK1 expression levels had a worse overall survival probability. For our validation set, this was also true when disease free survival was analyzed. This indicates a possible prognostic role for GIRK1 in ER positive breast cancer.

10 Discussion

In this project, we have analyzed a total of >1000 breast cancer patient samples regarding their GIRK1 expression. This was performed in two independent data sets: first, we used the TCGA gene expression data of 905 breast cancer patients for initial analysis of GIRK1 in different breast cancer subsets; second and based on the findings of the TCGA, a validation set of 298 estrogen receptor positive breast cancer patients was used (GEO ID GSE17705; (45)). Out of these 298 cases, 66 tumor tissue blocks were available to study GIRK1 expression *in situ*.

In general terms, ion channels are becoming increasingly interesting new targets in cancer research, especially in tumor development and metastasis. Mutations, overexpression and downregulation in different ion channel genes have been observed. These aberrant gene expressions seem to influence the hallmarks of cancer leading to higher malignancy (24,25,57-59). Potassium channels encounter the greatest attention when speaking about the oncogenic potential of different ion channels types. Several studies observed that potassium channels are involved in apoptosis and proliferation (60-65).

So far, only little evidence has existed for a role of GIRK1, the G-protein coupled inwardly rectifying potassium channel encoded by *KCNJ3*, in breast (37,38) or other cancers (35). The work presented here underlines and confirms the results of these findings in a considerably larger number of patient samples: a) analyzing the TCGA data, we found that patients who presented with positive lymph node status had significantly higher GIRK1 mRNA levels in the tumor than LN negative patients (n=876); and b) we could confirm that GIRK1 mRNA levels were significantly higher in breast tumors than in corresponding normal breast tissue (TCGA; n=105). This finding could be further corroborated using a highly sensitive and specific RNA *in situ* hybridization technique on samples of our validation set (Kammerer et al., “Critical evaluation of KCNJ3 gene product detection in human breast cancer: mRNA in situ hybridization is superior to immunohistochemistry”, accepted for publication in the Journal of Clinical Pathology).

Besides the confirmation of pre-existing results in a larger patient cohort, we also generated new knowledge. We clearly demonstrated a strong correlation between GIRK1 expression and ER positive tumors. Previous studies did not detect this correlation, most probably due to the rather low patient numbers (n=56 and n=31) used in these studies (37,38). To our knowledge, there is only one previous study suggesting a positive correlation between GIRK1 and ER positivity: Ko et al (66) performed expression profiling of a large ion channel panel in breast cancer. They reported downregulation of GIRK1 in p53 mutant breast tumor samples, whereby a p53 mutant status is negatively associated with ER status (67), and

GIRK1 upregulation in ER positive samples. However, this finding was not further investigated by any means, as the study's goal was to develop an ion channel gene signature for breast cancer and GIRK1 was not included in this prognostic IC30 signature (66). Our data not only show that GIRK1 is associated with ER positive breast cancer, but also that *KCNJ3* gene expression levels correlate with *ESR1* expression levels. No correlation was found between GIRK1 and the expression of the two other known estrogen receptors ESR2 and GPER. Most importantly, GIRK1 levels were not consistently high in ER positive tumors, but showed variability. The ER positive samples could be divided into two subgroups, one with low and one with high GIRK1 expression. This is a crucial finding, since ER positive patients with high GIRK1 expression had worse survival probabilities than the patients with low GIRK1 expression. This was first observed in the TCGA data set using RNASeq data in overall survival analysis and was further validated in our second data set using RNA *in situ* hybridization data in both overall and disease free survival analysis. Performing a multivariate Cox proportional hazard analysis, with tumor size, lymph node status, metastasis status, histology, Her2 expression status, menopausal status, age at diagnosis, and PAM50 classification as covariates, we could show that GIRK1 is an independent prognostic marker for ER positive breast cancer. Of note, GIRK1 was also independent from the PAM50 subtype of the patient, which indicates that GIRK1 does not just reflect the Luminal B status which is known as the more aggressive ER positive subtype (5). Therefore, GIRK1 might be used to stratify high and low risk ER positive patients.

Due to the strong correlation with the estrogen receptor, it seemed reasonable that transcription of GIRK1 might be activated by ER. Previous studies could not provide evidence for estrogen response elements (ERE) in the GIRK1 promoter region (68,69). This argues against a direct transcriptional activation of GIRK1 by ER. Our own *in silico* promotor analysis corroborates these findings. Our results also excluded gene locus amplification as possible mechanism for GIRK1 upregulation.

Further, we sought to study which genes are co-regulated with GIRK1 and to retrieve information about the cellular processes and pathways that might be controlled by GIRK1. Unfortunately, these analyses did not lead to any conclusive findings. The present work did not aim to elucidate the mechanisms that might lead to GIRK1 upregulation in ER positive breast tumors, and therefore, no *in vitro* assays addressing this question were performed. Functional effects of GIRK1 upregulation were studied by Simin Rezania of our working group (see Rezania et al., accepted for publication in BMC Cancer; or her thesis). She could show that MCF-7 cells stably overexpressing GIRK1 behaved more aggressively in terms of displaying increased invasion, velocity and motility as well as higher wound healing capacity (40). Further, MCF-7 cells showed higher self-renewal capacity than controls in a

mammosphere formation assay, which is indicative for stem cell like features (Kammerer et al., “KCNJ3 is a new independent prognostic marker for estrogen receptor positive breast cancer patients”, manuscript submitted to Oncotarget).

In conclusion, the work presented here suggests that GIRK1 might be used as prognostic biomarker for ER positive breast cancer in a clinical setting. Of note, we were also able to establish a reliable, specific and sensitive RNA ISH method for the detection of GIRK1 in a routine pathological setting (Kammerer et al., “Critical evaluation of KCNJ3 gene product detection in human breast cancer: mRNA in situ hybridization is superior to immunohistochemistry”, accepted for publication in the Journal of Clinical Pathology). Future studies are required to gain insights into the mechanisms that lead to GIRK1 upregulation in ER positive breast cancer, to unveil the pathways involved in invasion and metastasis upon GIRK1 upregulation, and to evaluate whether GIRK1 might be used as drugable target.

11 References

(1) Tinoco G, Warsch S, Gluck S, Avancha K, Montero AJ. Treating breast cancer in the 21st century: emerging biological therapies. J Cancer 2013;4(2):117-132.

(2) Jemal A, Bray F, Center MM, Ferlay J, Ward E, Forman D. Global cancer statistics. CA: A Cancer Journal for Clinicians 2011;61(2):69-90.

(3) Levitzki A, Klein S. Signal transduction therapy of cancer. Mol Aspects Med 2010 Aug;31(4):287-329.

(4) Van Meter ME, Kim ES. Bevacizumab: current updates in treatment. Curr Opin Oncol 2010 Nov;22(6):586-591.

(5) Kelly CM, Bernard PS, Krishnamurthy S, Wang B, Ebbert MTW, Bastien RRL, et al. Agreement in Risk Prediction Between the 21-Gene Recurrence Score Assay (Oncotype DX®) and the PAM50 Breast Cancer Intrinsic Classifier™ in Early-Stage Estrogen Receptor–Positive Breast Cancer. The Oncologist 2012 April 01;17(4):492-498.

(6) Mook S, Schmidt MK, Weigelt B, Kreike B, Eekhout I, van de Vijver MJ, et al. The 70-gene prognosis signature predicts early metastasis in breast cancer patients between 55 and 70 years of age. Annals of Oncology 2010 April 01;21(4):717-722.

(7) Pharoah PD, Caldas C. Genetics: How to validate a breast cancer prognostic signature. Nat Rev Clin Oncol 2010 Nov;7(11):615-616.

(8) Kesisis G, Kontovinis LF, Gennatas K, Kortsaris AH. Biological markers in breast cancer prognosis and treatment. J BUON 2010 Jul-Sep;15(3):447-454.

(9) Kurian A, Fish K, Shema S, Clarke C. Lifetime risks of specific breast cancer subtypes among women in four racial/ethnic groups. Breast Cancer Research 2010;12(6):R99.

(10) Ocana A, Pandiella A. Personalized therapies in the cancer "omics" era. Mol Cancer 2010 Jul 29;9:202-4598-9-202.

(11) Lappano R, Maggiolini M. G protein-coupled receptors: novel targets for drug discovery in cancer. Nat Rev Drug Discov 2011 print;10(1):47-60.

(12) Dorsam RT, Gutkind JS. G-protein-coupled receptors and cancer. Nat Rev Cancer 2007 print;7(2):79-94.

(13) Muller A, Homey B, Soto H, Ge N, Catron D, Buchanan ME, et al. Involvement of chemokine receptors in breast cancer metastasis. Nature 2001 Mar 1;410(6824):50-56.

(14) Arcangeli A, Crociani O, Lastraioli E, Masi A, Pillozzi S, Becchetti A. Targeting Ion Channels in Cancer: A Novel Frontier in Antineoplastic Therapy. Curr Med Chem 2009 JAN;16(1):66-93.

(15) Cotton M, Claing A. G protein-coupled receptors stimulation and the control of cell migration. Cell Signal 2009 7;21(7):1045-1053.

(16) Chambers AF, Groom AC, MacDonald IC. Dissemination and growth of cancer cells in metastatic sites. Nat Rev Cancer 2002 Aug;2(8):563-572.

(17) Pierce KL, Premont RT, Lefkowitz RJ. Seven-transmembrane receptors. Nat Rev Mol Cell Biol 2002 print;3(9):639-650.

(18) Luscher C, Slesinger PA. Emerging roles for G protein-gated inwardly rectifying potassium (GIRK) channels in health and disease. Nat Rev Neurosci 2010 May;11(5):301-315.

(19) Iwanir S, Reuveny E. Adrenaline-induced hyperpolarization of mouse pancreatic islet cells is mediated by G protein-gated inwardly rectifying potassium (GIRK) channels. Pflugers Arch 2008 Sep;456(6):1097-1108.

(20) Smith PA, Sellers LA, Humphrey PP. Somatostatin activates two types of inwardly rectifying K+ channels in MIN-6 cells. J Physiol 2001 Apr 1;532(Pt 1):127-142.

(21) Shankar H, Kahner BN, Prabhakar J, Lakhani P, Kim S, Kunapuli SP. G-protein-gated inwardly rectifying potassium channels regulate ADP-induced cPLA2 activity in platelets through Src family kinases. Blood 2006 Nov 1;108(9):3027-3034.

(22) Shankar H, Murugappan S, Kim S, Jin J, Ding Z, Wickman K, et al. Role of G protein-gated inwardly rectifying potassium channels in P2Y12 receptor-mediated platelet functional responses. Blood 2004 Sep 1;104(5):1335-1343.

(23) Perry CA, Pravetoni M, Teske JA, Aguado C, Erickson DJ, Medrano JF, et al. Predisposition to late-onset obesity in GIRK4 knockout mice. Proc Natl Acad Sci U S A 2008 Jun 10;105(23):8148-8153.

(24) Prevarskaya N, Skryma R, Shuba Y. Ion channels and the hallmarks of cancer. Trends Mol Med 2010 3;16(3):107-121.

(25) Li M, Xiong ZG. Ion channels as targets for cancer therapy. Int J Physiol Pathophysiol Pharmacol 2011;3(2):156-166.

(26) D'Amico M, Gasparoli L, Arcangeli A. Potassium Channels: Novel Emerging Biomarkers and Targets for Therapy in Cancer. Recent Patents Anti-Canc Drug Discov 2013 JAN;8(1):53-65.

(27) Bielanska J, Hernandez-Losa J, Perez-Verdaguer M, Moline T, Somoza R, Cajal SR, et al. Voltage-Dependent Potassium Channels Kv1.3 and Kv1.5 in Human Cancer. Current Cancer Drug Targets 2009 -12-01T00:00:00;9(8):904-914.

(28) Shen Z, Yang Q, You Q. Researches toward potassium channels on tumor progressions. Curr Top Med Chem 2009;9(4):322-329.

(29) Sundelacruz S, Levin M, Kaplan D. Role of Membrane Potential in the Regulation of Cell Proliferation and Differentiation. Stem Cell Reviews and Reports 2009 09/01;5(3):231-246.

(30) Han X, Wang F, Yao W, Xing H, Weng D, Song X, et al. Heat shock proteins and p53 play a critical role in K+ channel-mediated tumor cell proliferation and apoptosis. Apoptosis 2007 10/01;12(10):1837-1846.

(31) Zhanping W, Xiaoyu P, Na C, Shenglan W, Bo W. Voltage-gated K+ channels are associated with cell proliferation and cell cycle of ovarian cancer cell. Gynecol Oncol 2007 2;104(2):455-460.

(32) Zhou Q, Kwan HY, Chan HC, Jiang JL, Tam SC, Yao X. Blockage of voltage-gated K+ channels inhibits adhesion and proliferation of hepatocarcinoma cells. Int J Mol Med 2003 Feb;11(2):261-266.

(33) Choi M, Scholl UI, Yue P, Bjorklund P, Zhao B, Nelson-Williams C, et al. K+ channel mutations in adrenal aldosterone-producing adenomas and hereditary hypertension. Science 2011 Feb 11;331(6018):768-772.

(34) Scholl UI, Lifton RP. New insights into aldosterone-producing adenomas and hereditary aldosteronism: mutations in the K+ channel KCNJ5. Curr Opin Nephrol Hypertens 2013 Mar;22(2):141-147.

(35) Brevet M, Fucks D, Chatelain D, Regimbeau JM, Delcenserie R, Sevestre H, et al. Deregulation of 2 potassium channels in pancreas adenocarcinomas: implication of KV1.3 gene promoter methylation. Pancreas 2009 Aug;38(6):649-654.

(36) Takanami I, Inoue Y, Gika M. G-protein inwardly rectifying potassium channel 1 (GIRK 1) gene expression correlates with tumor progression in non-small cell lung cancer. BMC Cancer 2004 Nov 13;4:79.

(37) Stringer BK, Cooper AG, Shepard SB. Overexpression of the G-protein inwardly rectifying potassium channel 1 (GIRK1) in primary breast carcinomas correlates with axillary lymph node metastasis. Cancer Res 2001 Jan 15;61(2):582-588.

(38) Brevet M, Ahidouch A, Sevestre H, Merviel P, El Hiani Y, Robbe M, et al. Expression of K+ channels in normal and cancerous human breast. Histol Histopathol 2008 Aug;23(8):965-972.

(39) Wagner V, Stadelmeyer E, Riederer M, Regitnig P, Gorischek A, Devaney T, et al. Cloning and characterisation of GIRK1 variants resulting from alternative RNA editing of the KCNJ3 gene transcript in a human breast cancer cell line. J Cell Biochem 2010 Jun 1;110(3):598-608.

(40) Rezania S, Li C, Kammerer S, Gorischek A, Devaney T, Zarnani AH, et al. G-Protein Activated Inwardly Rectifying Potassium Channels Control Motility of Breast Cancer Cells. Biophys J 2014;106(2):543a.

(41) Gao J, Aksoy BA, Dogrusoz U, Dresdner G, Gross B, Sumer SO, et al. Integrative analysis of complex cancer genomics and clinical profiles using the cBioPortal. Sci Signal 2013 Apr 2;6(269):pl1.

(42) Cerami E, Gao J, Dogrusoz U, Gross BE, Sumer SO, Aksoy BA, et al. The cBio Cancer Genomics Portal: An Open Platform for Exploring Multidimensional Cancer Genomics Data. Cancer Discovery 2012 May 01;2(5):401-404.

(43) Cancer Genome Atlas Network. Comprehensive molecular portraits of human breast tumours. Nature 2012 Oct 4;490(7418):61-70.

(44) Hofer D, Lohberger B, Steinecker B, Schmidt K, Quasthoff S, Schreibmayer W. A comparative study of the action of tolperisone on seven different voltage dependent sodium channel isoforms. Eur J Pharmacol 2006 May 24;538(1-3):5-14.

(45) Symmans WF, Hatzis C, Sotiriou C, Andre F, Peintinger F, Regitnig P, et al. Genomic index of sensitivity to endocrine therapy for breast cancer. J Clin Oncol 2010 Sep 20;28(27):4111-4119.

(46) Gyorffy B, Lanczky A, Eklund AC, Denkert C, Budczies J, Li Q, et al. An online survival analysis tool to rapidly assess the effect of 22,277 genes on breast cancer prognosis using microarray data of 1,809 patients. Breast Cancer Res Treat 2010 Oct;123(3):725-731.

(47) Parker JS, Mullins M, Cheang MC, Leung S, Voduc D, Vickery T, et al. Supervised risk predictor of breast cancer based on intrinsic subtypes. J Clin Oncol 2009 Mar 10;27(8):1160-1167.

(48) Mihaly Z, Kormos M, Lanczky A, Dank M, Budczies J, Szasz MA, et al. A meta-analysis of gene expression-based biomarkers predicting outcome after tamoxifen treatment in breast cancer. Breast Cancer Res Treat 2013 Jul;140(2):219-232.

(49) Wang J, Zhuang J, Iyer S, Lin X, Greven MC, Kim B, et al. Factorbook.org: a Wiki-based database for transcription factor-binding data generated by the ENCODE consortium. Nucleic Acids Research 2013 January 01;41(D1):D171-D176.

(50) Wang J, Zhuang J, Iyer S, Lin X, Whitfield TW, Greven MC, et al. Sequence features and chromatin structure around the genomic regions bound by 119 human transcription factors. Genome Research 2012 September 01;22(9):1798-1812.

(51) Gerstein MB, Kundaje A, Hariharan M, Landt SG, Yan K, Cheng C, et al. Architecture of the human regulatory network derived from ENCODE data. Nature 2012 09/06;489(7414):91-100.

(52) De Bessa SA, Salaorni S, Patrao DF, Neto MM, Brentani MM, Nagai MA. JDP1 (DNAJC12/Hsp40) expression in breast cancer and its association with estrogen receptor status. Int J Mol Med 2006 Feb;17(2):363-367.

(53) Rhodes DR, Ateeq B, Cao Q, Tomlins SA, Mehra R, Laxman B, et al. AGTR1 overexpression defines a subset of breast cancer and confers sensitivity to losartan, an AGTR1 antagonist. Proc Natl Acad Sci U S A 2009 Jun 23;106(25):10284-10289.

(54) Namazi S, Sahebi E, Rostami-Yalmeh J, Jaberipour M, Razmkhah M, Hosseini A, et al. Effect of angiotensin receptor blockade on prevention and reversion of tamoxifen-resistant phenotype in MCF-7 cells. Tumour Biol 2014 Oct 11.

(55) Du N, Feng J, Hu LJ, Sun X, Sun HB, Zhao Y, et al. Angiotensin II receptor type 1 blockers suppress the cell proliferation effects of angiotensin II in breast cancer cells by inhibiting AT1R signaling. Oncol Rep 2012 Jun;27(6):1893-1903.

(56) Ateeq B, Tomlins SA, Chinnaiyan AM. AGTR1 as a therapeutic target in ER-positive and ERBB2-negative breast cancer cases. Cell Cycle 2009 Dec;8(23):3794-3795.

(57) Li C, Rezania S, Kammerer S, Sokolowski A, Devaney T, Gorischek A, et al. Piezo1 forms mechanosensitive ion channels in the human MCF-7 breast cancer cell line. Sci Rep 2015 Feb 10;5:8364.

(58) Hanahan D, Weinberg RA. Hallmarks of cancer: the next generation. Cell 2011 Mar 4;144(5):646-674.

(59) Hanahan D, Weinberg RA. The hallmarks of cancer. Cell 2000 Jan 7;100(1):57-70.

(60) Yang M, Brackenbury WJ. Membrane potential and cancer progression. Front Physiol 2013 Jul 17;4:185.

(61) Ouadid-Ahidouch H, Roudbaraki M, Delcourt P, Ahidouch A, Joury N, Prevarskaya N. Functional and molecular identification of intermediate-conductance Ca(2+)-activated K(+) channels in breast cancer cells: association with cell cycle progression. Am J Physiol Cell Physiol 2004 Jul;287(1):C125-34.

(62) Wang Z. Roles of K+ channels in regulating tumour cell proliferation and apoptosis. Pflugers Arch 2004 Jun;448(3):274-286.

(63) Ouadid-Ahidouch H, Le Bourhis X, Roudbaraki M, Toillon RA, Delcourt P, Prevarskaya N. Changes in the K+ current-density of MCF-7 cells during progression through the cell cycle: possible involvement of a h-ether.a-gogo K+ channel. Receptors Channels 2001;7(5):345-356.

(64) Ouadid-Ahidouch H, Chaussade F, Roudbaraki M, Slomianny C, Dewailly E, Delcourt P, et al. KV1.1 K(+) channels identification in human breast carcinoma cells: involvement in cell proliferation. Biochem Biophys Res Commun 2000 Nov 19;278(2):272-277.

(65) Pardo LA, del Camino D, Sanchez A, Alves F, Bruggemann A, Beckh S, et al. Oncogenic potential of EAG K(+) channels. EMBO J 1999 Oct 15;18(20):5540-5547.

(66) Ko JH, Ko EA, Gu W, Lim I, Bang H, Zhou T. Expression profiling of ion channel genes predicts clinical outcome in breast cancer. Mol Cancer 2013 Sep 22;12(1):106-4598-12-106.

(67) Borresen-Dale AL. TP53 and breast cancer. Hum Mutat 2003 Mar;21(3):292-300.

(68) Lin CY, Strom A, Vega VB, Kong SL, Yeo AL, Thomsen JS, et al. Discovery of estrogen receptor alpha target genes and response elements in breast tumor cells. Genome Biol 2004;5(9):R66.

(69) Schoots O, Voskoglou T, Van Tol HHM. Genomic Organization and Promoter Analysis of the Human G-Protein-Coupled K+Channel Kir3.1 (KCNJ3/HGIRK1). Genomics 1997 2/1;39(3):279-288.

(70) Stringer BK, Cooper AG, Shepard SB. Overexpression of the G-protein inwardly rectifying potassium channel 1 (GIRK1) in primary breast carcinomas correlates with axillary lymph node metastasis. Cancer Res 2001 Jan 15;61(2):582-588.

(71) Liang B, Nissen JD, Laursen M, Wang X, Skibsbye L, Hearing MC, et al. G-protein-coupled inward rectifier potassium current contributes to ventricular repolarization. Cardiovascular Research 2014 January 01;101(1):175-184.

(72) Kosti I, Jain N, Aran D, Butte AJ, Sirota M. Cross-tissue Analysis of Gene and Protein Expression in Normal and Cancer Tissues. Sci Rep 2016 May 4;6:24799.

(73) Nockemann D, Rouault M, Labuz D, Hublitz P, McKnelly K, Reis FC, et al. The K(+) channel GIRK2 is both necessary and sufficient for peripheral opioid-mediated analgesia. EMBO Mol Med 2013 Aug;5(8):1263-1277.

(74) Wang F, Flanagan J, Su N, Wang LC, Bui S, Nielson A, et al. RNAscope: a novel in situ RNA analysis platform for formalin-fixed, paraffin-embedded tissues. J Mol Diagn 2012 Jan;14(1):22-29.

(75) Ruggieri P, Mangino G, Fioretti B, Catacuzzeno L, Puca R, Ponti D, et al. The inhibition of KCa3.1 channels activity reduces cell motility in glioblastoma derived cancer stem cells. PLoS One 2012;7(10):e47825.

12 Appendix

12.1 Publications

- **Kammerer, S**; Sokolowski, A; Hackl, H; Platzer, D; Jahn, SW; El-Heliebe, A; Schwarzenbacher, D; Pichler, M; Rezania, S; Regitnig, P; Höfler, G; Schreibmayer, W; Bauernhofer, T.
  KCNJ3 is a new independent prognostic marker for estrogen receptor positive breast cancer patients.
  Manuscript submitted to Oncotarget; under review

- **Kammerer, S**; Jahn, SW; Winter, E; Eidenhammer, S; Rezania, S; Regitnig, P; Pichler, M; S; Schreibmayer, W; Bauernhofer, T.
  Critical evaluation of KCNJ3 gene product detection in human breast cancer: mRNA in situ hybridization versus immunohistochemistry.
  Accepted for publication in the Journal of Clinical Pathology

- Rezania, S; **Kammerer, S**; Li, C; Gorischek, A; DeVaney, T; Verheyen, S; Passegger, CA; Ghaffari-Tabrizi-Wizsy, N; Hackl, H; Platzer, D; Zarnani, AH; Malle, E; Jahn, S; Bauernhofer, T; Schreibmayer, W.
  Overexpression of KCNJ3 gene splice variants affects vital parameters of the malignant breast cancer cell line MCF-7 in an opposing manner.
  Accepted for publication in BMC cancer

- Li, C; Rezania, S; **Kammerer, S**; Sokolowski, A; DeVaney, T; Gorischek, A; Jahn, S; Hackl, H; Groschner, K; Windpassinger, C; Malle, E; Bauernhofer, T; Schreibmayer, W.
  Piezo1 forms mechanosensitive ion channels in the human MCF-7 breast cancer cell line.
  Scientific Reports 2015 Feb 10;5:8364; doi: 10.1038/srep08364

12.2 Oral Presentations

- **Kammerer, S**; Winter, E.
  RNAscope® in biomarker research: a field report.
  ACD Symposium: The RNA Revolution; OCT 15, 2015; Strasbourg, FRANCE. 2015.
  Invited Talk

- **Kammerer, S**; Sokolowski, A; Hackl, H; Platzer, D; Jahn, S; Schreibmayer, W; Bauernhofer, T.
  G protein-activated inward rectifier potassium channel 1 overexpression is associated with lymph node metastasis and poor prognosis in breast cancer.
  ÖGMBT 6th Annual Meeting; SEPT 15-18, 2014; Vienna, AUSTRIA.

- **Kammerer, S**; Sokolowski, A; Hackl, H; Platzer, D; Jahn, S; Asslaber, M; Schreibmayer, W; Bauernhofer, T.
  Overexpression of GIRK1 is associated with lymph node metastasis and poor prognosis in breast cancer.
  ZMF 10th Anniversary - Scientific Symposium; JUL 17-18, 2014; Graz, AUSTRIA.

12.3 Poster Presentations

- **Kammerer, S**; Sokolowski, A; Hackl, H; Platzer, D; Jahn, S; Peintinger, F; Symmans, F; Schreibmayer, W; Bauernhofer, T.
  GIRK1 overexpression correlates with ER positive breast cancer subtypes and is associated with poor prognosis.
  IMPAKT 2015 Breast Cancer Conference; MAY 7-9, 2015; Brussels, BELGIUM.
  Citation: Ann Oncol (2015) 26 (suppl 3): iii22. doi: 10.1093/annonc/mdv117.27

- **Kammerer, S**; Jahn, S; Winter, E; Sokolowski, A; Hackl, H; Platzer, D; Peintinger, F; Schreibmayer, W; Bauernhofer, T.
  GIRK1: a new prognostic biomarker for estrogen receptor positive breast cancer.
  OeGHO Frühjahrstagung 2015; APR 23-25, 2015; Salzburg, AUSTRIA.
  Poster Prize “Oncology“

- **Kammerer, S**; Sokolowski, A; Hackl, H; Platzer, D; Jahn, S; Schreibmayer, W; Bauernhofer, T.
  GIRK1 overexpression correlates with ER positive breast cancer subtypes and is associated with poor prognosis.
  Doctoral Day 2014; DEC 10, 2014; Graz, AUSTRIA.

- **Kammerer, S**; Sokolowski, A; Hackl, H; Platzer, D; Rezania, S; Jahn, S; Asslaber, M; Regitnig, P; Schreibmayer, W; Bauernhofer, T.
  G protein-activated inward rectifier potassium channel 1 (GIRK1) expression in breast cancer.
  Gordon Research Conference; JUN 8-13, 2014; Lucca (Barga), ITALY.

- **Kammerer, S**; Sokolowski, A; Hackl, H; Jahn, S; Asslaber, M; Symmans, F; Peintinger, F; Regitnig, P; Schreibmayer, W; Bauernhofer, T.
  Overexpression of G protein-activated inward rectifier potassium channel 1 (GIRK1) is associated with lymph node metastasis and poor prognosis in breast cancer.
  IMPAKT 2014 Breast Cancer Conference; MAY 8-10, 2014; Brussels, BELGIUM.
  Citation: Ann Oncol (2014) 25 (suppl 1):i8–i16; doi:10.1093/annonc/mdu066.21

- Li, C; Rezania, S; **Kammerer, S**; Gorischek, A; Bauernhofer, T; Schreibmayer, W.
  Mechano-sensitive ion channels (MSCs) provide human breast cancer cells with a sensorium for mechanical stress.
  Biophysical Society 58th Annual Meeting; FEB 15-19, 2014; San Francisco, USA.
  Citation: Biophysical Journal 2014;106(2), Supplement 1:549a–550a; doi: 10.1016/j.bpj.2013.11.3061

- Rezania, S; Li, C; **Kammerer, S**; Gorischek, A; Devaney, T; Zarnani, AH; Bauernhofer, T; Schreibmayer, W.
  G-Protein Activated Inwardly Rectifying Potassium Channels Control Motility of Breast Cancer Cells.
  Biophysical Society 58th Annual Meeting; FEB 15-19, 2014; San Francisco, USA.
  Citation: Biophysical Journal 2014;106(2), Supplement 1:543a; doi: 10.1016/j.bpj.2013.11.3026

- **Kammerer, S**; Sokolowski, A; Rezania, S; Gorischek, A; Hackl, H; Malle, E; Jahn, S; Asslaber, M; Schreibmayer, W; Bauernhofer, T.
  GIRK1 protein expression in primary tumours of breast cancer patients.
  Doctoral Day 2013; DEC 9, 2013; Graz, AUSTRIA.

- Li, C; Rezania, S; **Kammerer, S**; Gorischek, A; Bauernhofer, T; Schreibmayer, W.
  Mechano-sensitive ion channels (MSCs) provide human breast cancer cells with a sensorium for mechanical stress.
  Doctoral Day 2013; DEC 9, 2013; Graz, AUSTRIA.